# Regulation of bone formation and pathology by local actions of leptin in the bone marrow

**by**

**Erica L Scheller**

**A dissertation submitted in partial fulfillment**
**of the requirements for the degree of**
**Doctor of Philosophy**
**(Oral Health Sciences)**
**in The University of Michigan**
**2011**

**Doctoral Committee:**

**Professor Paul H. Krebsbach, Chair**
**Professor Laurie K. McCauley**
**Professor Renny T. Franceschi**
**Professor Ormond A. MacDougald**
**Assistant Professor Kurt D. Hankenson, University of Pennsylvania**

**Dedicated to Woo, Abbie, and AJ**

## TABLE OF CONTENTS

**Dedication** ii

**List of Figures** v

**List of Tables** vii

**Abstract** viii

**Chapters** 1

**1. Introduction** 1

1.1 Exploring the role of adipose in the bone marrow 1

1.2 Leptin 4

1.3 Clinical Challenges 23

1.4 Summary 24

**2. A Role for the Myeloid Lineage in Leptin-Regulated Bone Metabolism** 26

2.1 Summary 26

2.2 Introduction 27

2.3 Materials and Methods 29

2.4 Results 31

2.5 Discussion 37

2.6 Acknowledgements 37

**3. Leptin Functions Peripherally to Regulate Differentiation of Mesenchymal Progenitor Cells** 38

3.1 Summary 38

3.2 Introduction 39

3.3 Materials and Methods 42

3.4 Results 50

3.5 Discussion 70

3.6 Acknowledgements 75

**4. Ectopic Expression of Col2.3 and Col3.6 Promoters in the Brain – Association with Leptin Signaling and Contribution the 3.6$^{Cre+F/F}$ Phenotype** 77

4.1 Summary 77

4.2 Introduction 78

4.3 Materials and Methods 80

4.4 Results 82

4.5 Discussion 87

4.6 Acknowledgements 90

**5. Zoledronic Acid Inhibits Macrophage SOCS3 Expression and Enhances Cytokine Production** 91

5.1 Summary 91

5.2 Introduction 93

5.3 Materials and Methods 95

5.4 Results 101

5.5 Discussion ____ 111
5.6 Acknowledgements ____ 114

**6. Prospectus and Conclusions ____ 115**
6.1 Further consideration of the $3.6^{Cre+F/F}$ phenotype ____ 115
6.2 Potential use of recombinant leptin to treat human disease ____ 120

**References ____ 124**

## LIST OF FIGURES

1. Bone marrow adipose transition from thoracic to caudal vertebrae in mouse _____ 2

2. Leptin-deficient ob/ob mice have increased marrow fat in the distal femur but not in the lumbar vertebrae _____ 3

3. Leptin Signaling Diagram _____ 8

4. Leptin-deficient ob/ob mice have increased lumbar vertebral trabecular bone parameters _____ 15

5. Leptin-deficient ob/ob mice have decreased distal femoral trabecular bone parameters _____ 16

6. Immunohistochemistry for GFP of mice with ObRb-linked EGFP expression compared to control GFP negative mice _____ 19

7. GFP immunohistochemistry of mice with ObRb-linked EGFP expression reveals suspected ObRb expressing cells in vivo _____ 20

8. Summary of research direction _____ 25

9. Generation of $LysM^{Cre+F/F}$ Mice _____ 32

10. $LysM^{Cre+F/F}$ liver phenotype _____ 34

11. Primary bone marrow stromal cells (BMSCs) express ObRb _____ 51

12. Primary bone marrow stromal cell (BMSC) ObRb responds to leptin with phosphorylation of Stat3 _____ 52

13. Knockout of ObRb in vitro decreases the mineralization of primary bone marrow stromal cells _____ 54

14. Knockout of ObRb in vitro increases the adipogenesis of primary adipose derived stromal cells _____ 55

15. Bone marrow stromal cells (BMSCs) from ob/ob and db/db mice show increased mineralization _____ 57

16. Germline knockout of ObRb results in significant obesity. _____ 58

17. Characterization of LoxP recombination in mice expressing Col2.3-Cre or Col3.6-Cre and harboring the $ObRb^{F/F}$ site _____ 59

18. Gross phenotype of $3.6^{Cre+F/F}$ mice _____ 61

19. Minispec body composition analysis of $3.6^{Cre-}$ and $3.6^{Cre+F/F}$ mice _____ 62

20. Comprehensive lab animal monitoring system (CLAMS) analysis of $3.6^{Cre-}$ and $3.6^{Cre+F/F}$ mice 63

21. Femoral imaging and length analysis of transgenic mice 65

22. Knockout of ObRb in MPCs in vivo with Col3.6-Cre results in increased in vitro mineralization 68

23. Knockout of ObRb in MPCs in vivo with Col3.6-Cre results in increased in vitro adipogenesis 69

24. Peripheral model of leptin action on MPCs and osteoblasts 76

25. Diagram of the mouse brain 83

26. Ectopic expression of Col2.3 and Col3.6 promoters in the brain 84

27. Co-localization of Col3.6 driven loxP recombination and leptin induced P-Stat3 in the hypothalamus 85

28. Co-localization of Col2.3 driven loxP recombination and leptin induced P-Stat3 in the hypothalamus 86

29. Leptin induces a P-Stat3 response in both control and $3.6^{Cre+F/F}$ mice 88

29a. Longitudinal food intake analysis of $3.6^{Cre-}$ and $3.6^{Cre+F/F}$ mice 89

30. Zoledronic acid and leptin induce synergistic IL-6 production 102

31. Leptin-induced IL-6 production is mediated by ObRb tyrosine 985 103

32. Zoledronic acid (ZA) inhibits SOCS3 protein accumulation in primary bone marrow macrophages 105

33. Zoledronic acid (ZA) inhibits Stat3 phosphorylation 106

34. Farnesyl intermediates rescue zoledronic acid (ZA) mediated inhibition of P-Stat3 and SOCS3 mRNA 107

35. Rescue of P-Stat3 and SOCS3 mRNA with FOH does not correct SOCS3 protein inhibition 108

36. Bisphosphonates decrease SOCS3 in human CD68+ macrophages and human ONJ biopsies 109

37. Theoretical model of zoledronic acid (ZA) regulation of SOCS3 114

38. Summary of leptin modulation of bone formation 123

## LIST OF TABLES

1. Correlation of leptin and bone mineral density in males _____ 12

2. Correlation of leptin and bone mineral density in females _____ 13

3. Femoral microCT analysis of LysM transgenic mice _____ 35

4. Serum chemistries of $3.6^{Cre-}$ and $3.6^{Cre+F/F}$ mice _____ 60

5. Micro computed tomography analysis of $2.3^{Cre-}$ and $2.3^{Cre+F/F}$ femurs at 12 weeks _ 64

6. Micro computed tomography analysis of $3.6^{Cre-}$ and $3.6^{Cre+F/F}$ femurs at 12 and 42 weeks_____ 66

7. Micro computed tomography analysis of $2.3^{Cre-}$ and germline knockout (KO) femurs at 12 weeks _____ 67

8. Patient information, condition, treatment, and SOCS3 percent staining density of human specimens _____ 110

## ABSTRACT

**Regulation of bone formation and pathology by local actions of leptin in the bone marrow**

**by**

**Erica L Scheller**

**Chair: Paul H Krebsbach**

Site-specific adipose content of the bone marrow has been noted since the inclusion of meat into the hominid diet, evidenced by marrow removal from ungulate limb bones, 2.6 million years ago. Association between marrow fat and bone metabolism has since been documented, however the mechanism for this relationship remains unknown. Leptin, a secreted adipocytokine, possesses the ability to regulate bone formation both centrally through the hypothalamus and peripherally though marrow cells such as the osteoblast. Until the recent generation of a mouse with loxP sites flanking exon17 of the signaling-competent leptin receptor (ObRb), the physiologic contribution of peripheral leptin signaling to bone formation could not be determined. Leptin has been shown to increase mineralization of primary bone marrow stromal precursor cells (MPCs) and osteoblasts *in vitro*. Leptin is also a potent regulator of pro-inflammatory macrophage cytokine output. We therefore examined the ability of leptin to modulate bone formation through the myeloid lineage, the osteoblast, and the MPC by generating mice with conditional deletion of ObRb using LysozymeM

(LysM), Col2.3, and Col3.6 promoters driving Cre recombinase respectively. Myeloid-specific deletion of ObRb resulted in a mild, gender-specific bone phenotype in 52 week old animals with decreases in trabecular parameters noted in females and increases in cortical values in males. This change mimics associations between circulating leptin and bone mineral density (BMD) observed in adult humans. Osteoblast ObRb deletion using Col2.3-Cre did not produce a discernable bone phenotype. However, conditional removal of ObRb with Col3.6-Cre on more primitive MPCs increased femoral length and trabecular and cortical femoral parameters at 12 and 52 weeks of age. Our results imply that at physiologic equilibrium, leptin regulation of mature osteoblast function is negligible, however, early modulation of MPCs may contribute to properties such as bone length and trabecular formation. In contrast, regulation of myeloid lineage cells such as macrophages may explain adult gender-specific differences in associations between circulating leptin and BMD. Further modulation of macrophage-associated leptin signaling by compounds such as amino-bisphosphonates may enhance the ability of leptin to contribute to bone formation as well as the pathogenesis of diseases such as osteonecrosis of the jaw.

# CHAPTER 1

# INTRODUCTION

## 1.1 Exploring the role of adipose in the bone marrow

Largely due to the use of marrow as a food source, it has long been recognized that bone marrow composition varies by site with the more red marrow being confined toward the middle of the animal and the yellow, or fatty, marrow existing toward the periphery. Indeed, the initial inclusion of meat into the hominid diet 2.6 million years ago was inferred due to evidence of bone marrow removal shown by impact fractures from stone tools on sections of ungulate limb bones (Krech, McNeill et al. 2004). We have since learned that the functions of the adult bone marrow include blood cell formation, or hematopoiesis, and maintenance of skeletal structure through precise regulation of bone turnover and metabolism. Though osteoblasts and osteoclasts are recognized as the primary mediators of bone turnover, it is now appreciated that over thirty distinct cell populations reside in close proximity to the bone lining cells (Metcalf 2007; Phinney and Prockop 2007). These include hematopoietic lineage cells, mesenchymal lineage cells such as adipocytes, blood vessels, and neural tissue. Each of these cell populations, alone or in combination, may possess the capacity to influence bone growth and regeneration. This dissertation will focus on the contribution of the adipocyte to bone metabolism and pathology in the context of the secreted adipocytokine leptin.

Site specific differences in marrow adipose content are best illustrated in the vertebral column of rodents where marrow fat content increases as one progresses toward the tail (Figure 1). This initial observation of the bone marrow adipose transition in the caudal vertebrae of rats was made by Ranvier in Paris in 1889 (Ranvier 1889; Huggins and Blocksom Jr 1936). In addition to site-specific differences in marrow content, the number of fat cells present in the skeleton varies depending on age of the host, obesity, exogenous treatment, or disease state. For example, irradiation of the bone at a dose designed to prepare the host for a bone marrow transplant results in a transient filling of the bone cavity with adipose tissue for one to two weeks (Naveiras, Nardi et al. 2009). Alternatively, inhibition of expression of secreted adipocytokines such as leptin results in a robust accumulation of marrow fat in the distal femur (Hamrick, Pennington et al. 2004) (Figure 2). Though the presence of marrow fat appears to be tightly controlled, we do not yet understand its role or if the segregation of red and yellow marrow has any significance.

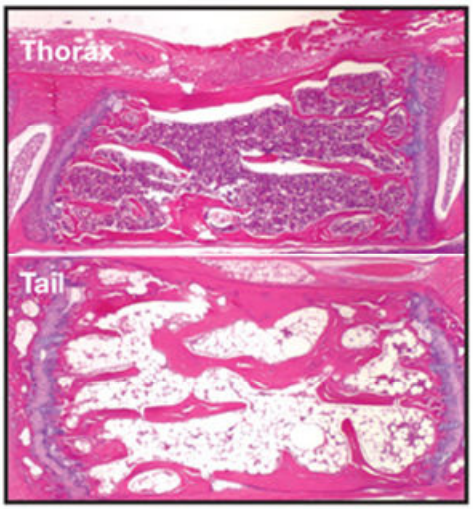


**Figure 1.** Bone marrow adipose transition from thoracic to caudal vertebrae in mouse. Credit: Reprinted by permission from Macmillan Publishers Ltd: Nature (Naveiras, Nardi et al. 2009), ©2009

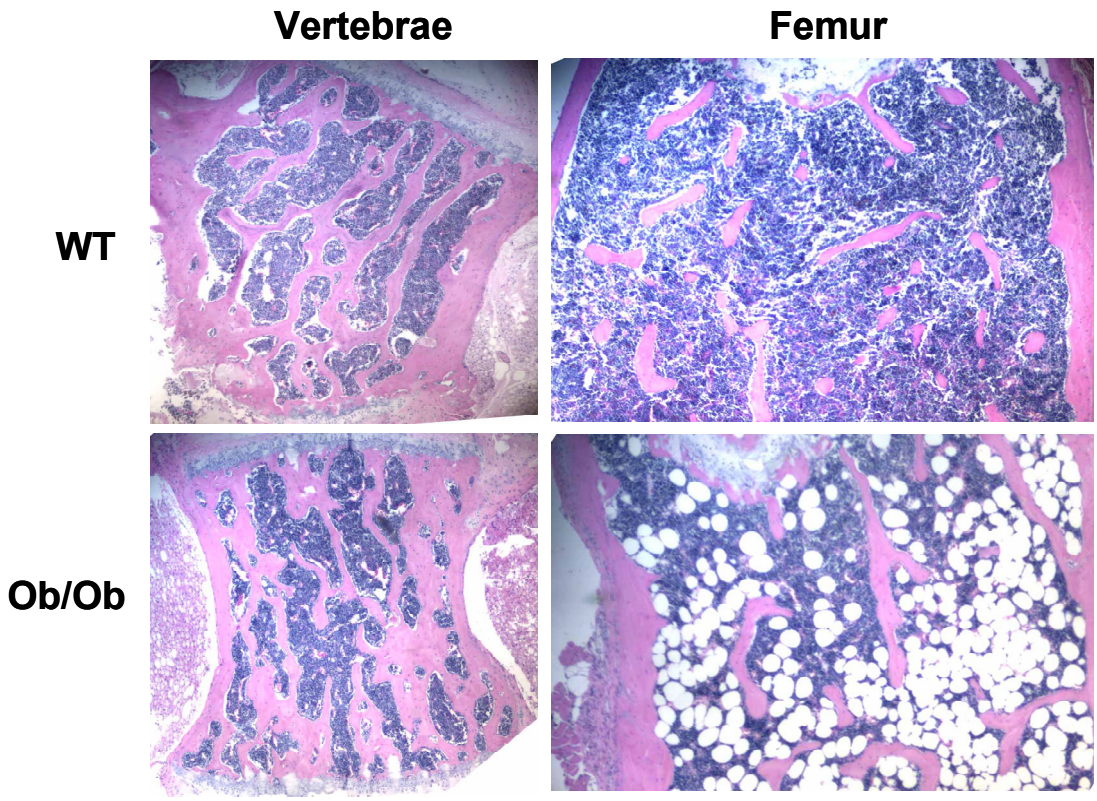


**Figure 2.** Leptin-deficient ob/ob mice have increased marrow fat in the distal femur but not in the lumbar vertebrae. 4x magnification. WT: wild type. Credit: E.L Scheller, unpublished data.

Since the formal description of marrow adipose site specificity in 1889 (Ranvier 1889), scientists have used this phenenomon to investigate its ability to regulate the two primary functions of the marrow, blood cell formation and bone turnover. It has recently been shown that increases in marrow adipose have the ability to decrease hematopoiesis (Naveiras, Nardi et al. 2009). In addition to the reported effects on blood cell formation, there is preliminary evidence to support that adipose tissue in the bone marrow may be a negative regulator of bone formation. For example, adipocytes co-cultured with osteoblasts or conditioned medium from marrow adipocytes can inhibit osteoblast proliferation and block alkaline phosphatase production *in vitro* (Benayahu, Zipori et al. 1993; Maurin, Chavassieux et al. 2000). Histopathological studies have demonstrated decreased osteoblast activity and osteoclast numbers in sites of high marrow fat such as

caudal vertebrae, distal tibia, proximal ulna, and distal radius when compared to sites of low marrow fat such as lumbar vertebrae, proximal tibia, proximal humerus, and pelvis (Wronski, Smith et al. 1981; Li, Shen et al. 1996). This is further supported by studies which demonstrate enhancement of trabecular bone formation after irradiation with suppression of marrow fat accumulation by a small molecule inhibitor of peroxisome proliferator-activated receptor-γ (PPAR-γ), a transcription factor required for adipocyte differentiation (Naveiras, Nardi et al. 2009). Despite initial evidence, the precise mechanism for adipose regulation of bone metabolism and the role of secreted adipocytokines such as leptin is currently unknown.

## 1.2 Leptin

### *Function of Leptin*

The discovery of leptin, a secreted 16 kDa alpha-helical adipocytokine, began in 1949 with the appearance of a spontaneous mutation in a non-inbred strain of mice at The Jackson Laboratory which produced offspring with severe obesity and sterility (Ingalls, Dickie et al. 1950). These studies were extended with a novel mutation in C57BL/Ks inbred stock in 1966 which resulted in severe metabolic disturbances resembling human diabetes mellitus and many similarities to the original mutant (Hummel, Dickie et al. 1966). These mutants were termed obese 'ob' and diabetes 'db', respectively. In 1978, following transfer of these mutants to a common inbred strain of mice, parabiosis experiments were performed which paired the circulation the mutant mice with one another as well as healthy donors (Coleman 1978). Pairing of db/db mice with control or ob/ob animals resulted in starvation and death, implying that a circulating factor

produced by db/db animals was severely restricting food intake of the paired mice (Coleman 1978). In contrast, pairing of ob/ob with control animals slowed weight gain and reduced food intake of the ob/ob mice suggesting that the control partner was producing a circulating factor responsible for regulation of satiety (Coleman 1978). In sum, these findings implied that the ob/ob mouse was unable to produce sufficient satiety factor to limit food intake while the db/db mouse produced the factor, but could not respond to it (Coleman 1978). Finally, forty-five years after the discovery of the obese mouse mutation, this circulating satiety factor was cloned and named leptin, derived from the greek 'leptos' meaning 'thin' (Zhang, Proenca et al. 1994). Leptin has structural similarities to IL-6, IL-12, IL-15, and G-CSF and is produced primarily by the adipocyte (Laharrague, Larrouy et al. 1998; La Cava and Matarese 2004). Leptin is recognized for its striking ability to regulate body mass and food intake. Human leptin deficiency, though rare, results in prominent obesity and hypogonadism (Ozata, Ozdemir et al. 1999). Additional findings in the human population include death during childhood due to infection, alterations in hormone function, and decreased bone mineral density in some individuals (Ozata, Ozdemir et al. 1999).

Serum leptin levels are strongly correlated to percent body fat and range from approximately 1 to 100ng/mL with an average of 8ng/mL in healthy controls and 31ng/mL in obese subjects (Considine, Sinha et al. 1996). Leptin signals through the hypothalamus and regulates food intake by producing a feeling of satiety after eating (Halaas, Gajiwala et al. 1995). There were high hopes for leptin as a weight loss drug and in 1994 Rockefeller University licensed the human protein to Amgen, Inc. for twenty

million dollars (Gura 1999). Subsequent human clinical trials were unfortunately disappointing with significant weight loss in only some of the human subjects and at only the highest doses tested (Heymsfield, Greenberg et al. 1999). These findings made it clear that obesity is not a result of insufficient leptin, but rather the inability of the body to respond to the hormone. Leptin resistance has since been demonstrated in control mice fed a high-fat diet (Lin, Thomas et al. 2000) and studies in rats have shown that obese animals require two to ten times more intracerebroventricular (ICV) leptin than controls for weight reduction (Cusin, Rohner-Jeanrenaud et al. 1996). We do not yet know if there is differential potential for leptin resistance to develop in central vs peripheral sites. Though leptin is not a generalized treatment for obesity due to central resistance, if peripheral resistance is less common leptin may be useful to treat peripheral imbalances including issues related to bone metabolism.

***Leptin Signaling***

Depending on its function, leptin has been classified as both a central neuroendocrine hormone and a peripherally acting cytokine. The leptin receptor exists in multiple isoforms which are splice variants of the originally identified leptin receptor gene (Tartaglia, Dembski et al. 1995). Only one of the isoforms retains the full signaling-competent cytoplasmic domain and is referred to as the long-form leptin receptor or ObRb (Lee, Proenca et al. 1996). The ObRa, ObRc, and ObRd isoforms are also membrane bound with an identical N-terminal segment to ObRb. They are highly expressed in most tissues and lack the concentrated expression pattern that ObRb demonstrates in the hypothalamus (Tartaglia, Dembski et al. 1995). The ObRe isoform,

termed the soluble of circulating leptin receptor, retains only the most proximal N-terminal leptin-binding segment (Lee, Proenca et al. 1996). The soluble receptor is highly expressed during early childhood and can reduce clearance of circulating leptin while both increasing its available pool or sequestering and inhibiting its actions depending on amount of molar excess ObRe available (Zastrow, Seidel et al. 2003).

The signaling form leptin receptor, ObRb, has several identified signaling moieties that include a Jak2 domain and two phosphotyrosines 985 and 1138 (Banks, Davis et al. 2000) (Figure 3). Activation of the receptor results in recruitment and activation of Jak2 which then phosphorylates and activates the cytoplasmic signaling phosphotyrosines. This conglomerate of signaling residues can then propagate signals through Stat3, SHP-2, mitogen-activated protein kinase (MAPK), phosphatidylinositol 3 kinase (PI3K), and AMP-activated protein kinase (AMPK) (Myers 2004) (Figure 3). Stat3 signaling is induced through phosphotyrosine 1138 and gene targeted mutation of this residue results in mice with hyperphagia and obesity (Banks, Davis et al. 2000; Bates, Stearns et al. 2003). Induction of P-Stat3 through Tyr1138 leads to mRNA transcription of suppressor of leptin signaling, SOCS3 (suppressor of cytokine signaling-3) (Bjorbaek, Elmquist et al. 1998). SOCS3, through its SH2 domain, can bind phosphorylated ObRb Tyr985 and Jak2 to inhibit Jak2 activity and block ObRb function (Banks, Davis et al. 2000). Accumulation of inhibitory SOCS3 has been implicated as a likely mechanism of leptin resistance and haplo-insufficiency for SOCS3 in mice protects against diet-induced obesity (Howard, Cave et al. 2004).

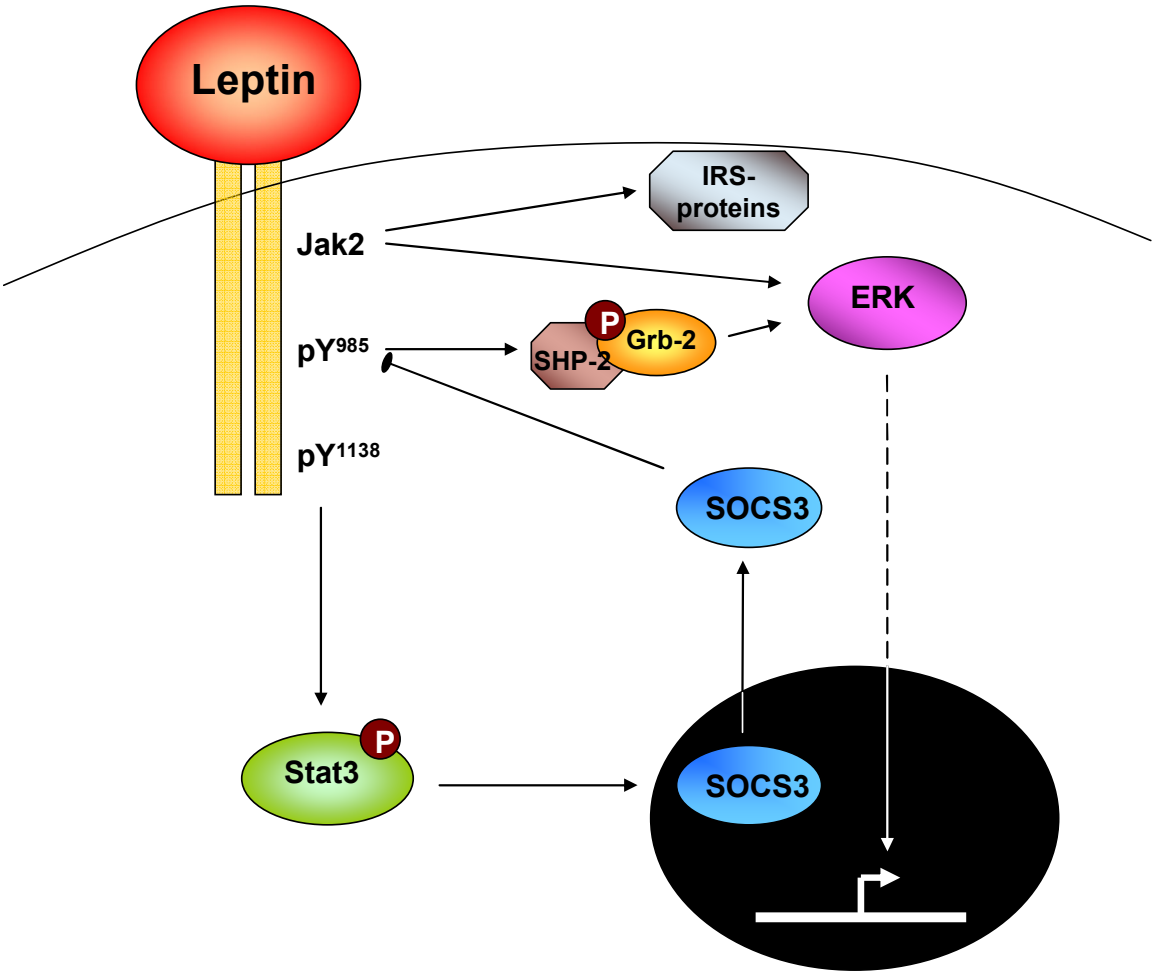


**Figure 3.** Leptin signaling diagram. Binding of leptin to its long-form receptor ObRb mediates signaling through receptor-based Jak2 and two signaling phosphotyrosines, Tyr985 (pY985) and Tyr1138 (pY1138). Jak2 can induce signals through insulin receptor substrate (IRS) proteins and extracellular signal related kinase (ERK). Phosphorylation of Tyr985 allows interaction with SH2-containing phosphatase 2 (SHP-2) and further signal perpetuation via growth receptor bound 2 (Grb-2). Tyr1138 induces phosphorylation of signal transducer and activation of transcription 3 (Stat3) and subsequent induction of suppressor of cytokine signaling 3 (SOCS3). SOCS3, through its SH2 domain, negatively interacts with Tyr985 to inhibit perpetuation of leptin-induced signals. Credit: Adapted from (Myers 2004).

Similar to the ability of SOCS3 to bind ObRb Tyr985 through its SH2 domain, SH2-containing phosphatase 2 (SHP-2) can also inhibit Tyr1138-mediated Stat3 activation while simultaneously activating MAP kinase (Banks, Davis et al. 2000). This can then activate extracellular signal-related kinase (Erk) and c-Fos (Morikawa, Ueyama et al.

2004). Phosphorylation of SHP-2 can also recruit growth receptor bound 2 (Grb-2) and link to small GTPases such as Ras and Raf (Zhang, Chen et al. 2005). Gene targeted mutation of Tyr985 dampens the ability of ObRb to receive auto-inhibitory negative feedback through SOCS3 and SHP-2 and results in lean female mice that have decreased feeding, increased leptin sensitivity and are protected from high-fat diet-induced obesity (Bjornholm, Munzberg et al. 2007).

The ability of ObRb to induce PI3K through Jak2-mediated phosphorylation of insulin-receptor substrate (IRS) and Grb-2 proteins links leptin and insulin signaling. Linkage of these pathways is implied by the fact that response to both leptin and insulin is impaired in most states of obesity. In mice, deficiency of IRS2 results in hyperphagia and obesity and PI3K inhibitors can inhibit the anorectic actions of leptin in rats further supporting the crosstalk of leptin and insulin signaling (Burks, Font de Mora et al. 2000; Niswender, Morton et al. 2001).

To summarize, ObRb signaling centrally through Stat3 via Tyr1138 has been shown to be responsible for mediating hyperphagia and obesity while Tyr985 is linked to auto-inhibitory negative feedback and is likely responsible for central leptin resistance. The function of these pathways exclusively in the hypothalamus fails to explain why targeted inhibition of ObRb in adipose tissue can result in peripheral fat accumulation (Huan, Li et al. 2003). This may be explained by direct leptin regulation of peripheral lipid metabolism through AMPK. AMPK activity is regulated by intracellular energy stores and can control fatty acid oxidation to generate ATP (Hardie and Carling 1997). Leptin

can stimulate AMPK phosphorylation in skeletal muscle both directly and centrally through the sympathetic nervous system to activate fatty acid oxidation (Minokoshi, Kim et al. 2002). There is also evidence that leptin inhibits differentiation of mesenchymal precursor cells to adipocytes *in vitro*, though the mechanism remains unknown (Thomas, Gori et al. 1999; Rhee, Sung et al. 2008; Scheller, Song et al. 2010). This action has also been observed *in vivo* as long-term 28-day treatment of type I diabetic mice inhibited accumulation of adipose in the bone marrow (Motyl and McCabe 2009).

***Leptin regulation of bone formation***

Given the rarity of complete leptin deficiency in the human population, the effects of leptin on bone formation have been derived mainly in the context of rodent models. In agreement with the decreased bone mineral density (BMD) observed in some leptin-deficient humans (Ozata, Ozdemir et al. 1999), many studies of leptin-replete humans have shown a positive correlation between serum leptin and BMD. The correlation between serum leptin and BMD has been published in over twenty-five reports containing information from over 10,000 patients (Table 1, 2). Even with the significant focus on this area of research, the data have yet to reveal a clear picture of leptin regulation of bone mass in humans. Interestingly, a dual pattern between males and females has emerged. Of the twelve studies on 5,659 male patients, six found a negative correlation between leptin and bone mass while only two found positive (Table 1) (Sato, Takeda et al. 2001; Thomas, Burguera et al. 2001; Yoneda, Maruyama et al. 2001; Ruhl and Everhart 2002; Morberg, Tetens et al. 2003; Roemmich, Clark et al. 2003; Sun, Jing et al. 2003; Zoico, Zamboni et al. 2003; Dennison, Syddall et al. 2004;

Chanprasertyothin, Piaseu et al. 2005; Lorentzon, Landin et al. 2006; Weiss, Barrett-Connor et al. 2006). Looking specifically at patient numbers, this equates to 80% of the male participants enrolled in a study with a negative correlation while only 2% were enrolled in one with positive correlation. Conversely, of the nineteen female studies, nine found a positive correlation (34% of study participants) while only two found negative correlation (4% of participants) (Table 2) (Ibanez, Potau et al. 2000; Martini, Valenti et al. 2001; Pasco, Henry et al. 2001; Thomas, Burguera et al. 2001; Yamauchi, Sugimoto et al. 2001; Yoneda, Maruyama et al. 2001; Ruhl and Everhart 2002; Roemmich, Clark et al. 2003; Roux, Arabi et al. 2003; Sahin, Polat et al. 2003; Ushiroyama, Ikeda et al. 2003; Zoico, Zamboni et al. 2003; Dennison, Syddall et al. 2004; Huang, Cheng et al. 2004; Chanprasertyothin, Piaseu et al. 2005; Yilmazi, Keles et al. 2005; Zhong, Wu et al. 2005; Weiss, Barrett-Connor et al. 2006; Oguz, Tapisiz et al. 2009). The percent of positive participants in the females may be deflated due to the large number of patients in one study (49% of total females) which found no correlation between leptin and bone mass (Ruhl and Everhart 2002). This study is, however, limited because dual-energy x-ray absorptiometry (DXA) was performed only on the femur and not the lumbar vertebrae or whole body, which means that a site-specific correlation may have been missed.

| Gender | Age | Number | Method | Reference | Correlation |
|---|---|---|---|---|---|
| Male | 43-70 | 26 | DXA - radius | Yoneda 2001 | Positive |
| Male | 68-75 | 92 | DXA - whole body, hip, femur | Zoico 2003 | Positive |
| Male | Youth 9-17 | 28 | DXA - whole body, femur, lumbar spine | Reommich 2003 | None |
| Male | 60-75 | 170 | DXA - lumbar spine, femur | Dennison 2004 | None |
| Male | 45-92 | 498 | DXA - hip, lumbar spine, radius | Weiss 2006 | None |
| Male | 23-90 | 343 | DXA - hip, lumbar spine, radius | Thomas 2001 | None |
| Male | 21-73 | 221 | SPA - right calcaneus (heel) | Sato 2001 | Negative |
| Male | 20+ | 2761 | DXA - femur | Ruhl 2002 | Negative |
| Male | 18-66 | 50 | DXA - whole body | Sun 2003 | Negative |
| Male | Avg 50 | 327 | DXA - whole body | Morberg 2003 | Negative |
| Male | 20-80 | 75 | DXA - lumbar spine, femur | Chanprasertyothin 2005 | Negative |
| Male | 18-20 | 1068 | DXA - lumbar spine, femur, whole body | Lorentzon 2006 | Negative |

**Table 1.** Correlation of leptin and bone mineral density in males. A summary of published manuscripts investigating the ability of circulating leptin concentration to correlate with bone mineral density. Correlations reported are the final values from the study and most have been normalized to factors such as body mass index and age.

| Gender | Age | Number | Method | Reference | Correlation |
|---|---|---|---|---|---|
| Female | 34-93 | 165 | DXA - hip, lumbar spine, radius | Thomas 2001 | Positive |
| Female | 48-78 | 139 | DXA - femur, lumbar spine, whole body | Yamauchi 2001 | Positive |
| Female | 68-75 | 171 | DXA - whole body, hip, femur | Zoico 2003 | Positive |
| Female | 45-92 | 411 | DXA - hip, lumbar spine, radius | Weiss 2006 | Positive |
| Female | Avg 51 | 122 | DXA - lumbar spine, femur | Oguz 2009 | Positive |
| Female | 21-54 | 137 | DXA - hip, lumbar spine, radius | Thomas 2001 | Positive |
| Female | 20-80 | 676 | DXA - lumbar spine, femur, whole body | Zhong 2005 | Positive |
| Female | Youth 5-14 | 52 | DXA - lumbar spine | Ibanez 2000 | Positive |
| Female | 20-91 | 214 | DXA - whole body, lumbar spine, femur | Pasco 2001 | Positive |
| Female | 39-82 | 123 | DXA - whole body | Martini 2001 | None |
| Female | 43-68 | 25 | DXA - radial bone | Yoneda 2001 | None |
| Female | 55+ | 1148 | DXA - femur | Ruhl 2002 | None |
| Female | 45-65 | 100 | DXA - lumbar spine, femur | Sahin 2003 | None |
| Female | Avg 54 | 121 | DXA - hip, lumbar spine | Roux 2003 | None |
| Female | 60-75 | 132 | DXA - lumbar spine, femur | Dennison 2004 | None |
| Female | 20-80 | 63 | DXA - lumbar spine, femur | Chanprasertyothin 2005 | None |
| Female | Avg 53 | 90 | DXA - lumbar spine, femur | Yilmazi 2005 | None |
| Female | 20-55 | 1906 | DXA - femur | Ruhl 2002 | None |
| Female | Youth 9-17 | 31 | DXA - whole body, femur, lumbar spine | Reommich 2003 | None |
| Female | Youth 10-19 | 105 | DXA - whole body | Huang 2004 | None |
| Female | 47-58 | 215 | DXA - lumbar spine | Ushiroyama 2003 | Negative |
| Female | 20-80 | 51 | DXA - lumbar spine, femur | Chanprasertyothin 2005 | Negative |

**Table 2.** Correlation of leptin and bone mineral density in females. A summary of published manuscripts investigating the ability of circulating leptin concentration to correlate with bone mineral density. Correlations reported are the final values from the study and most have been normalized to factors such as body mass index and age.

In leptin signaling deficient mice, two unique bone changes are observed with contrasting phenotypes in the limbs and spine (Hamrick, Pennington et al. 2004). The leptin deficient mouse, known as ob/ob, contains a nonsense mutation in codon 105 of the 16 kDa leptin transcript (Zhang, Proenca et al. 1994; MacDougald, Hwang et al. 1995). The leptin protein, expressed predominantly in adipose tissue of normal mice, is missing from homozygous mutant mice. The second model, known as db/db, is a leptin-receptor mutant mouse with a spontaneous autosomal recessive mutation that was discovered at The Jackson Laboratory, Bar Harbor, ME in 1966 (Hummel, Dickie et al. 1966). A G-to-T transversion in this allele created a donor splice site that causes abnormal splicing and a 106 nucleotide insertion in the transcript, leading to premature termination of the cytoplasmic domain of the long-form leptin receptor (ObRb) and loss of its signal transducing function (Lee, Proenca et al. 1996). Both mutant mice display a phenotype of uncontrolled eating and rapid weight gain. They also exhibit hyperphagia, glucose intolerance, elevated plasma insulin, subfertility, and impaired wound healing (Charlton 1984). Interestingly, leptin-deficient mice have significantly shorter femora, lower femoral bone mineral content (BMC), BMD, cortical thickness, and trabecular bone volume when compared to lean mice (Kawashima and Castro 1981; Steppan, Crawford et al. 2000; Hamrick, Pennington et al. 2004). However, these same mice have significantly increased vertebral length, lumbar BMC, lumbar BMD, and trabecular bone volume when compared to lean controls (Hamrick, Pennington et al. 2004) (Figure 4, Figure 5).

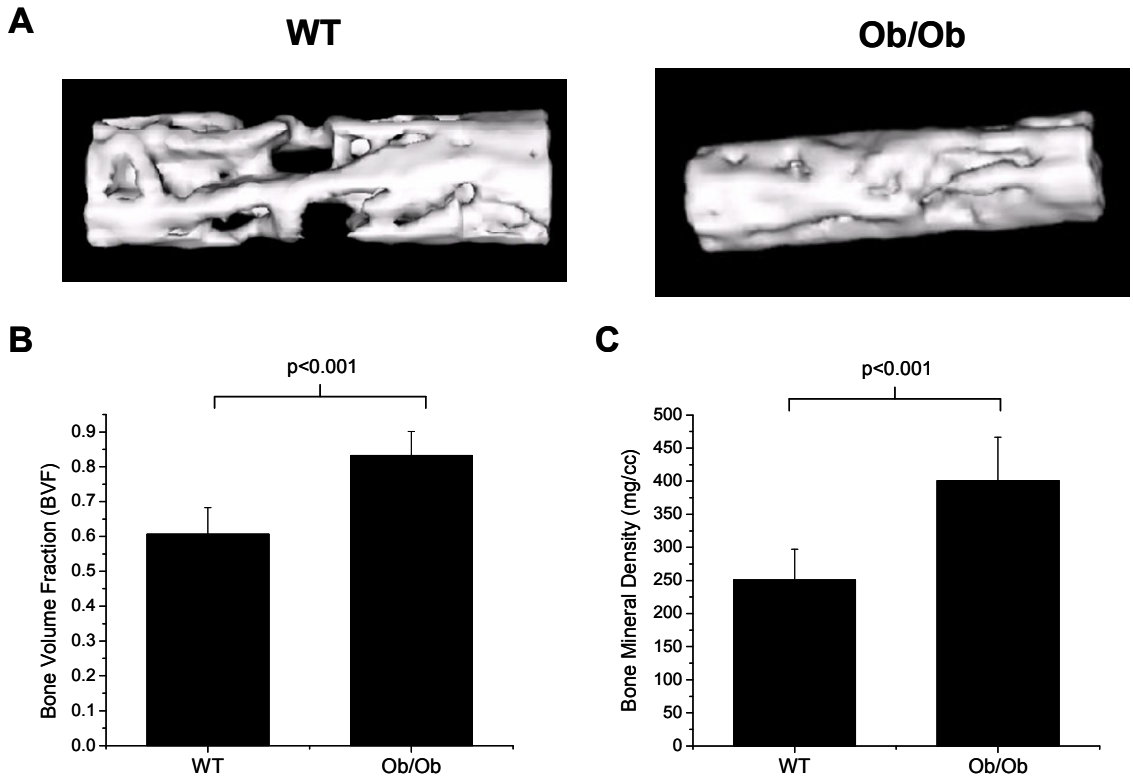


**Figure 4.** Leptin-deficient ob/ob mice have increased lumbar vertebral trabecular bone parameters. **(A)** L2 vertebrae were imaged with microCT and a core sample taken through the vertebral body, excluding the cortical bone, for analysis. **(B,C)** Trabecular bone volume fraction (%) and bone mineral density (mg/cc) were significantly higher in ob/ob mice when compared to controls. N=8 vertebrae. WT: wild type. Credit: E.L Scheller, unpublished data.

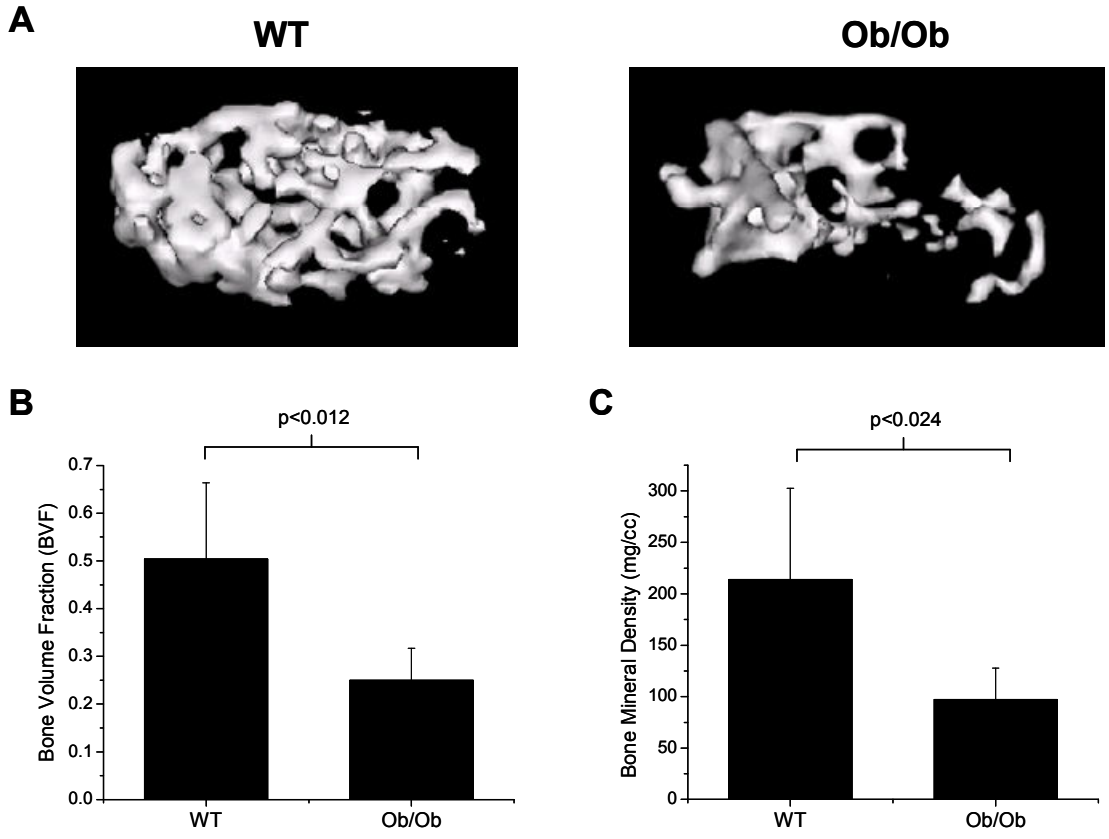


**Figure 5.** Leptin-deficient ob/ob mice have decreased distal femoral trabecular bone parameters. **(A)** Femurs were imaged with microCT and a sample taken at the distal femur, excluding the cortical bone and primary spongiosa, for analysis. **(B,C)** Trabecular bone volume fraction (%) and bone mineral density (mg/cc) were significantly lower in ob/ob mice when compared to controls. N=5 femurs. WT: wild type. Credit: E.L Scheller, unpublished data.

The phenotypic differences between the vertebral and long bone compartments of leptin transgenic mice have not yet been explained. *In vivo* studies have highlighted the importance of leptin administration modes and bone type analysis in determining the effects of leptin on bone mass. For example, intracerebroventricular (ICV) infusion of 8ng/hr leptin with subsequent analysis of vertebrae bone mass in 4 to 6 month old mice shows a 15 to 50% decrease in trabecular volume after twenty-eight days (Ducy, Amling et al. 2000; Takeda, Elefteriou et al. 2002). However, subcutaneous delivery of 10μg/day leptin in 15 week old leptin-deficient ob/ob mice for fourteen days results in greater than 30% increase in fluorochrome-labeled tibial endosteal surface (Steppan, Crawford et al. 2000; Hamrick, Della-Fera et al. 2005). Similarly, IP injection of 50μg/day leptin to 4 wk old ob/ob mice for 21 days produces a 6% increase in femoral length and an 84.2% increase in distal femoral trabecular mineral content when compared to controls (Steppan, Crawford et al. 2000). It is important to note that studies evaluating bone loss after leptin administration focus on the vertebrae while those focused on bone gain use long bone models. This dichotomy highlights the need for further investigation to definitively define the role of leptin in regulation of peripheral bone metabolism.

There are a few important points to consider when analyzing differences in the current literature. First, physiologic concentrations of circulating leptin average 8ng/mL in both mouse and human and rarely exceed 40ng/mL, even in states of high leptin production such as obesity (Hassink, Sheslow et al. 1996; Ahren, Mansson et al. 1997). It is possible that local levels of leptin adjacent to adipocytes in the bone marrow can significantly exceed this threshold. However, when considering serum concentrations only, in all but

one study highlighted above, stimulation was performed with leptin concentrations far exceeding physiologic levels. Second, the reported circulating half-life of recombinant leptin is only thirty minutes to three hours (Chehab 1997). Thus, continuous administration vs bolus injection could make a large difference in the actual circulating leptin concentration. Finally, leptin is a known mitogen that has even been classified as a growth factor in some circumstances (Hu, Juneja et al. 2002). Thus, administration of leptin to immature four week old mice may promote expansion of the growth plate through a mechanism entirely different than that required for later regulation of adult bone remodeling. A thorough understanding of these limitations is necessary to design experiments that directly relate to physiologic regulation of post-developmental bone mass.

***Ability of leptin to regulate peripheral cells***

Two possible mechanisms of leptin regulation of bone formation have been described. ICV leptin injection can increase sympathetic nerve activity when binding to its cognate receptors in the hypothalamus (Dunbar, Hu et al. 1997). This central regulation of sympathetic neural output can then alter osteoblast and osteoclast function and result in decreased bone mass (Ducy, Amling et al. 2000). The ability of leptin to directly regulate peripheral cells without a hypothalamic intermediate has been debated, but has become increasingly accepted as the presence of the signaling-competent leptin receptor (ObRb) has been reported on many cell types including mesenchymal stem cells, osteoblasts, skeletal muscle, adrenal glands, kidney, adipocytes, immune cells, liver, and pancreatic beta-cells (Emilsson, Liu et al. 1997; Hoggard, Mercer et al. 1997; Lollmann, Gruninger

et al. 1997; Kielar, Clark et al. 1998; Lord, Matarese et al. 1998; Thomas, Gori et al. 1999; Hess, Pino et al. 2005). Immunohistochemical staining for green fluorescent protein (GFP) of femurs from mice with enhanced-GFP (EGFP) linked to ObRb expression (Leinninger, Jo et al. 2009) reveals putative ObRb expressing cells including adipocytes, lymphocytes, and some bone lining cells (Figure 6, Figure 7).

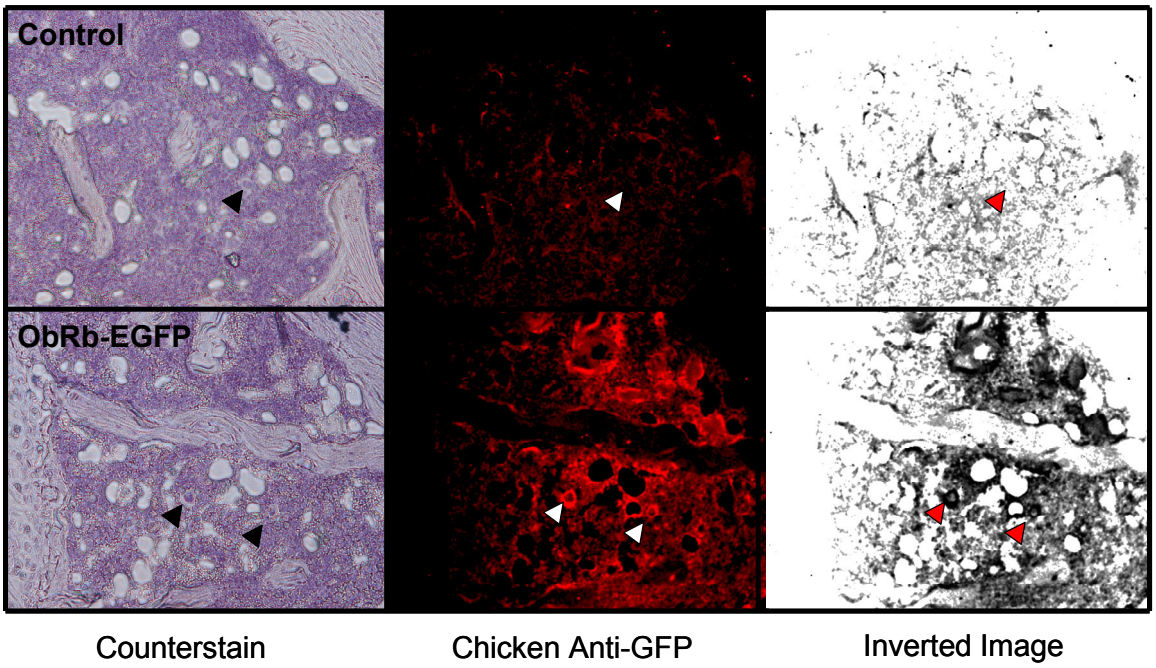


**Figure 6.** Immunohistochemistry for GFP of mice with ObRb-linked EGFP expression compared to control GFP negative mice. Left-most panel displays hematoxilyn counterstain image. Presence of GFP was determined with chicken anti-GFP primary antibody, followed by goat-anti chicken Cy3 secondary antibody. Center image reveals Cy3 positive areas. To aid in visualization, images were inverted and changed to black and white in Adobe Photoshop CS3 (right-most panel). Arrows highlight lymphocytes within the marrow. 10x magnification. EGFP: enhanced green fluorescent protein. GFP: green fluorescent protein. Credit: E.L Scheller, unpublished data.

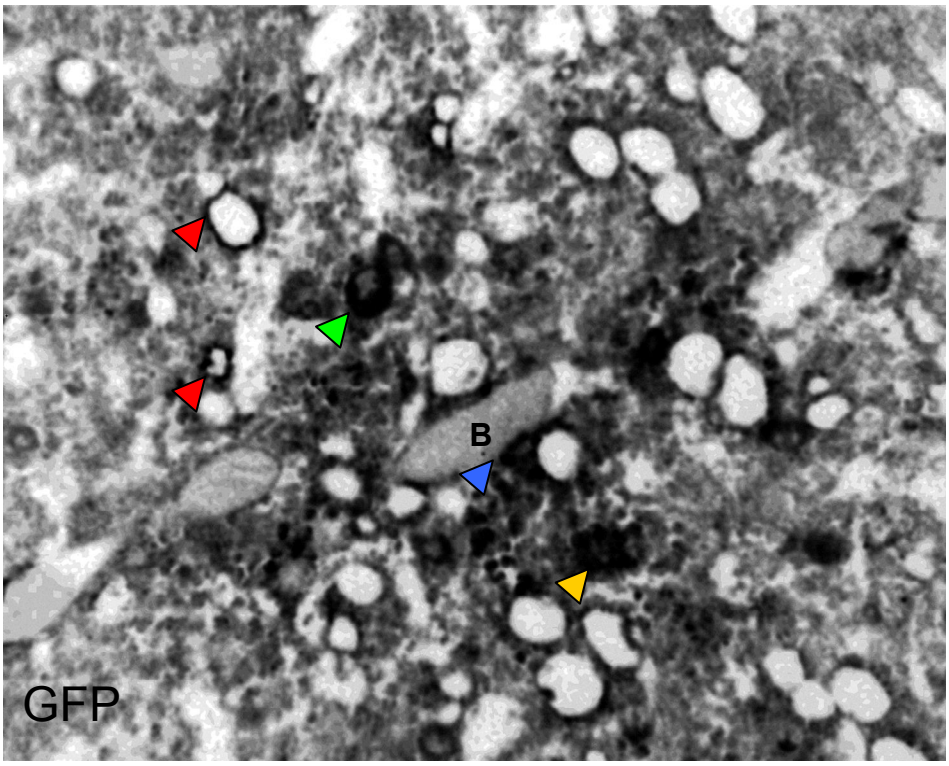


**Figure 7.** GFP immunohistochemistry of mice with ObRb-linked EGFP expression reveals suspected ObRb expressing cells *in vivo*. Image prepared as detailed in previous figure. Red arrows: adipocytes; Green arrow: lymphocyte; Blue arrow: bone lining cells; Yellow arrow: unknown positive cells; B: bone. Credit: E.L Scheller, unpublished data.

The physiologic relevance of peripheral leptin modulation of bone formation is currently unknown but preliminary *in vitro* evidence suggests that leptin has the ability to regulate bone forming cells such as the bone marrow stromal cell (BMSC) and the osteoblast. Leptin can enhance differentiation of human clonal BMSCs (hMS2-12) to osteoblasts as shown by increases in mineralization, alkaline phosphatase, and osteocalcin while inhibiting differentiation toward adipocytes (Thomas, Gori et al. 1999). Similarly, recombinant leptin stimulation of human primary BMSCs *in vitro* has been shown to promote osteogenic differentiation and partly inhibit adipogenic differentiation at 0.6 and 1.5µg/mL concentrations (Chang, Shih et al. 2006). Treatment of human iliac crest osteoblasts with lower concentrations of 100ng/mL leptin initially inhibited mineralization after two weeks *in vitro*, however, continued culture for 4-5 weeks

enhanced calcified nodule production (Reseland, Syversen et al. 2001; Gordeladze, Drevon et al. 2002). It has even been suggested that leptin is produced by primary human osteoblasts directly, though expression was not found in commercially available cells (Reseland, Syversen et al. 2001). However, unlike with human cells, similar studies with primary BMSCs isolated from C57BL/6J mice have failed to demonstrate any effects with 1.2μg/mL leptin stimulation of established cultures for 21 days (Ducy, Amling et al. 2000). We found similar negative results with BMSCs from control, ob/ob, and db/db mice after treatment with 100ng/mL leptin for fourteen days (Scheller, Song et al. 2010).

Though this dissertation will focus mainly on the ability of leptin to regulate mesenchymal lineages and macrophages, it should be noted that leptin may also be able to influence osteoclast activity. The nature of this influence is currently inconclusive. Histologically, ob/ob and db/db mice have a two-fold increase in osteoclast number when compared to controls (Ducy, Amling et al. 2000). However, the excretion of urinary deoxypyridinoline crosslink, a biochemical marker of bone resorption, was not impaired in these animals (Ducy, Amling et al. 2000). Conversely, leptin deficient rats have increased osteoclast surface, but no increase in numbers (Tamasi, Arey et al. 2003). Isolation of primary bone marrow osteoclast progenitors from leptin-deficient mice shows no deficiency in osteoclast differentiation or in their ability to form resorption lacunae on dentin (Ducy, Amling et al. 2000). Other *in vitro* studies show that leptin partially inhibits osteoclastogenesis at $10^{-11}$M in primary mouse marrow cultures but does not affect bone resorption of mature osteoclasts (Cornish, Callon et al. 2002). The scattered nature of the current published data are inconclusive as to the effects of leptin

on osteoclast formation and activity. However, this may be linked to leptin actions on the macrophage population since they share a common myeloid progenitor.

Monocytes and macrophages are produced in the bone marrow from hematopoietic stem cells and enter and exit this site through the vasculature. While the macrophage has long been appreciated as a key component of the immune system, an essential role for macrophages in bone homeostasis was only recently confirmed when induced depletion of macrophages in a mouse model ablated the mature osteoblast bone-forming surface (Chang, Raggatt et al. 2008). In addition to regulation of osteogenesis, macrophage-released cytokines are regulators of fibroblast and endothelial cell proliferation and studies have speculated that reduced macrophage infiltration may, in part, be responsible for increased rates of healing of oral mucosa compared to dermal sites (Szpaderska, Zuckerman et al. 2003). Macrophages are acutely sensitive to changes in their surrounding microenvironment and can respond to *in vitro* leptin concentrations as low as 1ng/mL, well under physiologic range (Maingrette and Renier 2003). Leptin is a potent monocyte/macrophage chemoattractant (Gruen, Hao et al. 2007) and plays a significant role in the regulation of pro-inflammatory immune responses (Loffreda, Yang et al. 1998; La Cava and Matarese 2004). Of note, leptin binding to macrophages has been shown to enhance secretion of the pro-inflammatory cytokines TNF-α, IL-6, and IL-12 (Gainsford, Willson et al. 1996; Santos-Alvarez, Goberna et al. 1999; Zhao, Hou et al. 2005). Many studies have highlighted the ability of monocytes and macrophages to interact with BMSCs and BMSCs have been implicated as negative regulators of monocyte differentiation (Jiang, Zhang et al. 2005). Furthermore, it has been demonstrated that the

macrophage can provide signals such as bone morphogenetic protein 2 (BMP-2) and TGF-β to promote osseous wound healing (Champagne, Takebe et al. 2002). Conversely, the absence of monocytes and macrophages as observed in the M-CSF deficient op/op mouse results in an osteopetrotic bone phenotype due to impaired osteoclastogenesis (Abboud, Woodruff et al. 2002). Since the macrophage can readily respond to sub-physiologic leptin levels with changes in cytokine production and migration, we hypothesized that regulation of macrophage activity by leptin may facilitate its actions as an osteoimmunologic intermediate and contribute to bone formation and metabolism.

### 1.3 Clinical Challenges

Osteoimmunology is defined as the interplay between the immune system and bone metabolism. This field was generated from the realization that during times of inflammation and stress, immune cells generated in the bone secrete factors that can profoundly affect bone regulation. For example, TNF-α and IL-4 can inhibit the differentiation of osteoblasts (Lewis, Liggitt et al. 1993; Gilbert, He et al. 2000; Ura, Morimoto et al. 2000). Conversely, conditioned media from inflammatory T cells can rapidly induce the differentiation of BMSCs to mature osteoblasts (Rifas, Arackal et al. 2003). This circle of creation and influence in the marrow cavity has important implications for the study of inflammation-linked bone disorders including osteoporosis, cancer metastasis to the bone, arthritis, osteomyelitis, periodontal disease, and osteonecrosis of the jaw. In addition to the contribution of osteoimmunology to bone disorders, it also plays a significant role in our ability to regenerate lost osseous tissues in

the presence of infection and inflammation. Understanding the ability of endogenous cytokines such as leptin to regulate bone formation directly or through an immunologic intermediate such as the macrophage will contribute to our ability to both regenerate tissues and to treat disease.

### 1.4 Summary

Accumulation of peripheral adipose tissue has significant consequences including increased risk for vascular disease, type 2 diabetes, cancer (endometrial, breast, and colon), high blood pressure, stroke, liver and gallbladder disease, sleep apnea, osteoarthritis, and even bisphosphonate-induced ONJ (CDC 1998; Wessel, Dodson et al. 2008). Peripheral adiposity or body mass index (BMI) has also been repeatedly linked to changes in bone mass. Despite recognition that, like the body, the bone marrow can also vary widely in degree of adiposity, we do not yet understand the ramifications of this tightly controlled presence of adipocytes. For example, osteoporosis has been linked to a dense infiltration of marrow by adipocytes (Burkhardt, Kettner et al. 1987). However, it is unclear if this infiltration is causal to the disease or rather an attempted protective response by the body.

Leptin is a potent adipocyte secretory product that can act both in a central neuroendocrine and a peripheral cytokine-like manner to regulate bone mass. The ability of leptin to act peripherally is controversial but is supported by positive associations between circulating leptin and BMD observed in human studies that can not be explained by negative central regulation (Table 1,Table 2). The majority of current research has

focused on the ability of leptin to regulate osteoblast function and mesenchymal stem cell differentiation *in vitro*. These studies have used concentrations of leptin well above physiologic norms and have failed to address the physiologic relevance of leptin actions on these cells. In addition, though leptin has been purported as a potent regulator of macrophage pro-inflammatory cytokine production, this ability has never been studied in the context of bone metabolism. In this body of work we will examine the physiologic relevance of leptin actions on bone formation through a macrophage osteoimmunologic intermediate, the osteoblast, and the mesenchymal precursor cell (Figure 8). We will also explore the relevance of these findings to a pathologic condition, osteonecrosis of the jaw.

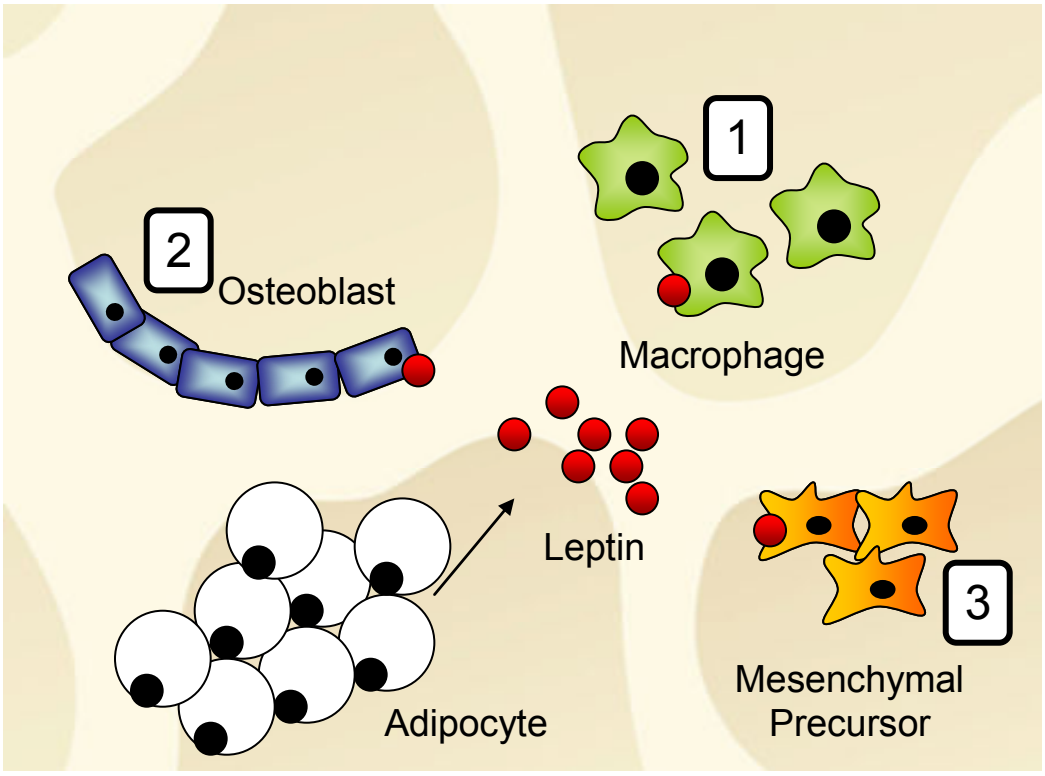


**Figure 8.** Summary of research direction. This dissertation will investigate the physiologic ability of leptin, an adipocytokine, to regulate bone formation though (1) a macrophage osteoimmunologic intermediate, (2) the osteoblast, and (3) the mesenchymal precursor cell.

# CHAPTER 2

# A ROLE FOR THE MYELOID LINEAGE IN LEPTIN-REGULATED BONE METABOLISM

## 2.1 Summary

Leptin influences bone formation centrally through the hypothalamus or peripherally by acting on osteoblasts or their precursors. However, neither mechanism explains the divergent, gender-specific correlation between leptin and bone mineral density in humans. Although leptin is a potent regulator of pro-inflammatory immune responses, a potential role for leptin as an osteoimmunologic intermediate in bone metabolism has not been tested. Mice with myeloid-specific ablation of the long-form leptin receptor (ObRb) were generated using mice expressing cre-recombinase from the lysoszyme M promoter. At 12 weeks of age the conditional knockout mice did not display any appreciable phenotype. However, at 52 weeks two changes were noted. First, there was a mild increase in liver inflammation. Second, a gender-specific, divergent bone phenotype was observed. Female mice displayed a consistent trend toward decreased trabecular bone parameters including reductions in bone volume fraction, trabecular number, and bone mineral content. Conversely, male mice lacked trabecular changes, but had statistically significant increases in cortical bone volume, thickness, and bone mineral density with equivalent total cortical volume. Since the year 2000, over twenty-five studies on more than 10,000 patients have attempted to determine the correlation between leptin and bone mineral density. The results have revealed a gender-specific correlation between leptin

and bone mineral density similar to that observed in our LysM transgenic animals. We hypothesize and show initial evidence that regulation of myeloid lineage cells such as macrophages by leptin may facilitate their actions as an osteoimmunologic intermediate and contribute to leptin-regulated bone formation and metabolism.

## 2.2 Introduction

Leptin, a pro-inflammatory cytokine synthesized primarily by adipocytes, is a neuroendocrine regulator of appetite (Pelleymounter, Cullen et al. 1995), energy metabolism (Breslow, Min-Lee et al. 1999), immune function (La Cava and Matarese 2004), and bone mass (Ducy, Amling et al. 2000; Scheller, Song et al. 2010). Leptin is also a potent monocyte/macrophage chemoattractant (Gruen, Hao et al. 2007) and plays a role in the regulation of pro-inflammatory immune responses (Loffreda, Yang et al. 1998; La Cava and Matarese 2004). Leptin binding to macrophages enhances secretion of the pro-inflammatory cytokines TNF-α, IL-6, and IL-12 (Gainsford, Willson et al. 1996; Santos-Alvarez, Goberna et al. 1999; Zhao, Hou et al. 2005). Macrophages are acutely sensitive to changes in their surrounding microenvironment and respond to leptin concentrations as low as 1ng/mL *in vitro* (Maingrette and Renier 2003). Though there are many studies that correlate obesity with increases in systemic inflammation and circulating leptin (Considine, Sinha et al. 1996), the physiologic significance of leptin interactions with the myeloid lineage has not yet been determined.

Over twenty-five studies on more than 10,000 patients have attempted to determine the relationship between circulating leptin and bone mineral density (BMD) in humans. The

sum of the results, though varied, has revealed divergent patterns between males and females. While leptin often correlates positively with BMD in females, the opposite is noted in males (Table 1,Table 2) (Thomas, Burguera et al. 2001; Ruhl and Everhart 2002; Zhong, Wu et al. 2005; Lorentzon, Landin et al. 2006). Despite extensive analysis, the mechanism of peripheral leptin regulation of bone mass is not entirely understood. Though it is accepted that leptin may act through a central neuroendocrine relay to negatively modulate bone metabolism (Ducy, Amling et al. 2000), the appearance of leptin resistance with age or obesity may impair these effects. Alternatively, leptin may act directly on osteoblasts. However, studies that examine this activity *in vitro* consistently use leptin concentrations far exceeding physiologic norms and mice conditionally lacking osteoblastic ObRb fail to demonstrate a bone phenotype (Thomas, Gori et al. 1999; Chang, Shih et al. 2006; Shi, Yadav et al. 2008; Scheller, Song et al. 2010). Lastly, it has been shown that leptin may negatively regulate mesenchymal precursor cell differentiation to influence bone length and BMD (Scheller, Song et al. 2010). However, this would likely contribute more to bone formation during growth and healing and not general bone turnover. We lack an experimental model that can mimic the modest, divergent, gender-specific changes in BMD that have been noted in adult humans. Since the macrophage can readily respond to subphysiologic leptin levels with changes in cytokine production and migration, we hypothesize that regulation of macrophage activity by leptin may facilitate its actions as an osteoimmunologic intermediate and contribute to bone formation and metabolism. To test this hypothesis, we generated a conditional myeloid lineage leptin-receptor (ObRb) deficient mouse.

## 2.3 Materials and Methods

### *Conditionally Regulated ObRb Mice*

All procedures were approved by the University Committee on the Use and Care of Animals. LysM-Cre mice were obtained from Jackson Laboratory (Bar Harbor, Maine, USA Cat:004781) (Clausen, Burkhardt et al. 1999). Flox/Flox Jak2-ObRb mice were obtained from Dr. Martin Myers (University of Michigan) with permission of Dr. Streamson Chua (Columbia University) (McMinn, Liu et al. 2004). To generate LysM-Cre crossed with ObRb floxed/floxed ($^{F/F}$) mice, one LysM$^{Cre+F/-}$ male was bred with two LysM$^{Cre-F/F}$ females and pups were genotyped via PCR analysis of tail biopsy DNA as reported previously (McMinn, Liu et al. 2004). Analysis was performed on LysM$^{Cre-}$, LysM$^{Cre+F/-}$ and LysM$^{Cre+F/F}$ littermates. Recombination and deletion of the loxP flanked allele was determined using the three-primer system designed by McMinn et al (McMinn, Liu et al. 2004).

### *MicroCT*

Femurs were scanned in a vivaCT 40 μCT system (Scanco Medical, Switzerland) with an isotropic voxel size of 10.5μm (55 kVp, 145μA, 1000 projections per 180 degrees, 200 ms integration time) as described previously (Scheller, Song et al. 2010). Briefly, 2D transverse slices were reconstructed into 2048x2048 pixel matrices. Cortical bone parameters were measured by analyzing 50 slices (0.525mm) of the mid-diaphysis. Trabecular bone parameters were measured by analyzing 101 slices (1.06mm) of the distal metaphysis 0.105 mm proximal to the primary spongiosa in the marrow cavity to assure that only trabecular bone was analyzed. For both analyses, a Gaussian low-pass

filter was used (σ=0.8, support=1). Analysis groups: 12 week female LysM$^{Cre-}$ (N=6), LysM$^{Cre+F/F}$ (N=6); 52 week female LysM$^{Cre-}$ (N=7), LysM$^{Cre+F/F}$ (N=4); 52 week male LysM$^{Cre-}$ (N=6), LysM$^{Cre+F/F}$ (N=6). One of the male 52 week old LysM$^{Cre+F/F}$ samples was eliminated as an outlier because values were greater than two standard deviations from the mean.

***Statistics***

A two-tailed, homoscedastic t test was used to calculate differences between control and experimental groups. Values are reported as the mean $^{+}/_{-}$ the standard deviation. $P<0.050$ was considered statistically significant. $P<0.150$ was considered to represent a non-significant trend.

## 2.4 Results

***Generation of Myeloid lineage-specific leptin receptor knockout mice***

Mice with loxP sites flanking the ObRb Jak2 signaling component (McMinn, Liu et al. 2004) were bred with mice expressing Cre recombinase under the control of the Lysozyme M (LysM) promoter (Clausen, Burkhardt et al. 1999) to specifically eliminate ObRb function in myeloid lineage cells (LysM$^{Cre+F/F}$). DNA was isolated from tissues of 12 week old LysM$^{Cre+F/F}$ mice and used for PCR amplification to determine the extent of deletion of the floxed locus. DNA was also harvested from macrophages differentiated from primary bone marrow with 50ng/mL M-CSF for two days. Results revealed the highest level of deletion in cultured macrophages, whole bone marrow (WBM), tail, and spleen extracts (Figure 9). Low-level recombination was observed in all other tissues

except for the hypothalamus (Figure 9). Mice were phenotypically similar with exception of slight obesity observed in both the male heterozygote $LysM^{Cre+F/-}$ (14% increase, p=0.007) and homozygote $LysM^{Cre+F/F}$ (11% increase, p=0.062) mice at 50 weeks (Data Not Shown). No differences were noted in the mass of females from 3 to 52 weeks of age (Figure 9).

Because mice with complete ObRb knockout are known to have significant hepatomegaly (Menahan 1983), we quantified liver mass at necropsy. At 52 weeks, the $LysM^{Cre+F/F}$ female mice had an $11.3^{+}/_{-}0.9$% reduction in liver mass/body mass ratio (P=0.016) when compared to the $LysM^{Cre-}$ mice that was not present in the heterozygotes (Figure 10). Histological analysis revealed moderate steatohepatitis with microscopic features including hepatocyte ballooning, finely divided fat droplets in the hepatocyte cytoplasm, intracytoplasmic accumulations of Mallory hyaline, and inflammatory infiltrates consisting predominately of neutropils with some lymphocytes (Figure 10). Histological features of steatohepatitis were present in both the 12 month old $LysM^{Cre-}$ and $LysM^{Cre+F/F}$ mice, however, the presence of inflammatory islands of ten or more cells was significantly increased in the $LysM^{Cre+F/F}$ mice (Figure 10). No changes in spleen size were noted (Data Not Shown).

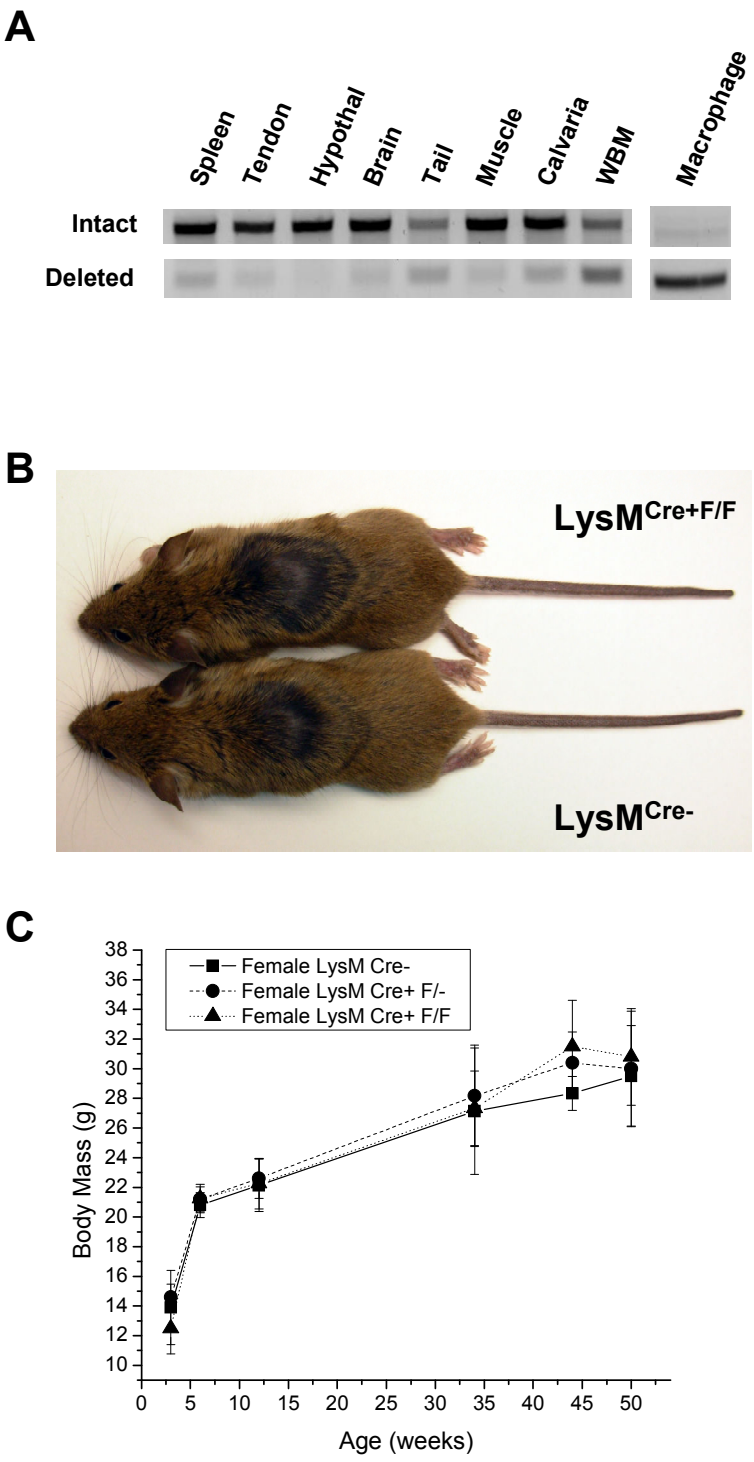


**Figure 9.** Generation of LysM$^{Cre+F/F}$ Mice. LysM-Cre mice were mated with mice with loxP sites flanking exon 17 of the long-form leptin receptor (ObRb) to generate myeloid-specific ObRb knockout mice. **(A)** Genomic DNA PCR of tissues from 12 week old animals or primary bone marrow macrophages cultured *in vitro* showing the intact (~646 base pairs) and deleted (~200 base pairs) bands, lanes cropped from the same gel. **(B)** Representative photo, female, 3 months old. **(C)** Body mass of transgenic female mice from 3 to 52 weeks. N=6-8. WBM: Whole Bone Marrow. Hypothal: hypothalamus. Credit: E.L. Scheller, unpublished data.

Because complete ObRb KO mice have altered femoral bone parameters (Hamrick, Pennington et al. 2004), femurs were harvested from mice at 12 and 52 weeks of age and cortical and trabecular bone parameters were analyzed with microCT. Statistically significant differences in bone parameters were not present at 12 weeks of age (Table 3) (Scheller, Song et al. 2010). At 52 weeks, females demonstrated a trend toward decreased trabecular bone volume fraction (-31%, p=0.105), trabecular number (-18%, p=0.081), and bone mineral content (-31%, p=136) (Table 3). This corresponded to an increase in trabecular spacing (+16%, p=0.129) (Table 3). These trends were not present in the males, however, increases in cortical parameters were observed including bone volume (+9.3%, p=0.036), cortical bone fraction (+9.0%, p=0.089), cortical thickness (+10.5%, p=0.038), BMC (+13.7%, p=0.006), and BMD (+4.0%, p<0.001), but total volume was unchanged (Table 3).

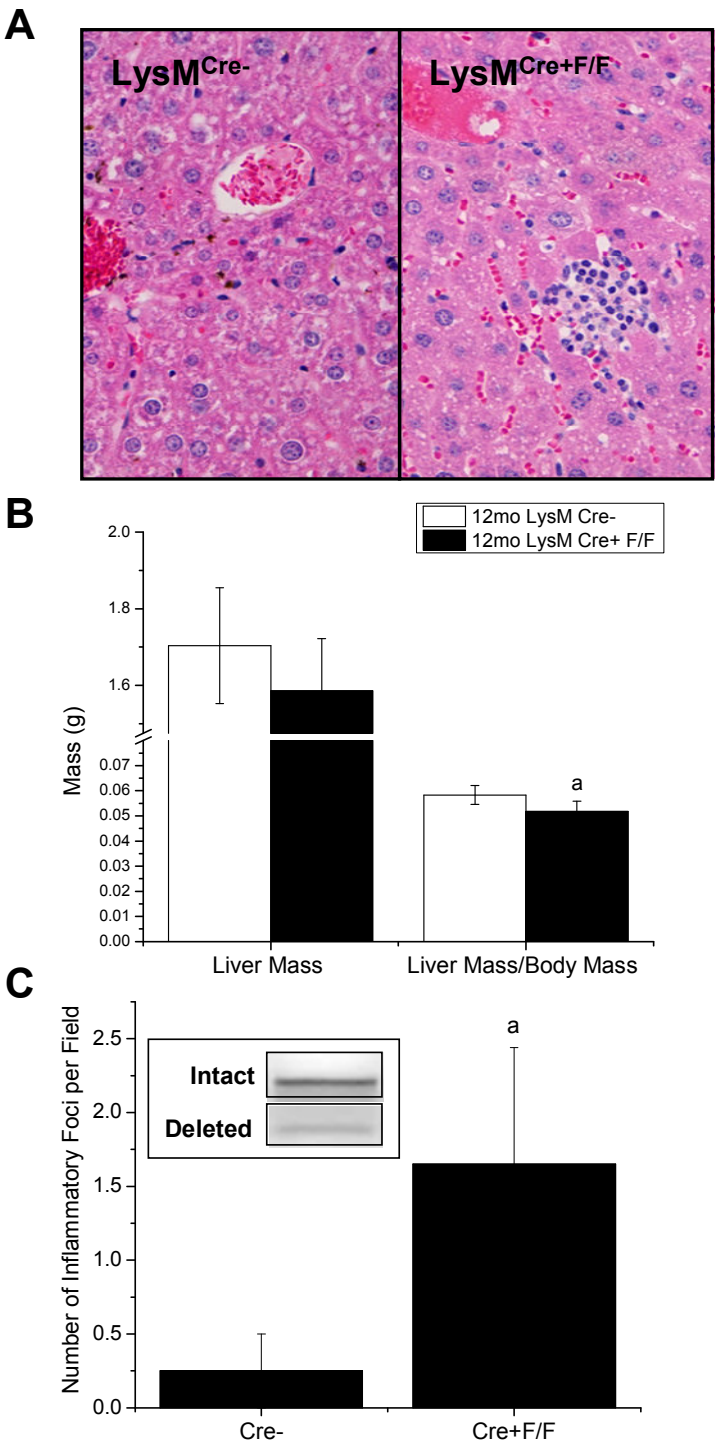


**Figure 10.** LysM$^{Cre+F/F}$ liver phenotype. **(A)** Liver histology. **(B)** 52 week old female liver mass and liver mass/body mass ratio (N=6-8). **(C)** Number of inflammatory islands per field (N=3 mice, 3 liver sections each, 10 fields/section). Inset contains genomic DNA PCR to check for Cre-lox recombination. Credit: E.L. Scheller, unpublished data.

| LysMCre+F/F % Change vs Cre- Control | | | | | | | | | |
|---|---|---|---|---|---|---|---|---|---|
| | 12 wk Female | | | 52 wk Female | | | 52 wk Male | | |
| **Trabecular** | **Control** | **LysM+** | **p value** | **Control** | **LysM+** | **p value** | **Control** | **LysM+** | **p value** |
| Bone Volume Fraction (%) | 24+/-3.9 | 25+/-5.0 | 0.581 | 6.9+/-1.9 | 4.8+/-1.9 | 0.105 | 7.4+/-1.3 | 7.7+/-3.1 | 0.842 |
| Tb. Number (1/mm) | 5.96+/-0.54 | 5.79+/-0.67 | 0.625 | 2.19+/-0.35 | 1.80+/-0.23 | 0.081 | 2.35+/-0.27 | 2.48+/-0.62 | 0.642 |
| Tb. Thickness (mm) | 0.061+/-0.002 | 0.060+/-0.005 | 0.759 | 0.063+/-0.007 | 0.063+/-0.006 | 0.982 | 0.058+/-0.007 | 0.058+/-0.007 | 0.879 |
| Tb. Spacing (mm) | 0.175+/-0.016 | 0.183+/-0.022 | 0.488 | 0.487+/-0.082 | 0.566+/-0.060 | 0.129 | 0.442+/-0.059 | 0.440+/-0.114 | 0.970 |
| BMC (mg HA) | 463+/-74 | 452+/-105 | 0.837 | 142+/-46 | 98+/-36 | 0.136 | 176+/-46 | 184+/-78 | 0.843 |

| **Cortical** | **Control** | **LysM+** | **p value** | **Control** | **LysM+** | **p value** | **Control** | **LysM+** | **p value** |
|---|---|---|---|---|---|---|---|---|---|
| Total Volume (mm^3) | 0.86+/-0.04 | 0.84+/-0.05 | 0.379 | 1.08+/-0.09 | 1.06+/-0.07 | 0.787 | 1.18+/-0.08 | 1.19+/-0.09 | 0.902 |
| Bone Volume (mm^3) | 0.408+/-0.010 | 0.398+/-0.036 | 0.512 | 0.509+/-0.047 | 0.512+/-0.021 | 0.900 | 0.538+/-0.046 | 0.588+/-0.020 | 0.036 |
| Cortical Bone Fraction (%) | 47.5+/-2.0 | 47.5+/-2.7 | 0.978 | 47.2+/-3.0 | 48.2+/-2.3 | 0.581 | 45.5+/-4.0% | 49.6+/-3.4 | 0.089 |
| Cortical Thickness (mm^3) | 0.201+/-0.006 | 0.199+/-0.015 | 0.769 | 0.222+/-0.016 | 0.225+/-0.007 | 0.684 | 0.219+/-0.020 | 0.242+/-0.013 | 0.038 |
| BMC (mg HA) | 480+/-14 | 472+/-46 | 0.682 | 627+/-64 | 638+/-33 | 0.758 | 656+/-57 | 746+/-25 | 0.006 |
| BMD (mg HA/ccm) | 1176+/-18 | 1186+/-34 | 0.561 | 1232+/-27 | 1236+/-29 | 0.778 | 1219+/-6 | 1268+/-17 | <0.001 |

**Table 3.** Femoral microCT analysis of LysM transgenic mice. No differences were noted in femoral cortical or trabecular parameters at 3 months of age. At 12 months, the $LysM^{Cre+F/F}$ females showed a trend toward decreased bone volume fraction and trabecular number. Conversely, the males had no noted changes in trabecular parameters, but had significant increases in cortical bone volume, bone mineral content (BMC) and bone mineral density (BMD). Female $LysM^{Cre-}$ N=7, $LysM^{Cre+F/F}$ N=4. Male $LysM^{Cre-}$ N=6, $LysM^{Cre+F/F}$ N=6. Credit: E.L. Scheller, unpublished data.

## 2.5 Discussion

Osteoimmunology is an emerging field of research that views regulation of bone metabolism within the context of immune function. While the macrophage has long been appreciated as a key component of the immune system, an essential role for macrophages in bone homeostasis was only recently confirmed when induced depletion of osteal tissue macrophages in a mouse model ablated the mature osteoblast bone-forming surface (Chang, Raggatt et al. 2008). In addition to the bone changes, we report the liver phenotype of the 52 week old $LysM^{Cre+F/F}$ animals as an interesting finding, though we do not yet understand its significance. The slight increase in liver inflammation observed in the conditionally regulated mice may indicate that leptin actions on myeloid lineage cells could regulate homing to the liver.

The trend toward decreased trabecular bone observed in the aged female but not the male $LysM^{Cre+F/F}$ mice and the increase in cortical bone mass in the male but not the female closely mimics the association between leptin and BMD observed in humans. For example, many studies cite a modest positive correlation between leptin and BMD in post-menopausal adult females (Thomas, Burguera et al. 2001; Zhong, Wu et al. 2005). Thus, removal of the leptin receptor should decrease bone parameters as was observed in our $LysM^{Cre+F/F}$ 52 week old females. Conversely, the negative association between circulating leptin and BMD in males would point toward increases in bone parameters after receptor ablation as was also noted in our animals. Though it is not yet possible to completely ascribe the effects of leptin on post-natal bone remodeling to the macrophage, this mouse model provides compelling evidence for the existence of a novel leptin-

responsive myeloid osteoimmunologic intermediate. This is also the first leptin transgenic mouse model to mimic the human condition with a divergent gender-specific phenotype. Based on our findings, we hypothesize that with age, leptin receptors on the myeloid lineage may play a role in leptin-regulated maintenance of bone mass.

### 2.6 Acknowledgments

Supported by R01 DE13835 (PHK/KDH), T32 DE07057 (ELS/PHK) and F30 DE019577 (ELS).

# CHAPTER 3

# LEPTIN FUNCTIONS PERIPHERALLY TO REGULATE DIFFERENTIATION OF MESENCHYMAL PROGENITOR CELLS

## 3.1 Summary

Leptin functions through a well-documented central neuroendocrine pathway to regulate bone mass. However, the ability of leptin to modulate bone mass through a peripheral mechanism has been debated due to conflicting *in vitro* results and lack of sufficient *in vivo* models. We utilized mice with loxP sites introduced into the long-form leptin receptor (ObRb) gene to determine how leptin regulates mesenchymal progenitor cell (MPC) differentiation and osteoblast function *in vitro* and *in vivo.* Rapid phosphorylation of Stat3 after leptin treatment of bone marrow stromal cells (BMSCs) from mice with conditional deletion of ObRb in macrophages ($LysM^{Cre+F/F}$) confirmed expression of functional leptin receptors by BMSCs. Adenovirus-Cre mediated disruption of ObRb in primary stromal cells decreased mineralization while increasing adipogenesis. In contrast, BMSCs harvested from leptin-signaling deficient ob/ob or db/db mice showed increased mineralization. To determine the physiologic relevance of these differences, mice with cell-specific deletion of ObRb in mesenchymal precursors ($3.6^{Cre+F/F}$) or osteoblasts ($2.3^{Cre+F/F}$) were generated. Though the $2.3^{Cre+F/F}$ mice were grossly normal, the $3.6^{Cre+F/F}$ mice displayed mild obesity that was not attributed to food intake. Femurs of $3.6^{Cre+F/F}$ animals showed a 58-61.9% increase in trabecular bone volume and a 65.5-74% increase in bone mineral density. Cortical volume and mineral content were also

increased 18-22%. Primary $3.6^{Cre+F/F}$ BMSCs recapitulated the high mineralization phenotype of ob/ob and db/db BMSCs. We conclude that leptin may have multiple peripheral roles depending on the differentiation state of MPC. Leptin (1) helps maintain MPCs in an undifferentiated state and (2) promotes mineralization of more differentiated osteoblasts.

### 3.2 Introduction

Leptin, named after the Greek '*leptos'* meaning 'thin', was discovered in 1994 during the analysis of a colony of spontaneously obese mice (Zhang, Proenca et al. 1994). This 16kDa cytokine has since been found to play a prominent role in regulation of energy metabolism and appetite (Pelleymounter, Cullen et al. 1995; Breslow, Min-Lee et al. 1999; Cohen, Zhao et al. 2001). Many secondary functions of leptin have also been uncovered (Myers 2004), including modulation of immune cell responses (La Cava and Matarese 2004) and maintenance of bone mass (Ducy, Amling et al. 2000; Steppan, Crawford et al. 2000; Hamrick, Della-Fera et al. 2005). The ability of leptin to regulate bone formation through peripheral mechanisms has been debated due to conflicting *in vitro* results and a lack of sufficient *in vivo* models. The challenge to study the peripheral effects of leptin with conditional regulated gene recombination (Cre-loxP) systems was proposed in 1998 (Friedman and Halaas 1998), but these experiments were not possible until the recent generation of a mouse model with loxP sites flanking the Jak2 signaling component of the long-form leptin receptor (ObRb) (McMinn, Liu et al. 2004). To help clarify the controversy of leptin's peripheral actions on bone through regulation of mesenchymal progenitor cell (MPC) differentiation and osteoblast function

we have used this model and generated three cell-specific knockouts of ObRb using LysM-Cre ('macrophage'), Col2.3-Cre ('osteoblast') and Col3.6-Cre ('MPC') mice.

Previous research demonstrates two mechanisms of leptin regulation of bone mass. First, elegant *in vivo* studies support the central hypothesis which states that binding of leptin to ObRb in the hypothalamus can stimulate bone loss by regulating osteoblast activity through the sympathetic nervous system (Ducy, Amling et al. 2000; Takeda, Elefteriou et al. 2002; Elefteriou, Ahn et al. 2005). Conversely, the peripheral hypothesis postulates that there are mechanisms through which local leptin can directly regulate bone formation by acting on cells in the bone marrow. The existence of such mechanisms has been explored by multiple groups who have compiled key pieces of evidence. For example, leptin receptors are expressed on the surface of human BMSCs (Hess, Pino et al. 2005) and recombinant leptin stimulation of human BMSCs *in vitro* has been shown to promote mineralization and partly inhibit adipogenic differentiation (Chang, Shih et al. 2006). It has further been demonstrated *in vitro* that BMSC fate decisions can be regulated by suppression of leptin expression after addition of adipogenic factors (Yang, Tsay et al. 2008). Lastly, *in vivo,* peripheral (subcutaneous or intra-peritoneal) delivery of supra-physiologic doses of leptin to leptin-deficient ob/ob mice resulted in a >30% increase in fluorochrome-labeled tibial endosteal surface and an 84.2% increase in distal femoral trabecular mineral content respectively (Steppan, Crawford et al. 2000; Hamrick, Della-Fera et al. 2005). Despite this evidence, the existence of physiologically relevant peripheral mechanisms is debated due to conflicting studies that have failed to demonstrate pro-osteogenic effects of leptin stimulation of primary mouse osteoblast

cultures (Ducy, Amling et al. 2000) and one *in vivo* publication with osteoblast-specific ObRb deletion that lacked significant differences in vertebral bone mass (Shi, Yadav et al. 2008). Though conflicting, these studies have laid the groundwork for a more in-depth examination of leptin's peripheral actions with additional delineation of effects on primitive MPCs and more differentiated osteoblast populations.

The true mesenchymal stem cell (MSC) is an elusive *in vivo* precursor to mesenchymal lineage cells such as osteoblasts, adipocytes, and chondrocytes. MSCs have been identified in tissues including bone marrow (Friedenstein, Deriglasova et al. 1974), adipose (Zuk, Zhu et al. 2001), and dental pulp (Gronthos, Mankani et al. 2000). Though many groups have focused on characterizing the MSC, specific cell surface markers have not been identified (Bianco, Riminucci et al. 2001; Gronthos, Franklin et al. 2001). Thus, our methods for *in vitro* isolation date back to the 1970s (Friedenstein, Deriglasova et al. 1974; Friedenstein, Gorskaja et al. 1976) and rely on the adherence of a subpopulation of cells to tissue culture plastic and subsequent passaging to enrich for MSCs (Aust, Devlin et al. 2004). *In vivo* the MSC is defined as a multipotent cell that undergoes self-renewal until stimulated to differentiate into a daughter lineage. Culturing these cells *in vitro* results in cells that are more differentiated and proliferative, yet not fully lineage committed. Thus, studies which disrupt gene expression *in vitro* may result in a phenotype that is different than effects found when the gene is deleted *in vivo*. In recognition of the limited knowledge of the 'true' MSC, this report will use the term mesenchymal progenitor cell (MPC) to refer to the *in vivo* precursor populations targeted

by Col3.6-Cre and bone marrow stromal cells (BMSCs) or adipose-derived stromal cells (ADSCs) to refer to MSCs that have been isolated and cultured *in vitro*.

Analysis of current models of leptin signaling deficiency such as the ob/ob mouse (leptin deficient) and the db/db mouse (ObRb deficient) are limited by secondary complications of diabetes and obesity. Mutant mice display a phenotype of uncontrolled eating and rapid weight gain. They also exhibit hyperphagia, glucose intolerance, elevated plasma insulin, subfertility, impaired wound healing, and both low (femoral) and high (vertebral) trabecular bone mass (Charlton 1984; Hamrick, Pennington et al. 2004). To circumvent these systemic complications we utilized a mouse model with loxP sites flanking exon 17 of the ObRb gene, deletion of this gene segment by Cre recombinase terminates receptor function (McMinn, Liu et al. 2004). This study was designed to critically evaluate the ability of leptin to modulate differentiation of MPCs and the function of their osteoblast progeny. We hypothesized that leptin exerts differential effects on lineage committed cells such as osteoblasts when compared to their more primitive MPC precursors. To clarify these differences we have used *in vitro* adenovirus Cre and *in vivo* Col2.3-Cre ('osteoblast') and Col3.6-Cre ('MPC') mediated recombination of ObRb to explore the inherent role of physiologic, circulating leptin in bone formation and maintenance.

## 3.3 Materials and Methods

### *Primary Cell Culture*

BMSCs were harvested as described previously (Krebsbach, Kuznetsov et al. 1997) with slight modification. Femora, tibiae, and humeri were dissected free of surrounding

muscle. Marrow was removed with phosphate buffered saline (PBS) and filtered through a 70μm cell filter. The marrow content of 6-9 bones was plated into a 75-$cm^2$ culture flask in BMSC growth medium (α-Modified Eagle's Medium (α-MEM; Invitrogen/Gibco), 10% fetal bovine serum (Gibco, Lot no.451459), 100U/ml penicillin, 100mg/ml streptomycin sulfate (Gibco Cat:15140), 100nm dexamethasone (Sigma Cat:D8893)). To harvest adipose-derived stromal cells (ADSCs) intra-abdominal and paralumbar fat pads were collected, washed with PBS, and minced. Minced adipose was incubated for one hour at 37°C in α-MEM + 0.2% Collagenase II (Gibco Cat:17101). ADSCs were pelleted at 1100rpm for 10 minutes at 4°C and plated at 6-8 million cells per 10cm plate in ADSC growth medium (Dulbecco's Modified Eagle Medium (DMEM, Invitrogen/Gibco), 10% fetal bovine serum (Gibco, Lot no.451459), 100U/ml penicillin, 100mg/ml streptomycin sulfate). Cells were cultured at 37°C in an atmosphere of 100% humidity and 5% $CO_2$. Colonies of adherent cells were formed by 11-14 days. The colonies were harvested and the sub-cultured cells were re-plated at 15,000 cells/$cm^2$.

***PCR***

RNA was harvested using Trizol reagent (Invitrogen Cat:15596) and 0.3 to 1μg of total RNA was processed using the SuperScript™ First-Strand RT-PCR kit (Invitrogen Cat:12371) to generate cDNA. Leptin receptor expression was analyzed as previously reported (Lamghari, Tavares et al. 2006). GAPDH primers were used as a loading control, GAPDH_F: TTCCAGTATGACTCCACTCACGGCAAAT; GAPDH_R: TGGTGAAGACACCAGTAGACTCCACGAC. Genomic DNA was harvested using the DNeasy Blood & Tissue Kit (Qiagen Cat:69506). Expression of osteocalcin was

determined with computed threshold method qPCR using SYBR® Green PCR master mix (Applied Biosystems Cat:4309155) with GAPDH as a loading control. OCN_F: CAAGCAGGGTTAAGCTCACA; OCN_R: GGTAGTGAACAGACTCCGGC; GAPDH_F: TGAAGCAGGCATCTGAGGG; GAPDH_R: CGAAGGTGGAAGAGTGGGAG.

***Western Blot***

Protein was harvested using NP-40 lysis buffer (10% glycerol, 1% NP-40, 50mM Tris pH7.4, 200mM NaCl, 2mM MgCl2, 1mM PMSF, 1xProtease Inhibitor Cocktail (Sigma Cat:P8340)) + phosphatase inhibitors (Roche Cat:04906845001). Cells were washed with cold PBS + phosphatase inhibitors, collected and pelleted at 4$^{o}$C. Cell pellets were resuspended in 50-100μL of lysis buffer and incubated for 30min on ice. Protein concentration was measured at 595nm with Bio-Rad protein assay dye concentrate (Cat:500-0006). Protein extracts (50 μg) were boiled in 2x SDS sample buffer 10min and separated on a 10% Tris-HCl polyacrylamide gel (Bio-Rad). Protein was transferred to PVDF membranes using a wet transfer system (Bio-Rad Cat:170-3930). Membranes were blocked in 5% milk (Bio-Rad Cat:170-6404) one hour and probed overnight with 1:500 Stat3 (Cell Signaling Cat:9132), 1:500 P-Stat3 (Cell Signaling Cat:9131), or 1:1000 GAPDH (Chemicon® International Cat:MAB374). Signals were amplified with 1:1500 HRP-conjugated secondary antibody (Santa Cruz Biotechnology) and SuperSignal® West Pico Chemiluminescent Substrate (Thermo Scientific, Pierce Product) and developed using film exposure.

### *Adenoviral Transduction*

Passage one BMSCs were plated at a density of 15,000cells/$cm^2$ in T75 flasks. After four hours virus was added at 800 multiplicity of infection (MOI) for BMSC or 400 MOI for ADSC in 4mL α-MEM+0.5% FBS. Complete media was added after four hours. Adenovirus was used in accordance with NIH guidelines and obtained from the University of Michigan vector core (Ann Arbor, Michigan, USA). Adenovirus expressing cre recombinase, harvest date 2/19/09, viral titer 2.40E11 PFU/mL. Adenovirus CMVpLpA.dlE3 #1 (AdBlank), harvest date 9/18/01, viral titer 1.30E11 PFU/mL.

### *In vitro Mineralization Assay*

Primary BMSCs in passage 2-3 were used for this assay. Cells were plated in 12-well or 6-well plates at 25,000-30,000 cells/$cm^2$. Plated cells were allowed to grow to confluence in complete medium for 2-4 days. After reaching confluence cells were cultured in osteogenic medium (BMSC Growth Medium+100nm dexamethasone (Sigma Cat:D8893), 10mM beta-glycerophosphate (Sigma Cat:G9891), and 50μm ascorbic acid 2-phosphate (Sigma Cat:A8960)) for up to 14 days. Cells were fixed with 70% ethanol at $4^oC$ for one hour, rinsed with water, stained for 10 minutes in 40mM, pH 4.2 alizarin red, and washed extensively with water. Dye was eluted in 10% w/v hexadecylpyridinium chloride monohydrate (Wako, Japan) in 10mM sodium phosphate pH 7.0 and concentration determined by absorbance measurement at 562nm.

### *In Vitro Adipogenic Differentiation*

ADSCs were plated at 30,000 cells/cm2 and grown to confluence for two days. Cells were induced with adipogenic medium (ADSC Growth Medium+ 50µM Isobutylmethylxanthine (Sigma Cat:I7018), 1µM dexamethasone (Sigma Cat:D8893, 167nM insulin (Sigma Cat:I5500), and 5µg/mL Troglitazone (Cayman Chemical Cat:71750)) for two days. Adipogenic maintenance media (ADSC Growth Medium+ 167nM insulin (Sigma Cat:I5500)) was then added for two days. This process of induction media followed by maintenance media was repeated once. Cells were then fixed in zinc buffered formalin (Z-fix, Anatech LTD, Battle Creek, MI) for one hour and stained with Oil Red O solution (Sigma Cat:O0625). Dye was eluted in 100% isopropanol and quantified at 500nm.

### *Animals*

All procedures were approved by the University Committee on the Use and Care of Animals (UCUCA). Col2.3-Cre and Col3.6-Cre mice were obtained from Dr.Fei Liu (University of Michigan) (Liu, Woitge et al. 2004). LysM-Cre mice were obtained from Jackson Laboratory (Bar Harbor, Maine, USA Cat:004781) (Clausen, Burkhardt et al. 1999). Flox/Flox Jak2-ObRb mice were obtained from Dr.Martin Myers (University of Michigan) with permission of Dr.Streamson Chua (Columbia University) (McMinn, Liu et al. 2004). Breeding cages contained one male with two females. Pups were genotyped via PCR analysis of tail biopsy DNA with primers as reported previously (McMinn, Liu et al. 2004). Deletion of the floxed allele was determined using the three-primer system designed by McMinn et al (McMinn, Liu et al. 2004). Analysis of food intake was

performed daily for one week. Mice were housed 2-3 animals per cage, mass of chow was determined every 24 hours, chow intake was averaged per housed animals to determine daily intake.

***Blood Collection and Serum Analysis***

Blood was collected from the mice by nicking the lateral tain vein and pooling blood drops into BD Microtainer® tubes (New Jersey, USA). Blood was allowed to clot at room temperature for 30-45 minutes. Samples were spun at 3000rpm for 10min at 4$^{o}$C and serum supernatant removed. Analysis of serum chemistries was performed by the Animal Diagnostic Laboratory of the University of Michigan (Ann Arbor, Michigan, USA). For glucose and cholesterol analyses animals were placed on a 6 hour fast prior to serum collection. Leptin analysis was performed using an ELISA assay kit as described for serum leptin (R&D Systems Cat: MOB00).

***Comprehensive Lab Animal Monitoring System (CLAMS) and Body Composition Analysis***

Measurements and analysis were performed by the University of Michigan Animal Phenotyping Core with approval by the University Committee on the Use and Care of Animals (UCUCA). Body composition was determined using Nuclear Magnetic Resonance based analysis with a Minispec LF90$_{II}$ (Bruker, Optics) to quantify percent fat, lean mass, and fluid in live, conscious animals. For CLAMS analysis, mice were single-housed in an open-circuit calorimetry system capable of simultaneous monitoring of whole animal oxygen consumption, carbon dioxide production, spontaneous activity

(photocell detection with X and Z coverage), and food intake. Measurements for each parameter were recorded every 10-20 minutes for 72 hours.

***MicroCT***

Femurs were wrapped in 70% ethanol-soaked gauze and scanned using a vivaCT 40 μCT system (Scanco Medical, Switzerland) with an isotropic voxel size of 10.5μm (55 kVp, 145μA, 1000 projections per 180 degrees, 200 ms integration time). 2D transverse slices were reconstructed into 2048x2048 pixel matrices. Cortical bone parameters were measured by analyzing 50 slices (0.525mm) of the mid-diaphysis. This region was defined to be the central portion between the proximal and distal ends of the femur. A semi-automated contouring method was used to determine the outer cortical bone perimeter. Briefly, a user-defined contour was drawn around the cortical bone perimeter of the first slice. This initial estimate is then subjected to automated edge detection. This semi-automated contour then serves as the initial estimate for the second slice, and the automated contouring process continues for all 50 slices. A fixed, global threshold of 375 (1/1000 gray scale) corresponding to 635.9 mg of HA/ml was used to distinguish cortical bone from soft tissue and marrow. Trabecular bone parameters were measured by analyzing 101 slices (1.06mm) of the distal metaphysis. Briefly, the distal end of the analysis region was chosen to be 0.105 mm proximal to the primary spongiosa in the marrow cavity. This assured that only trabecular bone was analyzed. Starting at this image, a user-defined contour was drawn to include only the marrow cavity and exclude any cortical bone. User-defined contours were drawn every 10 images (0.105mm) and an automated morphing program was used to interpolate the contours for all images in

between. A fixed, global threshold of 230 (1/1000 gray scale) corresponding to 321.6mg of HA/ml was used to distinguish trabecular bone from soft tissue and marrow. For both analyses, a Gaussian low-pass filter was used ($\sigma$=0.8, support=1).

***Statistics and Image Editing***

A two-tailed, homoscedastic t test was used to determine any difference between control and experimental groups. Values are reported as the mean +/- the standard deviation. $P<0.050$ was considered statistically significant. $P<0.100$ was considered to represent a non-significant trend. In images with 'intact' and 'deleted' bands lanes were cropped from the same parent gel. Brightness and contrast were optimized equally across all lanes for improved visibility.

## 3.4 Results

### *Primary bone marrow stromal cells (BMSCs) express functional ObRb*

Primary BMSCs were harvested from wild type C57BL/6J mice and analyzed for expression of leptin receptor mRNA at passage two (P2). Consistent with previous reports in human BMSCs (Hess, Pino et al. 2005) and mouse clonal MC3T3-E1 osteoblasts, (Lamghari, Tavares et al. 2006) both short form ObRa and long form ObRb leptin receptors were expressed as the progenitor cells differentiated to mature osteoblasts for 7, 14, or 21 days (Figure 11). Since primary BMSCs are a heterogeneous population that is contaminated by cells of the macrophage lineage, we generated a mouse model with floxed ObRb deletion driven by the LysozymeM locus ($LysM^{F/F}$) to disrupt ObRb function in macrophages (Clausen, Burkhardt et al. 1999). Cre-lox recombination is a tool that is used to mediate site-specific recombination of genomic DNA (Sauer and Henderson 1988). DNA sequences that are flanked by loxP nucleotide sequences or 'floxed' are susceptible to deletion and recombination by the enzyme Cre recombinase. When expression of Cre is placed under the control of a specific promoter, such as LysM, gene deletion can be limited to the cell populations where that promoter is expressed. In our experiments the flox sites were designed to flank exon 17 of ObRb. When probed with primers designed to surround this exon, cre-mediated deletion of the segment was determined based on the appearance of a shorter ~200bp PCR band when compared to the intact 646bp band (Figure 11). Stimulation of marrow derived monocytes from these mice with 50ng/mL M-CSF for two days resulted in recombination of the ObRb locus in macrophages *in vitro* (Figure 11). As expected, culture of primary BMSCs from $LysM^{F/F}$ mice demonstrated that macrophage contamination of BMSC cultures decreased with

passaging of the cells (Figure 11). Primary BMSCs (P2) derived from LysM$^{F/F}$ mice were stimulated with 1000ng/mL leptin for 0, 5, 10 or 20 minutes and downstream phosphorylation of Stat3 (P-Stat3) was analyzed. In response to leptin stimulation, rapid induction of P-Stat3 was observed after 5-10 minutes that could be attributed to the non-macrophage portion of the primary BMSC preparation (Figure 12).

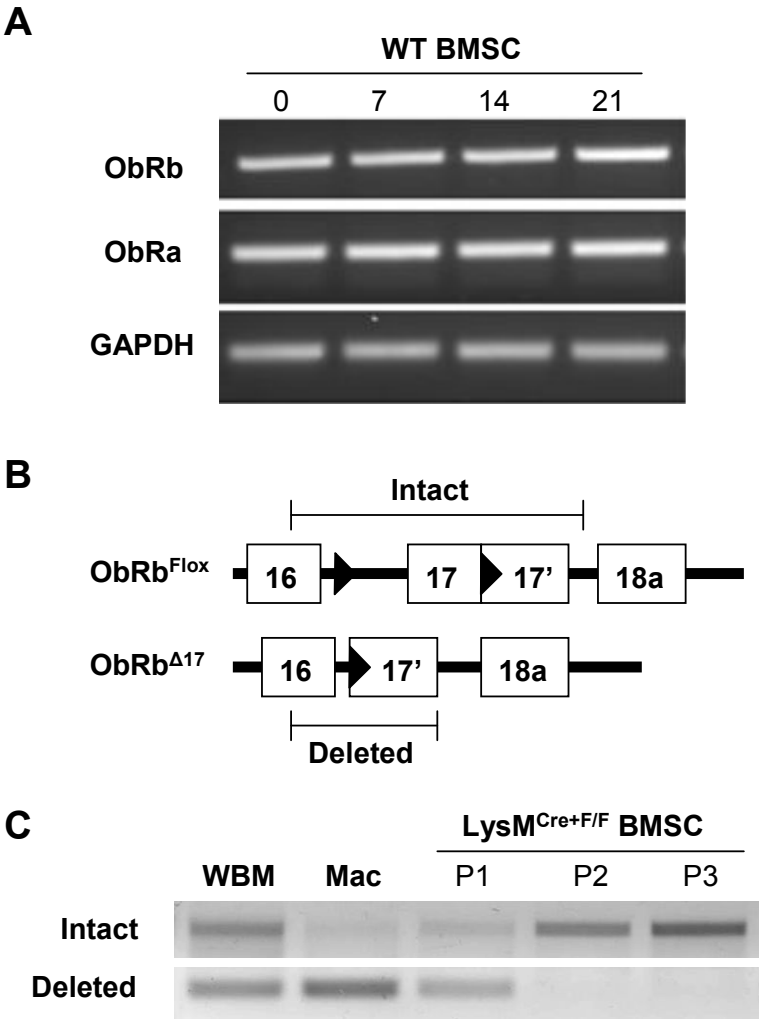


**Figure 11.** Primary bone marrow stromal cells (BMSCs) express ObRb. **(A)** PCR analysis of long-form (ObRb) and short-form (ObRa) leptin receptor. RNA from C57BL/6J (WT) P2 BMSCs. **(B)** Diagram of anticipated PCR products from intact or cre-recombined (deleted) genomic DNA. **(C)** LoxP recombination in genomic DNA from whole bone marrow (WBM), primary macrophage (Mac) and passage one to passage 3 (P1-P3) BMSC from LysM$^{Cre+F/F}$ mice. WT: wild type. GAPDH: glyceraldehyde-3-phosphate dehydrogenase. Credit: (Scheller, Song et al. 2010).

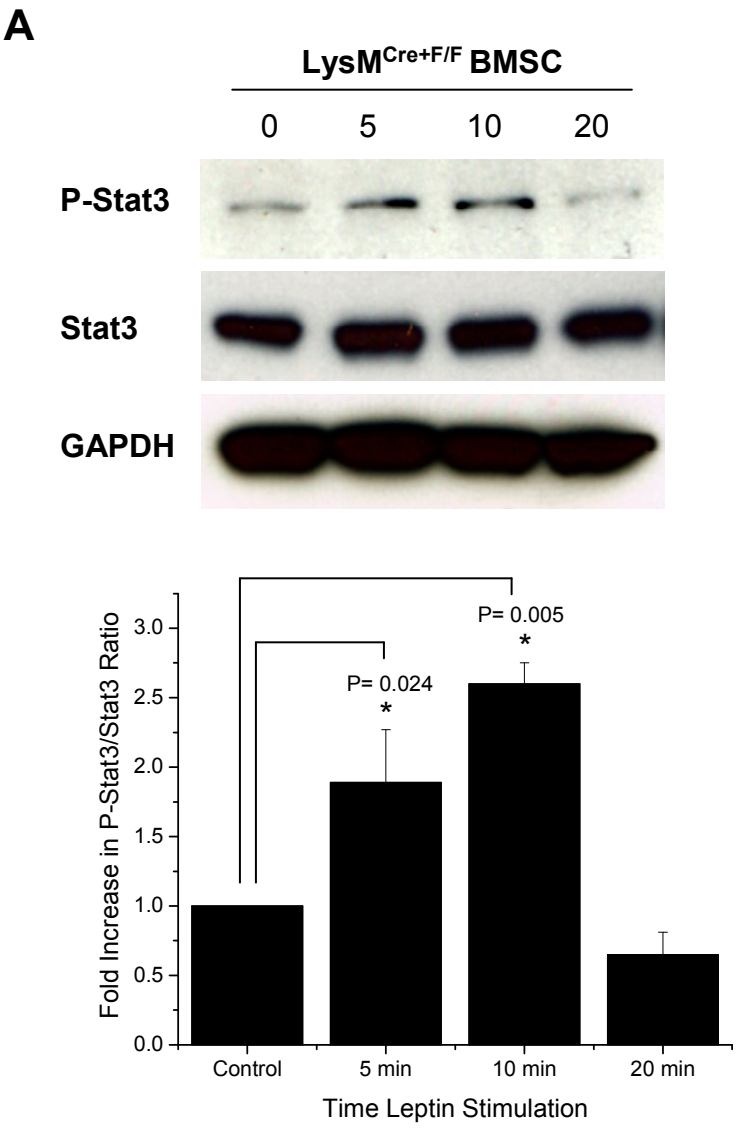


**Figure 12.** Primary bone marrow stromal cell (BMSC) ObRb responds to leptin with phosphorylation of Stat3. P-Stat3 induction after 1000ng/mL leptin administration for 0 to 20 minutes. The ratio of P-Stat3 to Stat3 was quantified using densitometry and fold induction determined with time 0 normalized to 1.0. N=3. *: statistically significant over control time zero. GAPDH: glyceraldehyde-3-phosphate dehydrogenase. Stat3: signal transducer and activator of transcription 3. Credit: (Scheller, Song et al. 2010).

***Knockout of ObRb in vitro decreases mineralization and increases adipogenesis of primary stromal cells***

To evaluate the significance of endogenous leptin production *in vitro*, primary BMSCs were harvested from long bones of control mice harboring the ObRb loxP mutation. Cells were treated at P1 with adenovirus expressing Cre recombinase (AdCre) or a non-functional poly-L-poly-A sequence (AdBlank) and monitored for ObRb gene deletion. Complete recombination of the loxP site occurred after AdCre treatment (Figure 13, Figure 14). Treated BMSCs were harvested and re-plated at a density of 25,000 cells/$cm^2$ in 12-well plates and induced to differentiate toward osteoblasts. AdCre treated cells exhibited significantly less *in vitro* mineral deposition at Day 7 of osteogenic culture that was equalized by Day 14 (Figure 13). This deletion study is the converse of previous experiments that have added leptin directly to primary BMSCs *in vitro* and observed an increase in mineralization (Chang, Shih et al. 2006). Similarly, primary ADSCs were harvested from para-lumbar and intra-abdominal fat pads and treated with AdCre or AdBlank as described above. Ablation of ObRb function increased the adipogenic differentiation of the confluent cell monolayers by 99.8+/-25% (Figure 14). This is also consistent with previous results that have demonstrated inhibition of adipogenesis *in vitro* by recombinant leptin (Rhee, Sung et al. 2008).

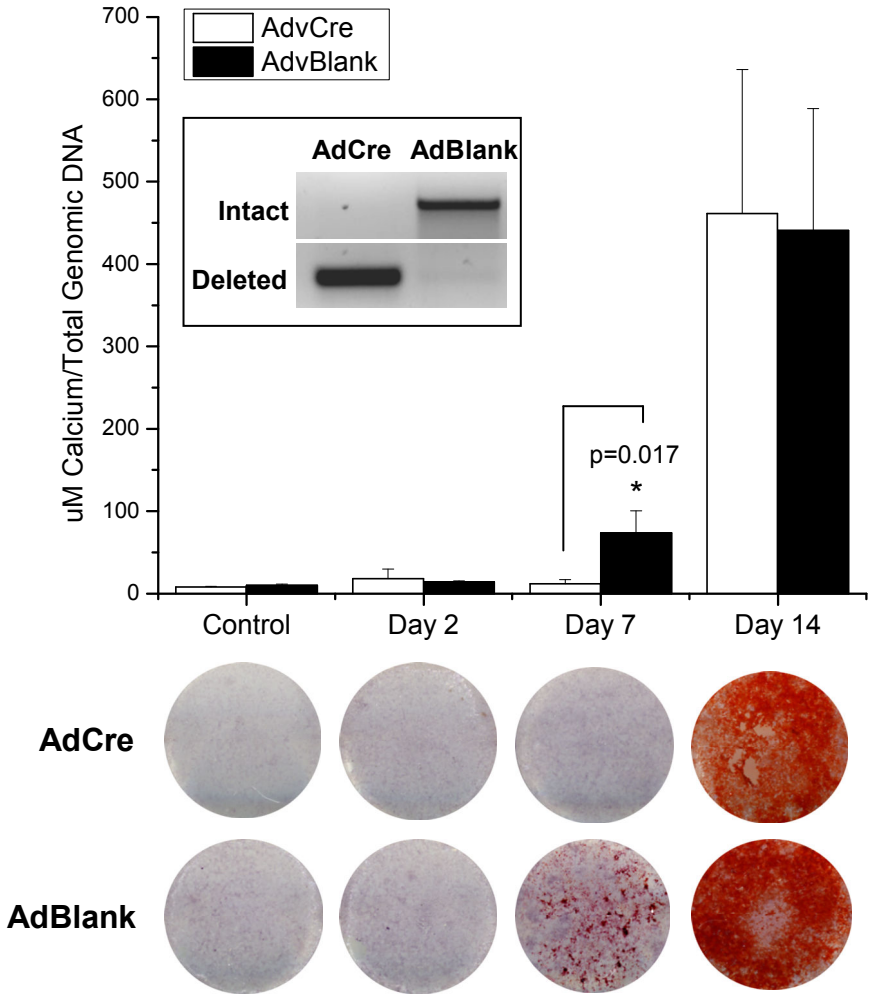


**Figure 13.** Knockout of ObRb *in vitro* decreases the mineralization of primary bone marrow stromal cells. Alizarin red stain and stain quantification of BMSCs treated with adenovirus expressing Cre recombinase (AdCre) or adenovirus expressing an inert poly-L-poly-A sequence (AdBlank) at 800MOI. Inset shows PCR of genomic DNA after virus treatment and confirms recombination of the loxP site. Bands are cropped from the same gel. N=3. *: statistically significant over matched day. Credit: (Scheller, Song et al. 2010).

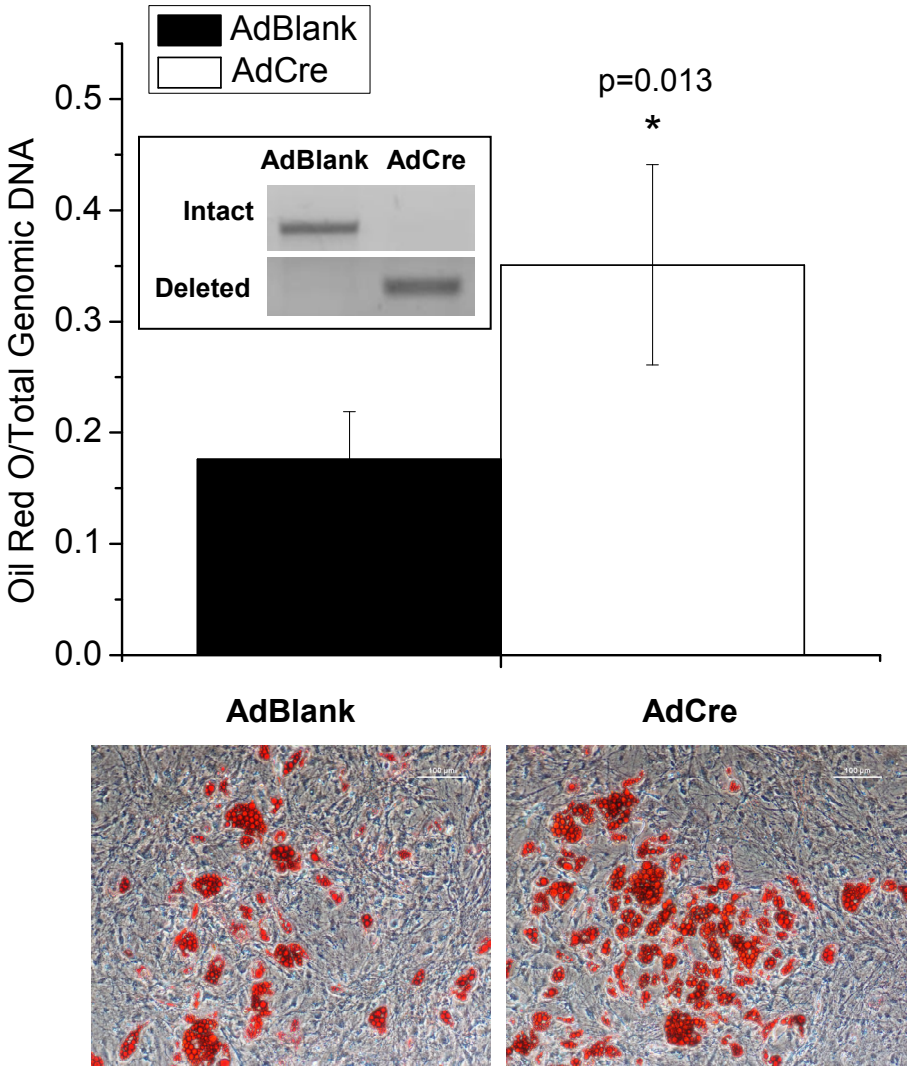


**Figure 14.** Knockout of ObRb *in vitro* increases the adipogenesis of primary adipose derived stromal cells (ADSCs). Adipogenesis, Oil Red O stain, of ADSCs treated with adenovirus expressing Cre recombinase (AdCre) or adenovirus expressing an inert poly-L-poly-A sequence (AdBlank) at 400MOI. Inset shows PCR of genomic DNA after virus treatment and confirms recombination of the loxP site. Bands are cropped from the same gel. N=4. *: statistically significant over control. Credit: (Scheller, Song et al. 2010).

***BMSCs obtained from mice with an absence of total body ObRb signaling show increased mineralization potential in vitro***

Surprisingly, while the in vitro disruption of leptin signaling resulted in reduced mineralization, primary BMSCs from leptin-deficient ob/ob and ObRb-deficient db/db mice showed a high mineralization phenotype. At Day 14, mineralization of ob/ob and db/db cultures was increased by 50.7+/-6.4% or 45.1+/-5.4% respectively (Figure 15). Addition of 100ng/mL recombinant leptin to the medium failed to rescue the high mineralization phenotype (Figure 15). Osteocalcin expression at Day 14 was also increased by 2.9+/-0.08-fold (ob/ob) or 2.4+/-0.23-fold (db/db) (Figure 15). Alkaline phosphatase activity was significantly higher per total protein in ob/ob but not db/db cells (Figure 15).

***Generation of transgenic mice expressing Col2.3-Cre or Col3.6-Cre and harboring the $ObRb^{F/F}$ site***

To determine the physiologic relevance of the divergent *in vitro* mineralization patterns, we generated osteoblast (Col2.3) and MPC (Col3.6) cell-specific knockout mice. The Col3.6 promoter is active in osteoblast precursors while the 2.3 promoter is active when cells differentiate to become osteoblasts (Liu, Woitge et al. 2004). Mice harboring the $ObRb^{F/F}$ site were mated with Col2.3-Cre $ObRb^{F/-}$ or Col3.6-Cre $ObRb^{F/-}$ mice to generate litters consisting of Cre-F/F, Cre-F/-, Cre+F/-, and Cre+F/F mice in a 1:1:1:1 ratio. Breeding conformed to expected Mendelian ratios, however, complete gene disruption was observed in a significant number of female pups and some of the males for both Col3.6-Cre and Col2.3-Cre litters (observation, not quantified).

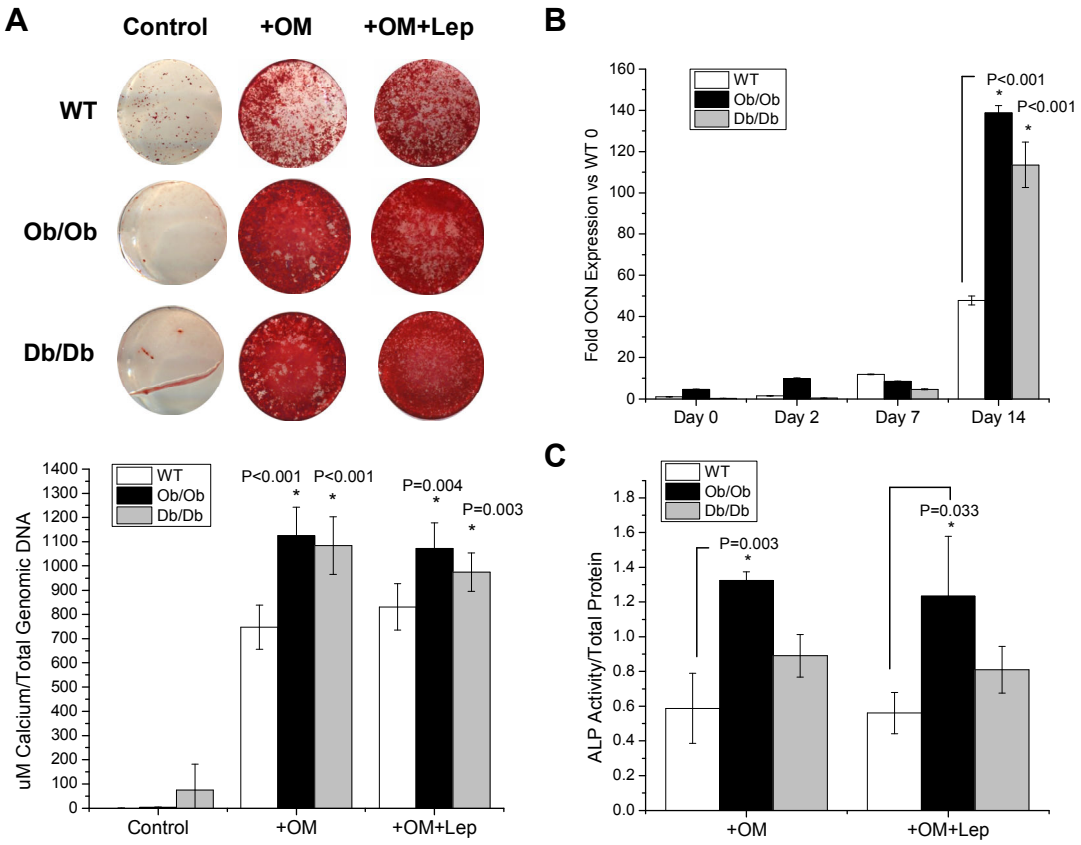


**Figure 15.** Bone marrow stromal cells (BMSCs) from ob/ob and db/db mice show increased mineralization. **(A)** Alizarin red stained mineral after fourteen days in osteogenic media (OM) with or without 100ng/mL leptin. Mineral was quantified and normalized to total genomic DNA per well. Passage 2 BMSCs. N=5-6. **(B)** Quantitative PCR for osteocalcin (OCN) expression. N=3. **(C)** Alkaline phosphatase activity as measured by conversion of p-nitrophenol phosphate to nitrophenol, normalized to total protein. N=3. WT: wild type. *: statistically significant over matched wild type. Credit: (Scheller, Song et al. 2010).

This is consistent with previous reports of sporadic germline recombination (Cochrane, Clark et al. 2007) when using the Col2.3 and Col3.6 promoters. Complete knockout (KO) mice were easily identified phenotypically by their frank obesity and genetically by 100% band excision in harvested DNA (Figure 16). Tissue analysis of genomic DNA revealed some recombination in all tissues of $3.6^{Cre+F/F}$ mice with the highest deletion rate in adipose, tendon, and calvaria (Figure 17). Consistent with previous reports, the majority of *in vitro* primary $3.6^{Cre+F/F}$ BMSCs harbored the deleted form of the ObRb locus (Liu, Woitge et al. 2004) (Figure 17). We speculate that the background

recombination in $3.6^{Cre+F/F}$ whole tissues can be attributed to expression of Col3.6 in tissue-associated MPC or vascular endothelial cells. Recombination in $2.3^{Cre+F/F}$ mice was highest in muscle, calvaria, and whole marrow (Figure 17).

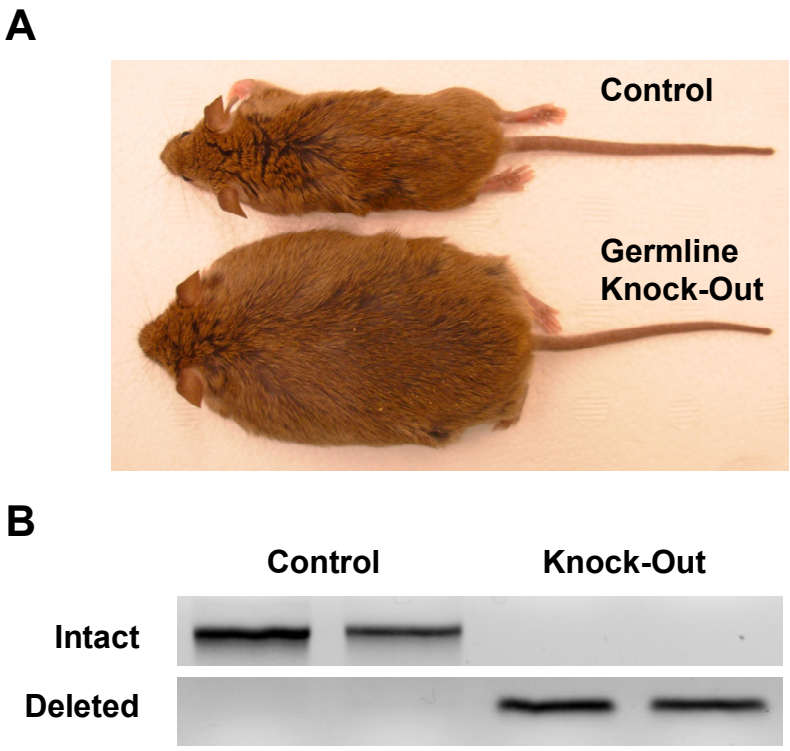


**Figure 16.** Germline knockout of ObRb results in significant obesity. **(A)** Representative mouse photographs of control Cre negative and complete ObRb knockout mice. **(B)** Genomic DNA PCR confirming complete loxP recombination of genomic DNA in bone marrow macrophages derived from the knockout animals and intact ObRb the controls. Bands are cropped from the same gel and replicate duplicate samples. Credit: (Scheller, Song et al. 2010; Scheller, Hankenson et al. 2011).

The gross phenotype of $2.3^{Cre+F/F}$ mice was identical to $2.3^{Cre-}$ controls. The $3.6^{Cre+F/F}$ mice demonstrated mild obesity that remained statistically significant after approximately 12 weeks of age (Figure 18). Body composition analysis of 16 week old female mice revealed that the mass increase was due predominantly to increased adiposity, however, total lean and fluid mass were also significantly increased (Figure 19).

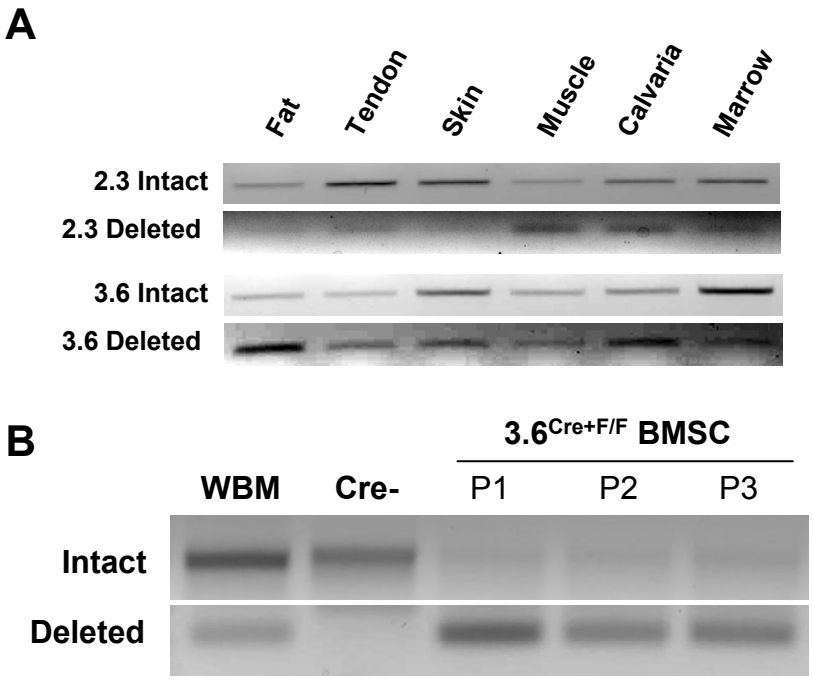


**Figure 17.** Characterization of loxP recombination in mice expressing Col2.3-Cre or Col3.6-Cre and harboring the $ObRb^{F/F}$ site. **(A)** Representative PCR of tissue genomic DNA from 12 week old animals. **(B)** PCR of whole bone marrow (WBM) and passage one to passage three (P1-P3) bone marrow stromal cells (BMSCs) from $3.6^{Cre+F/F}$mice. Cre-: P1 BMSCs harvested from mice lacking Col3.6 driven Cre recombinase expression. Bands are cropped from the same gel. Credit: (Scheller, Song et al. 2010).

This translated to a significant increase in percent body fat, decrease in lean mass, and no change in percent fluid (Figure 19). Mice were examined for alterations in fasting serum chemistries including cholesterol, calcium, ALT, albumin, alkaline phosphatase, amylase, blood urea nitrogen, creatinine, hemoglobin, phosphate, total bilirubin, total protein, glucose, and leptin (Table 4). The only significant differences in these values between the $3.6^{Cre-}$ and $3.6^{Cre+ F/F}$ mice were a slight increase in serum calcium (within normal range), a small increase in total protein driven by an increase in albumin and a significant elevation of serum leptin (Table 4). Thus, unlike the complete knockout mice, $3.6^{Cre+ F/F}$ mice were not diabetic and had no significant alterations in liver or kidney function.

| Col3.6 Serum Chemistries | | | |
|---|---|---|---|
| Labs | Cre- | Cre+ F/F | p value |
| Cholesterol (mg/dL) | 142.3 | 156.6 | 0.137 |
| Alkaline Phosphatase (units/L) | 41 | 49 | 0.101 |
| Alanine aminotransferase (units/L) | 51.2 | 49.4 | 0.777 |
| Amylase (units/L) | 2581 | 2411 | 0.389 |
| Blood Urea Nitrogen (mg/dL) | 22.5 | 21.3 | 0.645 |
| Calcium (mg/dL) | 8.66 | 9.3 | 0.041 |
| Creatanine (mg/dL) | 0.275 | 0.3 | 0.437 |
| Phosphate (mg/dL) | 9.425 | 8.4 | 0.392 |
| Total Bilirubin (mg/dL) | 0.825 | 0.75 | 0.368 |
| Albumin (g/dL) | 2 | 2.425 | 0.047 |
| Globulin (g/dL) | 2.85 | 2.875 | 0.171 |
| Total Protein (g/dL) | 4.725 | 5.3 | 0.021 |
| Fasted Glucose (mg/dL) | 150.3 | 149.8 | 0.969 |
| Leptin (ng/mL) | 4.8 | 44.5 | 0.006 |

**Table 4.** Serum chemistries of $3.6^{Cre-}$ and $3.6^{Cre+F/F}$ mice. Analysis reveals a significant increase in circulating calcium in the $3.6^{Cre+F/F}$ mice. There is also a significant increase in total protein that is driven by increases in albumin. N=4-6. Credit: (Scheller, Song et al. 2010).

### *Metabolic analysis of $3.6^{Cre+F/F}$ mice*

Food intake of 42 week old mice was monitored for one week. No significant differences were observed between the three groups (Data Not Shown). To enhance sensitivity of food intake monitoring and examine additional metabolic parameters, $3.6^{Cre-}$ and $3.6^{Cre+F/F}$ females at 16 weeks of age were subjected to three day metabolic analysis. Similar to the aged males, the output did not reveal a statistically significant increase in intake of the $3.6^{Cre+F/F}$ animals when compared to controls (Figure 20). Total activity was similarly unchanged between groups (Figure 20). The only consistent difference was a highly significant decrease in oxygen consumption per body mass per hour in the $3.6^{Cre+F/F}$ animals (Figure 20). This was likely driven by the increased mass of the $3.6^{Cre+F/F}$ mice and disappeared when normalized to lean instead of total body mass (Figure 20).

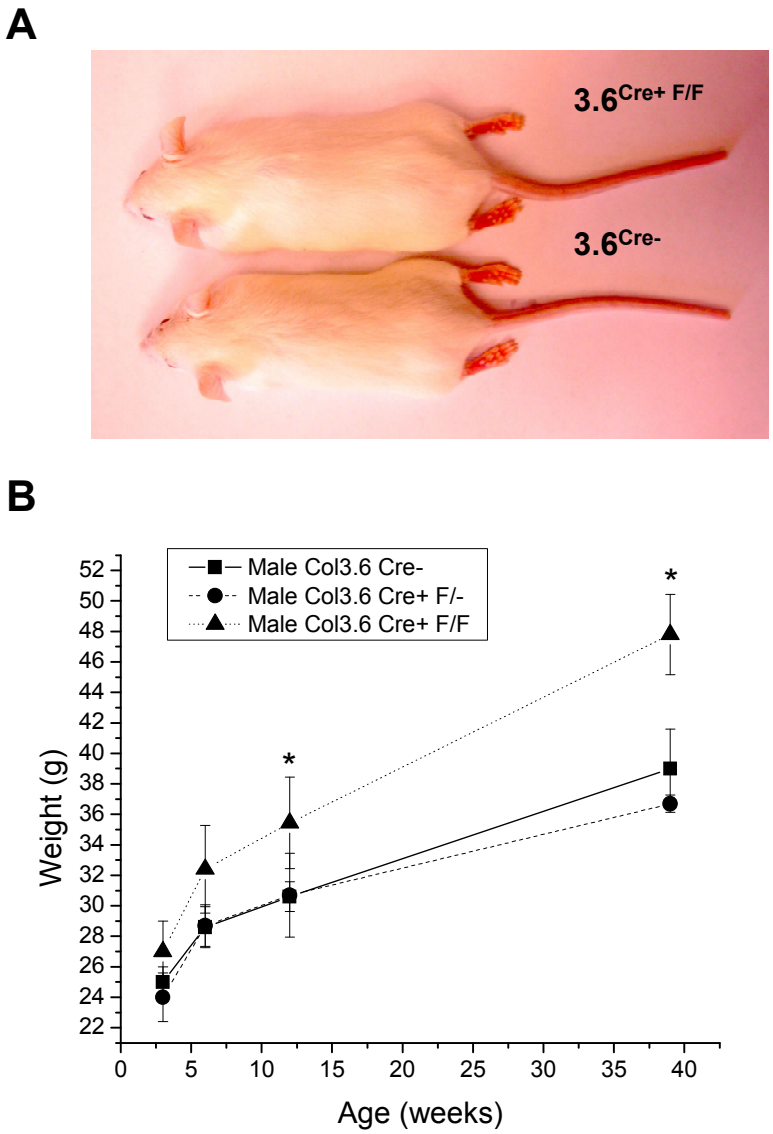


**Figure 18.** Gross phenotype of $3.6^{Cre+F/F}$ mice. **(A)** Representative photo of 12 week old male $3.6^{Cre-}$ and $3.6^{Cre+F/F}$ mice showing increase in peripheral adiposity and body size. **(B)** Mass of male transgenic mice from 3 to 38 weeks of age. *: significant over matched time point $3.6^{Cre-}$. N=4-6. Credit: (Scheller, Song et al. 2010); E.L Scheller, unpublished data.

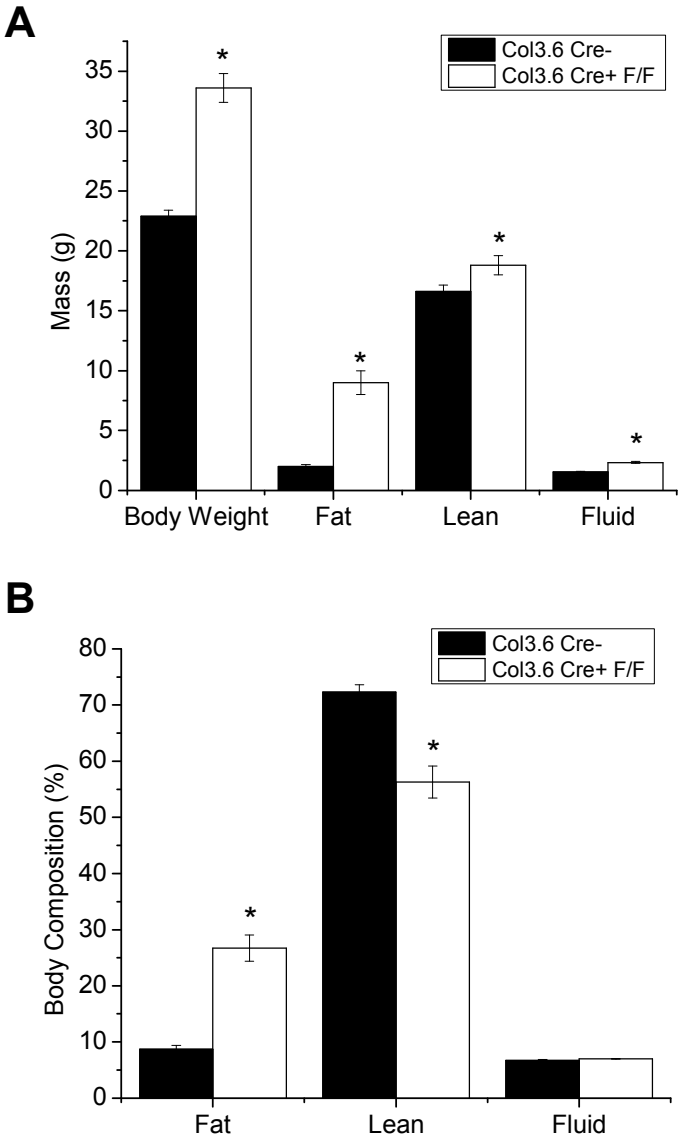


**Figure 19.** Minispec body composition analysis of $3.6^{Cre-}$ and $3.6^{Cre+F/F}$ mice. Female mice at 16 weeks of age were analyzed with Nuclear Magnetic Resonance based imaging on a Minispec LF90II (Bruker, Optics) to quantify percent fat, lean mass, and fluid in live, conscious animals. **(A)** Absolute mass of whole body, fat, lean mass, and fluid. **(B)** Percent fat, lean, and fluid mass relative to whole body weight. $3.6^{Cre-}$ N=10, $3.6^{Cre+F/F}$ N=7. *: statistically significant relative to $3.6^{Cre-}$. Credit: E.L Scheller, unpublished data.

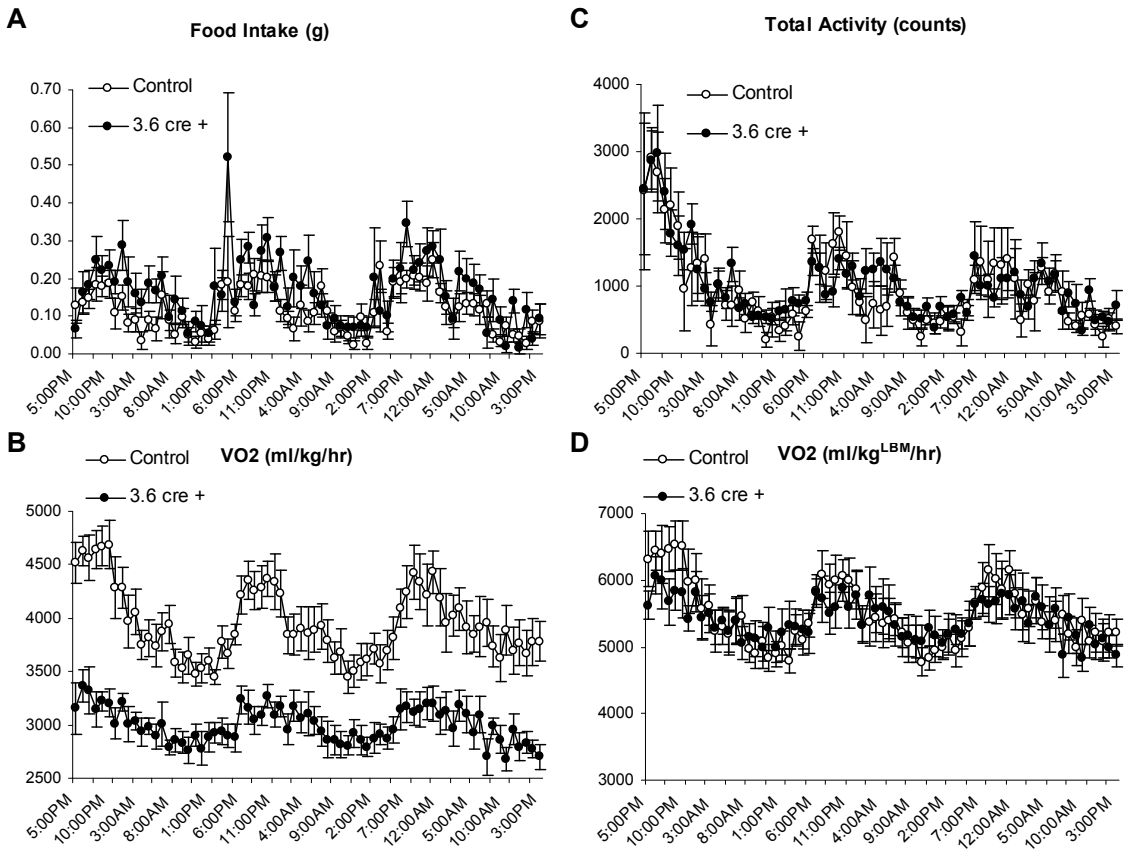


**Figure 20.** Comprehensive lab animal monitoring system (CLAMS) analysis of $3.6^{Cre-}$ and $3.6^{Cre+F/F}$ mice. Mice were single-housed in an open-circuit calorimetry system capable of simultaneous monitoring of **(A)** food intake, **(B)** whole animal oxygen consumption (VO2), **(C)** spontaneous activity (photocell detection with X and Z coverage). **(D)** Oxygen consumption was normalized to lean body mass. Measurements for each parameter were recorded every 10-20 minutes for 72 hours. $3.6^{Cre-}$ N=10, $3.6^{Cre+F/F}$ N=7. Credit: E.L Scheller, unpublished data.

### *Contrasting bone phenotypes of $2.3^{Cre+F/F}$ and $3.6^{Cre+F/F}$ mice*

Femurs were dissected free of muscle and radiographed at 32kV for 45 seconds (Figure 21). Femoral microCT analysis revealed no difference in trabecular parameters of the $2.3^{Cre+F/F}$ femurs (Table 5). However, cortical parameters showed a non-significant trend ($P<0.100$) toward increased bone volume and bone area (Table 5).

| | 12 weeks Col2.3 | | |
|---|---|---|---|
| **Trabecular** | **2.3Cre-** | **2.3Cre+F/F** | **p value** |
| Bone Volume (mm^3) | 0.523+/-0.063 | 0.462+/-0.103 | 0.245 |
| Bone Volume Fraction (%) | 22.4+/-2.5 | 19.3+/-3.9 | 0.131 |
| Tb. Number (1/mm) | 5.24+/-0.42 | 4.90+/-.41 | 0.183 |
| Tb. Thickness (mm) | 0.060+/-0.003 | 0.058+/-0.004 | 0.393 |
| Mineral Density of Total Volume (mg HA/ccm) | 181+/-22 | 156+/-34 | 0.171 |
| Total Mineral Content (mg HA) | 422+/-60 | 373+/-88 | 0.288 |
| Bone Mineral Content (mg HA) | 436+/-61 | 383+/-84 | 0.239 |
| | | | |
| **Cortical** | **2.3Cre-** | **2.3Cre+F/F** | **p value** |
| Total Volume (mm^3) | 0.86+/-0.05 | 0.90+/-0.02 | 0.160 |
| Bone Volume (mm^3) | 0.398+/-0.017 | 0.416+/-0.016 | 0.099 |
| Mineral Density of Total Volume (mg HA/ccm) | 555+/-28 | 550+/-25 | 0.759 |
| Total Mineral Content (mg HA) | 478+/-18 | 493+/-21 | 0.221 |
| Bone Mineral Content (mg HA) | 467+/-17 | 481+/-20 | 0.221 |
| Total Area (mm^2) | 1.68+/-0.01 | 1.74+/-0.04 | 0.183 |
| Bone Area (mm^2) | 0.79+/-0.03 | 0.82+/-0.03 | 0.098 |

**Table 5.** Micro computed tomography analysis of $2.3^{Cre-}$ and $2.3^{Cre+F/F}$ femurs at 12 weeks. Trabecular and cortical bone parameters of male mice as determined by microCT. N=6. Credit: (Scheller, Song et al. 2010).

Due to the presence of significant differences, femurs of $3.6^{Cre+F/F}$ mice were analyzed at both 12 and 42 weeks of age. At 42 weeks femur length was increased by 0.78+/-0.02mm (5.5+/-0.16%) in male $3.6^{Cre+F/F}$ mice when compared to $3.6^{Cre-}$ controls (Figure 21). At both ages trabecular parameters including bone volume fraction (BVF) and mineral density of total volume (MD of TV) were significantly increased by 58-61.9% and 65.5-74% respectively (Table 6). Increased cortical parameters at 12 weeks mimicked those present in complete knockout mice with an 18.3+/-1.7% and a 21.7+/-2.2% increase in bone volume and total mineral content respectively (Table 6). The decrease in femoral trabecular BVF and increased cortical parameters of our spontaneous complete KO mice recapitulates what has been reported previously for ob/ob mice (Hamrick, Pennington et al. 2004) (Table 7).

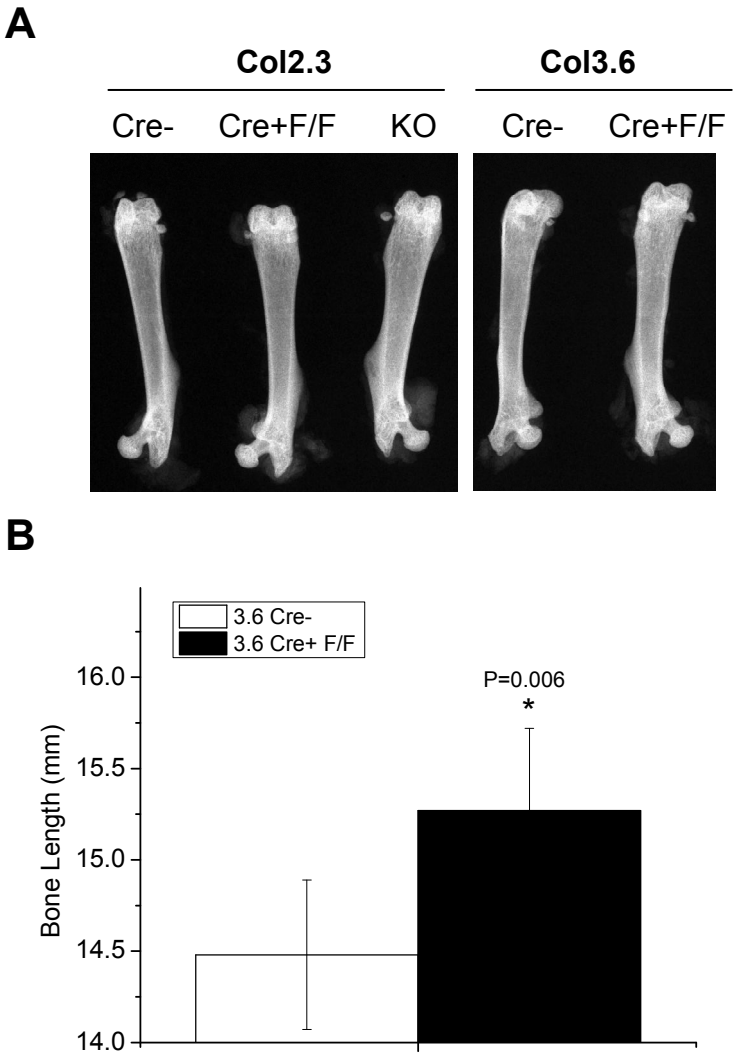


**Figure 21.** Femoral imaging and length analysis of transgenic mice. **(A)** Representative faxitron x-ray image of femurs from 12 week old Col2.3, Col3.6, and germline knockout (KO) mice. Decreased length of the KO and increased length of the $3.6^{Cre+F/F}$ femurs relative to control can be noted. **(B)** Quantification of femur length of $3.6^{Cre-}$ and $3.6C^{re+F/F}$ mice at 42 weeks. N=6-8. Credit: (Scheller, Song et al. 2010).

| | 12 week Col3.6 | | | 42 week Col3.6 | | |
|---|---|---|---|---|---|---|
| **Trabecular** | **Control** | **Col3.6+** | **p value** | **Control** | **Col3.6+** | **p value** |
| Bone Volume (mm^3) | 0.380+/-0.099 | 0.684+/-0.099 | 0.006 | 0.270+/-0.111 | 0.416+/-0.123 | 0.056 |
| Bone Volume Fraction (%) | 16+/-4.1 | 25.9+/-3 | 0.011 | 9.1+/-3.5 | 14.4+/-4.2 | 0.035 |
| Tb. Number (1/mm) | 4.56+/-0.56 | 5.51+/-0.52 | 0.056 | 2.72+/-0.69 | 3.35+/-0.47 | 0.089 |
| Tb. Thickness (mm) | 0.056+/-0.003 | 0.065+/-0.003 | 0.005 | 0.058+/-0.006 | 0.064+/-0.007 | 0.154 |
| Mineral Density of Total Volume (mg HA/ccm) | 127+/-28 | 210+/-30 | 0.008 | 78+/-37 | 135+/-51 | 0.050 |
| Total Mineral Content (mg HA) | 300+/-66 | 552+/-92 | 0.004 | 229+/-109 | 389+/-147 | 0.059 |
| Bone Mineral Content (mg HA) | 312+/-80 | 565+/-87 | 0.006 | 233+/-100 | 367+/-116 | 0.057 |

| **Cortical** | **Control** | **Col3.6+** | **p value** | **Control** | **Col3.6+** | **p value** |
|---|---|---|---|---|---|---|
| Total Volume (mm^3) | 0.89+/-0.07 | 0.99+/-0.02 | 0.060 | 1.22+/-0.11 | 1.25+/-0.06 | 0.629 |
| Bone Volume (mm^3) | 0.398+/-0.012 | 0.471+/-0.046 | 0.012 | 0.552+/-0.047 | 0.593+/-0.064 | 0.238 |
| Mineral Density of Total Volume (mg HA/ccm) | 534+/-26 | 582+/-46 | 0.104 | 579+/-61 | 615+/-39 | 0.253 |
| Total Mineral Content (mg HA) | 473+/-28 | 576+/-58 | 0.013 | 705+/-70 | 768+/-69 | 0.145 |
| Bone Mineral Content (mg HA) | 467+/-25 | 554+/-51 | 0.015 | 687+/-62 | 744+/-73 | 0.169 |
| Total Area (mm^2) | 1.72+/-0.14 | 1.92+/-0.04 | 0.057 | 2.38+/-0.22 | 2.44+/-0.12 | 0.605 |
| Bone Area (mm^2) | 0.84+/-0.09 | 0.93+/-0.09 | 0.012 | 1.09+/-0.09 | 1.18+/-0.13 | 0.234 |

**Table 6.** Micro computed tomography analysis of $3.6^{Cre-}$ and $3.6^{Cre+F/F}$ femurs at 12 and 42 weeks. Trabecular and cortical bone parameters of male mice as determined by microCT. N=3-6. Credit: (Scheller, Song et al. 2010

| | 12 week Complete Knockout | | |
|---|---|---|---|
| **Trabecular** | **Control** | **KO** | **p value** |
| Bone Volume (mm^3) | 0.523+/-0.063 | 0.462+/-0.072 | 0.170 |
| Bone Volume Fraction (%) | 22.4+/-2.5 | 18.6+/-3.0 | 0.050 |
| Tb. Number (1/mm) | 5.24+/-0.42 | 4.75+/-0.36 | 0.071 |
| Tb. Thickness (mm) | 0.060+/-0.003 | 0.058+/-0.003 | 0.332 |
| Mineral Density of Total Volume (mg HA/ccm) | 181+/-22 | 163+/-19 | 0.190 |
| Total Mineral Content (mg HA) | 422+/-60 | 403+/-43 | 0.582 |
| Bone Mineral Content (mg HA) | 436+/-61 | 376+/-56 | 0.124 |

| **Cortical** | **Control** | **KO** | **p value** |
|---|---|---|---|
| Total Volume (mm^3) | 0.86+/-0.05 | 0.99+/-0.08 | 0.008 |
| Bone Volume (mm^3) | 0.398+/-0.017 | 0.477+/-0.062 | 0.015 |
| Mineral Density of Total Volume (mg HA/ccm) | 555+/-28 | 594+/-25 | 0.036 |
| Total Mineral Content (mg HA) | 478+/-18 | 591+/-65 | 0.002 |
| Bone Mineral Content (mg HA) | 467+/-17 | 568+/-65 | 0.005 |
| Total Area (mm^2) | 1.68+/-0.01 | 1.93+/-0.15 | 0.009 |
| Bone Area (mm^2) | 0.79+/-0.03 | 0.94+/-0.12 | 0.014 |

**Table 7.** Micro computed tomography analysis of $2.3^{Cre-}$ and germline knockout (KO) femurs at 12 weeks. Trabecular and cortical bone parameters of male mice as determined by microCT. N=4-6. Credit: (Scheller, Song et al. 2010).

### *Primary BMSCs from mice $3.6^{Cre+\ F/F}$ mice have increased osteoblast and adipocyte differentiation potential in vitro*

To verify that deletion of ObRb *in vivo* results in an increased differentiation *in vitro* we harvested primary stromal cells from both $3.6^{Control}$ and $3.6^{Cre+\ F/F}$ mice. Mineralization of the BMSCs at P2 *in vitro* revealed a robust mineralization phenotype that mimicked that of BMSCs from ob/ob and db/db mice. Mineralization was increased by 422+/-215% at Day 7 and 192+/-17% at Day 14 (Figure 22). Differentiation of primary BMSCs also showed a 97.7+/-23.1% increase in adipogenic potential (Figure 23).

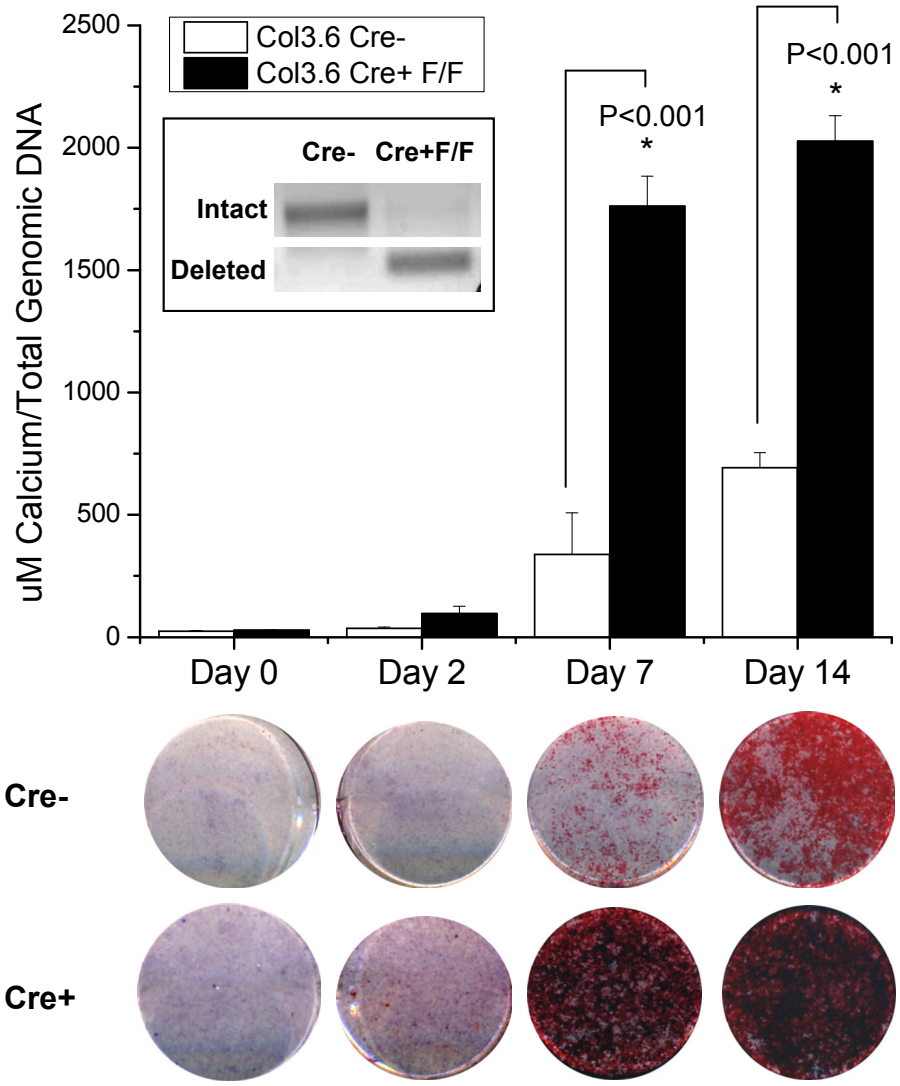


**Figure 22.** Knockout of ObRb in MPCs *in vivo* with Col3.6-Cre results in increased *in vitro* mineralization. Mineralization, alizarin red stain and quantification of passage two bone marrow stromal cells (BMSCs) from $3.6^{Cre-}$ and $3.6^{Cre+F/F}$ mice. Inset shows PCR of genomic DNA and confirms recombination of the loxP site. Bands are cropped from the same gel. N=3. *: statistically significant over $3.6^{Cre-}$. Credit: (Scheller, Song et al. 2010).

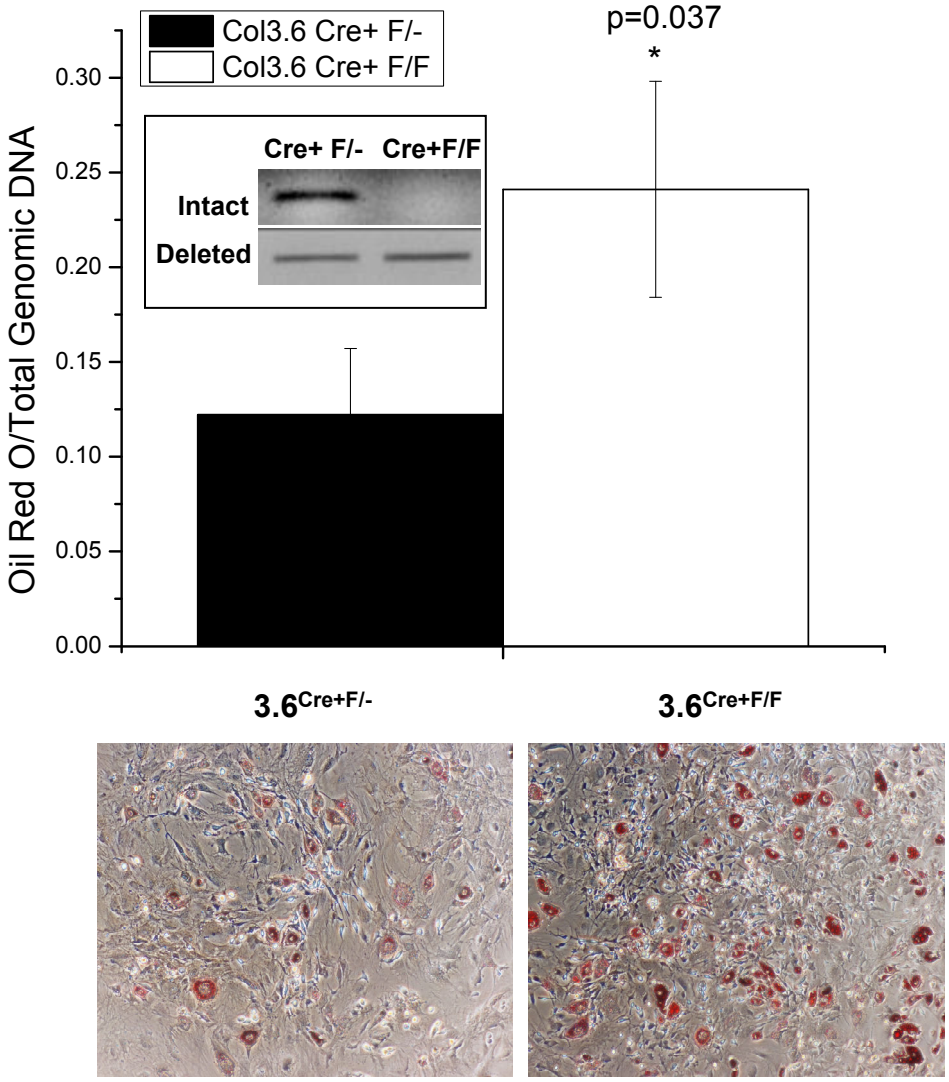


**Figure 23.** Knockout of ObRb in MPCs *in vivo* with Col3.6-Cre results in increased *in vitro* adipogenesis. Adipogenesis, oil red o stain and quantification of passage two bone marrow stromal cells (BMSCs) from $3.6^{Cre-}$ and $3.6^{Cre+F/F}$ mice. Inset shows PCR of genomic DNA and confirms recombination of the loxP site. Bands are cropped from the same gel. N=3. *: statistically significant over $3.6^{Cre-}$. Credit: (Scheller, Song et al. 2010).

### 3.5 Discussion

It is well established that leptin acts primarily through the hypothalamus to regulate weight gain through food intake (Pelleymounter, Cullen et al. 1995; Breslow, Min-Lee et al. 1999; Cohen, Zhao et al. 2001). Generation of a mouse with conditional disruption of the long-form leptin receptor gene in the MPC and osteoblast has allowed us to begin to understand the physiologic contributions of peripheral leptin in bone. We used a mouse with loxP sites flanking exon 17 of ObRb to critically evaluate physiologic regulation of bone formation by peripheral leptin *in vitro* and *in vivo*. To do this, three transgenic mouse lines were generated with cell-specific knockout of ObRb function using the LysM, Col2.3 and Col3.6 promoters. Use of the Col2.3 and Col3.6 promoters is somewhat limited by high levels (15-50%) of germline recombination that decreases the number of usable offspring (Cochrane, Clark et al. 2007) as well as non-specific expression of Col3.6 in tendon, skin, and muscle (Liu, Woitge et al. 2004). However, both promoters have previously been used successfully (Lengner, Steinman et al. 2006; Gutierrez, Kong et al. 2008) and an alternative promoter that drives reliable recombination in the mesenchymal precursor compartment without also affecting neighboring bone cells is not yet available.

The Col3.6 promoter is known to be expressed in multiple tissues including tendon, skin, calvaria, and long bone (Liu, Woitge et al. 2004). Analysis with ROSA reporter mice shows widespread expression in the bone cavity that encompasses the osteocyte, osteoblast, and stromal fibroblast population with additional expression observed in some clustered areas of proliferative and hypertrophic chondrocytes (Liu, Woitge et al. 2004).

Adipose tissue was not analyzed in this previous publication, though our current study reveals high levels of recombination in the fat pads (Figure 17). Since the Col3.6 promoter mediates loxP recombination in osteoblasts, adipocytes, and some chondrocytes we believe that it likely deletes the gene a precursor population for these lineages, the MPC. BMSC from Col3.6-Cre mice crossed with ROSA Cre-reporter mice in low-density CFU-F cultures show high expression of Cre-recombinase in primitive colonies which is additional evidence that Col3.6 forces recombination at an early MPC-like level (Liu, Woitge et al. 2004). Thus, we propose that recombination driven by Col3.6-Cre is one method that can be used to study effects of gene deletion on MPC function *in vivo*. However, it is still possible that an unidentified population of neurons express Col3.6 and that ObRb deletion in these cells is contributing to the $3.6^{Cre+\ F/F}$ mouse phenotype. When leptin receptors are completely deleted in the hypothalamus *in vivo* this results in decreased length and trabecular bone of the femur (Hamrick, Pennington et al. 2004). Since the $3.6^{Cre+F/F}$ mice have longer femurs with increased trabecular bone, it is not yet clear how non-specific brain recombination would contribute to the bone phenotype. However, future studies will continue to explore this possibility. Col2.3 promoter expression is more restricted and shows deletion primarily in more differentiated osteoblasts (Liu, Woitge et al. 2004). We have used the above premise to explore the contrasting *in vitro* mineralization phenotypes found in leptin-signaling deficient BMSCs that were generated *in vitro* (AdCre) or *in vivo* (ob/ob and db/db).

When determining the ability of ob/ob and db/db cells to mineralize *in vitro,* an unanticipated finding was that despite decreases in femoral trabecular bone content *in*

*vivo* (Hamrick, Pennington et al. 2004) the cells actually mineralized more than their controls *in vitro*. This was matched by increases in osteocalcin expression and for ob/ob, increases in alkaline phosphatase activity. ALP activity is variable in murine BMSC cultures and we do not yet understand the significance, if any, of the non-significant differences between WT and db/db BMSCs. This finding of high mineralization was initially assumed to be due to unknown systemic complications of diabetes and obesity. Addition of recombinant leptin did not reduce the mineralization of the cells to baseline levels implying that the starting population derived from ob/ob mice is unique when compared to WT. Previous publications have shown that leptin is able to enhance mineralization at higher concentrations (0.6-1.2μg/mL) (Chang, Shih et al. 2006). The systemically healthy $3.6^{Cre+F/F}$ ObRb mouse model which exhibited an opposite *in vivo* phenotype of increased trabecular BVF and BMD in the femur also showed increased mineralization potential *in vitro* similar to the ob/ob and db/db mice. This suggests that *in vivo* the systemic environment is driving differentiation of the MPCs in opposite directions in the ob/ob (increased medullary fat) and $3.6^{Cre+F/F}$ (increased trabecular bone) mice. Despite these differences *in vivo*, culture of the cells *in vitro* revealed uniform increased sensitivity to osteoblast differentiation. In contrast, deletion of ObRb in cultured and passaged P2 BMSCs *in vitro* decreased mineralization. We believe that this *in vitro* deletion occurs when mesenchymal lineage cells are fundamentally very different and more differentiated than the *in vivo* deletion that occurs in primitive in MPC of ob/ob, db/db and $3.6^{Cre+F/F}$ mice. While an absence of leptin signaling in primitive cells results in MPC with enhanced differentiation potential, ObRb disruption in differentiated cells *in vitro* is inhibitory to osteoblast differentiation but promotes adipogenic

differentiation. As observed with the $2.3^{Cre+F/F}$ mouse and one previous publication (Shi, Yadav et al. 2008), inhibition of leptin's actions on osteoblasts does not appear to be physiologically relevant to trabecular bone parameters during states of healthy equilibrium *in vivo*.

Even in the presence of intact leptin signaling, obesity can have significant effects on bone cell function *in vitro* and bone mass *in vivo* (Cao, Gregoire et al. 2009; Iwaniec, Dube et al. 2009). Studies that have analyzed bone parameters in mice due to diet-induced obesity observed increases in cortical parameters of the femur (Iwaniec, Dube et al. 2009) with no change (Iwaniec, Dube et al. 2009) or decreases (Cao, Gregoire et al. 2009) in trabecular parameters. These studies observed changes in obese mice of age 14-25 weeks that were approximately 32-38g. Despite being of comparable age and body mass to the diet-induced obese mice, our $3.6^{Cre+F/F}$ mice presented with statistically significant increases in trabecular bone parameters instead of decreases. Consistent with previous results (Iwaniec, Dube et al. 2009), we also observed cortical changes in our $3.6^{Cre+F/F}$ mice at 12 weeks that failed to persist and equalized by 42 weeks. Thus, we conclude that the trabecular bone phenotype is due to ObRb deletion and not increased load bearing.

Since systemic leptin is increased in the $3.6^{Cre+F/F}$ animals due to adipose accumulation, one must also consider the effects of leptin on osteoclast function. It is possible that the high bone mass observed in these animals is related to inhibition of osteoclast differentiation or activity. However, *in vivo* knockout of ObRb in osteoclast precursor

macrophages with the LysM-Cre promoter did not change body mass or bone parameters at 12 weeks (Table 3). In addition, published data do not support a consistent role for leptin in mature osteoclast function. For example, even though ob/ob and db/db mice have over two-fold increase in osteoclast number the excretion of urinary deoxypyridinoline crosslink, a biochemical marker of bone resorption, was not impaired when compared to controls (Ducy, Amling et al. 2000). Conversely, leptin deficient rats have increased osteoclast surface, but no increase in numbers (Tamasi, Arey et al. 2003). Isolation of primary bone marrow osteoclast progenitors from leptin-deficient mice showed no deficiency in osteoclast differentiation or their ability to form resorption lacunae on dentin (Ducy, Amling et al. 2000). Other *in vitro* studies demonstrated that leptin partially inhibits osteoclastogenesis of primary mouse marrow cultures but did not affect bone resorption of mature osteoclasts (Cornish, Callon et al. 2002).

Based on our data we propose a working model for peripheral leptin regulation of bone mass that includes divergent mechanisms depending on the differentiation state of the MPC (Figure 24). Generally, it is thought that a factor that controls MPC differentiation to adipocytes will inhibit differentiation toward osteoblasts and vice versa. However, in some situations a factor may block differentiation of primitive MPCs without regard for the downstream possibilities, in effect maintaining stemness. Here, we demonstrate that leptin may be one of the factors that functions to maintain MPCs in an undifferentiated state. Thus, in mice with leptin signaling deficient MPC there is enhanced bone formation and increased adipogenesis, and cells *in vitro* show increased differentiation to these fates. Future studies will pursue this hypothesis and work to uncover any potential

Col3.6 expressing neurons that may contribute to the bone and metabolic phenotype. Though we do not yet understand the full implications of this finding, there are multiple clinical scenarios that should be tested to uncover its relevance. For example, it has been previously reported that sites with high marrow fat content (and thus higher local leptin concentration) have a decreased rate of bone turnover (Wronski, Smith et al. 1981). It is possible that leptin's inhibition of MPC differentiation may play a role in this process. Or, perhaps limited fracture healing potential in obese individuals (Foulk and Szabo 1995) with increased systemic leptin may be related to leptin's limitation of *de novo* mesenchymal activation, osteoblast recruitment and subsequent matrix synthesis. In the future we hope to address these questions and expand our molecular understanding of leptin's regulation of MPC function. In summary, we conclude that though the effect of leptin on mature osteoblast function may not be physiologically significant *in vivo*, leptin has previously unrecognized peripheral roles in bone that include regulation of MPC differentiation.

### 3.6 Acknowledgments

Supported by R01 DE13835 (PHK/KDH), T32 DE07057 (ELS/PHK) and F30 DE019577 (ELS). Thank you to Martin Myers and Gina Leinninger for their comments regarding central leptin signaling.

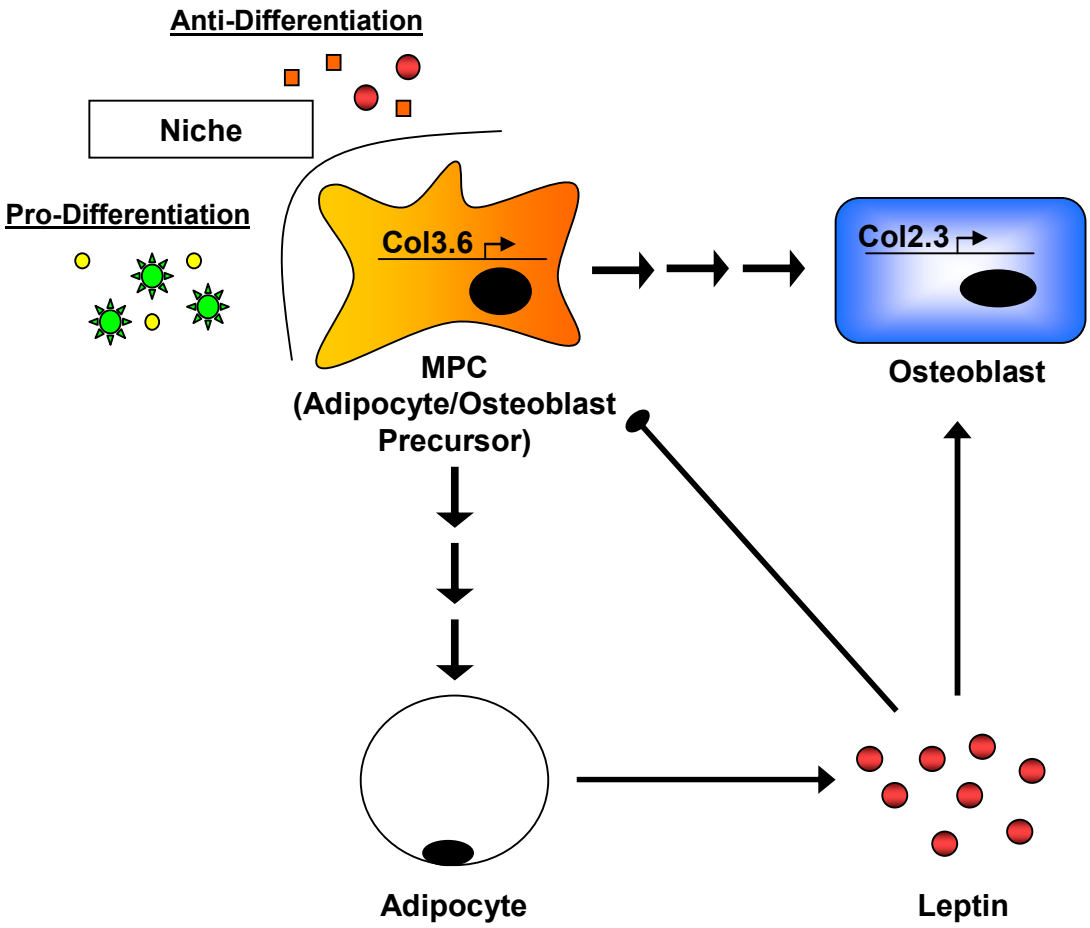


**Figure 24.** Peripheral model of leptin action on MPCs and osteoblasts. Leptin (1) helps to maintain MPCs in an undifferentiated state and (2) promotes differentiation and mineralization of *in vitro* pre-osteoblasts and osteoblasts. Credit: (Scheller, Song et al. 2010).

# CHAPTER 4

# ECTOPIC EXPRESSION OF COL-2.3 AND COL-3.6 PROMOTERS IN THE BRAIN – ASSOCIATION WITH LEPTIN SIGNALING AND CONTRIBUTION TO THE $3.6^{CRE+F/F}$ PHENOTYPE

## 4.1 Summary

We have used the collagen 2.3 and 3.6 promoters to drive Cre expression for generation of conditional transgenic mutant mice. Within the bone, Col3.6 is expressed by mesenchymal precursor cells (MPC) and their downstream progeny while Col2.3 is more osteoblast-specific. Our generation of transgenic mice with Col2.3-Cre and Col3.6-Cre driven deletion of the long-form leptin receptor (ObRb) necessitated a thorough analysis of non-specific expression of these promoters in the central nervous system. Both Col2.3 and Col3.6 were capable of forcing loxP recombination in the brain as demonstrated by EGFP expression in ROSA reporter mice. Expression of Col2.3 was limited to the central base of the brain near the third ventricle. In contrast, robust expression of Col3.6 was noted throughout the brain centering near the distal third ventricle, third ventricle, and aqueduct. We subsequently analyzed co-localization of leptin-responsive P-Stat3 neurons with Col3.6 expressing neurons. Approximately 5-10% co-localization was noted in leptin-responsive brain areas such as the arcuate nucleus, dorsal medial hypothalamus, ventral premammillary nucleus, and lateral hypothalamus. Injection of $3.6^{Cre+F/F}$ ObRb knockout mice with leptin confirmed the presence of an intact P-Stat3 response that was dampened in the lateral hypothalamus ($p<0.050$). This test was done to

explore the contribution of neural leptin signaling to the bone phenotype of the $3.6^{Cre+F/F}$ mice. Our analysis indicates that neural ObRb deletion, while present, is likely not the sole driver of the femoral changes through traditional sympathetic circuits.

## 4.2 Introduction

We previously reported a significant increase in both femur length and trabecular density in mice with conditional deletion of the long-form leptin receptor (ObRb) driven by Col3.6-Cre ($3.6^{Cre+F/F}$) (Scheller, Song et al. 2010). No bone changes were noted in Col2.3-Cre driven ObRb knockout animals ($2.3^{Cre+F/F}$). The Col2.3 and Col3.6 promoters are derived from the full-length collagen 1A1 (Col1A1) (Krebsbach, Harrison et al. 1993). Col3.6 contains a 3.6kb fragment (-3521 to +115) of the Col1A1 gene. Col2.3 consists of approximately 2.3kb of Col1A1 DNA upstream of the transcription start site (Krebsbach, Harrison et al. 1993). Col2.3-Cre is known to drive loxP recombination in the osteoblast and odontoblast populations (Kalajzic, Liu et al. 2002; Liu, Woitge et al. 2004). Col3.6-Cre in the marrow shows recombination in an earlier mesenchymal precursor cell (MPC) and its downstream progeny (Liu, Woitge et al. 2004). There is also evidence that Col3.6-Cre induces non-specific recombination in other tissues including tendon, muscle, skin, and adipose (Liu, Woitge et al. 2004; Scheller, Song et al. 2010).

Leptin is an adipokine and central regulator of food intake and metabolism (Pelleymounter, Cullen et al. 1995). Development of a leptin-signaling related bone phenotype is thought to have two potential sources. The first, and most common, occurs

due to alterations in leptin signaling in the brain (Ducy, Amling et al. 2000). Femur length is shortened in both leptin deficient ob/ob and ObRb knockout (KO) db/db mice as well as mice with a point mutation in ObRb that prohibits Stat3 signaling which suggests an anabolic effect of leptin (Myers personal communications)(Hamrick, Pennington et al. 2004; Ealey, Fonseca et al. 2006; Scheller, Song et al. 2010). Femur length deficits of leptin-deficient ob/ob mice can be fully corrected after 15 weeks by leptin gene therapy in the brain (Iwaniec, Boghossian et al. 2007) and also partially restored by peripheral intra-peritoneal (IP) injection of 50μg/day leptin for four weeks (Steppan, Crawford et al. 2000). The second possible mechanism of leptin-mediated bone changes occurs when leptin acts directly on a peripheral cell such as the MPC to regulate differentiation and subsequent bone formation (Scheller, Song et al. 2010).

Generation of a mouse model with floxed ObRb has allowed use of conditional ObRb KO mice to determine the relative contributions of the central and peripheral mechanisms of leptin regulation on bone formation (McMinn, Liu et al. 2004). Leptin or ObRb deficient mice have decreased femur length that is due to a central depletion of leptin signaling. In contrast, the femur length of our $3.6^{Cre+F/F}$ mice was increased by 5.4+/-0.16% in addition to approximately 80% increases in trabecular bone volume fraction and bone mineral density (Figure 21). We hypothesize that this is driven by peripheral deletion of leptin receptors on the MPC, but due to the non-specific recombination in other tissues can not yet rule out the contribution of central leptin actions. In this study we systematically investigated the ability of both Col2.3-Cre and Col3.6-Cre to drive non-specific loxP recombination in the brain. In addition, to determine the contribution

of central leptin signaling to the Col3.6 bone phenotype, we evaluated the ability of leptin to force recombination in leptin-responsive P-Stat3 positive neurons. Lastly, to determine if central leptin resistance may be contributing to the obesity of $3.6^{Cre+F/F}$ animals, we quantified the ability of leptin to induce phosphorylation of hypothalamic Stat3 in 42 week old $3.6^{Cre-}$ and $3.6^{Cre+F/F}$ mice.

## 4.3 Materials and Methods

### *Animals*

All procedures were approved by the University Committee on the Use and Care of Animals. Col2.3-Cre and Col3.6-Cre mice were obtained from Dr.Fei Liu (University of Michigan) (Liu, Woitge et al. 2004). ROSA-EGFP mice were obtained from Jackson Laboratory (Stock no: 004077). Col-Cre mice were crossed with ROSA reporter mice and three F1 pups per promoter were analyzed at 12-16 weeks of age. Cre genotyping primers: CreF CGCAGAACCTGAAGATGTTCGCGATTA; CreR TCTCCCACCGTCAGTACGTGAGATATC. $3.6^{Cre+F/F}$ mice were generated as described previously (Scheller, Song et al. 2010).

### *Leptin injection*

Co-localization studies: Mice were anesthetized with isoflurane and a 26 gauge ICV cannula was implanted into the lateral ventricle at A/P -0.34, M/L -1.0, D/V -2.4 (Franklin and Paxinos 1997). The cannula pedestal was affixed to the skull with surgical adhesive, wound closed, and a dummy injector placed for the duration of recovery. Recovery lasted for one week with analgesia (Buprenex) prior to and 12h post surgery.

Mice were then treated with 3µg leptin (3µL of 1mg/mL Leptin [a generous gift from Amylin] injected at a rate of 1 µL per minute).

Aged $3.6^{Cre+F/F}$ studies: 42 week old mice were injected intraperitoneally (IP) with 5 mg/kg leptin. Two hours post-treatment mice were anesthetized with an overdose of IP pentobarbitol and transcardially perfused with 10% normal buffered formalin.

***IHC***

Brains were removed, postfixed overnight and dehydrated in a 30% sucrose solution. Immunostaining was performed as described previously (Leinninger, Jo et al. 2009). A freezing microtome was used to collect 30µm serial coronal sections, collected in four consecutive series. Brain sections were incubated in rabbit anti-P-STAT3 (1:250, Cell Signaling) and chicken anti-GFP (1:1000, AbCam) overnight at room temperature, then visualized by using a biotin-conjugated secondary antibody (1:250, Jackson Immuno Research) and DAB (Vectastain ABC kit, Thermo Scientific) or secondary immunofluorescence using species-specific Alexa-488 or −568 antibodies (1:200, Invitrogen). Stained sections were mounted onto gelatin-coated slides using ProLong Gold Antifade reagent (Invitrogen).

***Image Analysis and Statistics***

Sections were imaged with NIS-Elements on a Nikon Eclipse E600 and grouped into composite images for each brain region to be analyzed. ImageJ was used to threshold the composites and determine the number of positive neurons per unit area in each brain region (Abramoff, Magelhaes et al. 2004). A two-tailed, homoscedastic t test was used to

determine significance between control and experimental groups at $p<0.050$. Values are reported as mean ± the standard deviation.

## 4.4 Results

### *Both Col3.6-Cre and Col2.3-Cre induce neural loxP recombination*

Col2.3-Cre and Col3.6-Cre were bred with ROSA-EGFP reporter mice (Scheller, Leinninger et al. 2011). Cre recombinase forces recombination of loxP sites and excision of the intervening DNA in tissues that express Col2.3 or 3.6. Coronal sections of the mouse brain were collected and stained, our figure presents representative images from four brain regions measured with respect to Bregma (Figure 25). Deletion of loxP removed a stop sequence in front of an enhanced green fluorescent protein (EGFP) locus (Figure 26) (Mao, Fujiwara et al. 2001). Expression of EGFP in the brain of $2.3^{ROSA\text{-}EGFP}$ and $3.6^{ROSA\text{-}EGFP}$ was analyzed indirectly with an anti-GFP antibody. Few positive neural cells in the $2.3^{ROSA\text{-}EGFP}$ mice were noted with most expression located near the base of the brain around the bottom of the third ventricle (3V), including the arcuate nucleus of the hypothalamus (Figure 26). The $3.6^{ROSA\text{-}EGFP}$ mice showed significantly more positive cells in regions spanning from the forebrain to the hindbrain centered predominantly around the third ventricle (3V), dorsal third ventricle (D3V) and aqueduct (Aq) (Figure 26). In the hypothalamus the ventral medial hypothalamus (VMH,*) was specifically negative for $EGFP^{+}$ neurons (Figure 26).

### *Col3.6 induces mild co-localization with leptin-responsive neurons*

Injection of leptin IP or directly into the lateral ventricle produced a robust P-Stat3 response in hypothalamic brain regions including the posterior hypothalamus (PH), ventral premammillary nucleus (PMv), arcuate nucleus (Arc), dorsal and ventral medial hypothalamus (DMH/VMH), and lateral hypothalamic area (LHA), consistent with previous reports (Faouzi, Leshan et al. 2007). We also examined representative sections from one of four series per brain including the ventral tegmental area and pre-optic areas. An average of 5-10% of P-Stat3 positive neurons co-localized with $EGFP^{+}$ cells in the ARC, VMH, PMv, and LHA (Figure 27). When repeated with Col2.3 mice, very little co-localization was noted (0-1%) with the highest levels present in the arcuate nucleus (Figure 28).

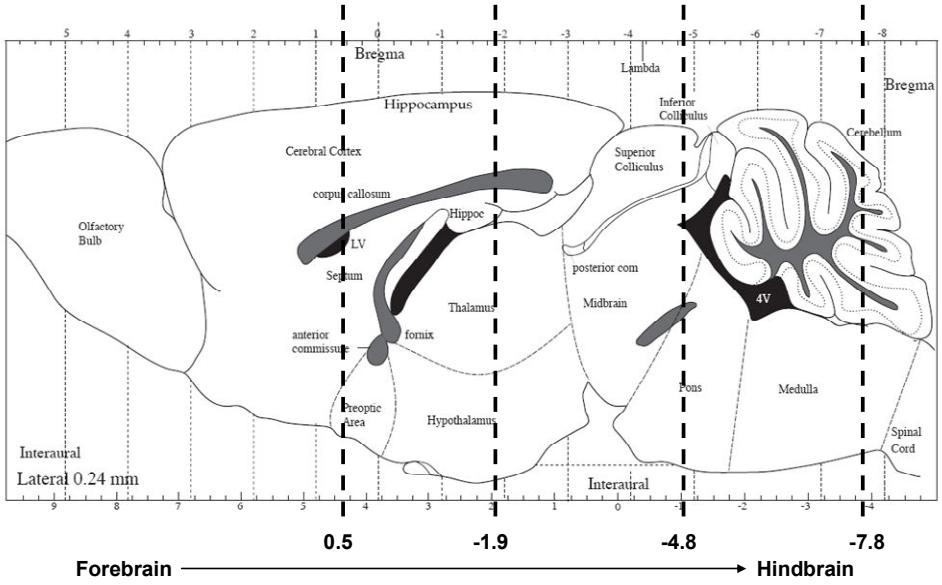


**Figure 25.** Diagram of the mouse brain. Serial frozen sections were harvested through the entire mouse brain. Sections were evenly divided into four groups to generate four representative sets of brain tissue. One set was stained and analysed for enhanced green fluorescent protein expression. Presented images represent sections as indicated with dashed lines and are labeled in relation to the landmark Bregma. Image Credit: The Mouse Brain in Stereotaxic Coordinates, 2nd Edition, G Paxinos and K. B. J. Franklin. ©2001 by Academic Press. Used with permission.

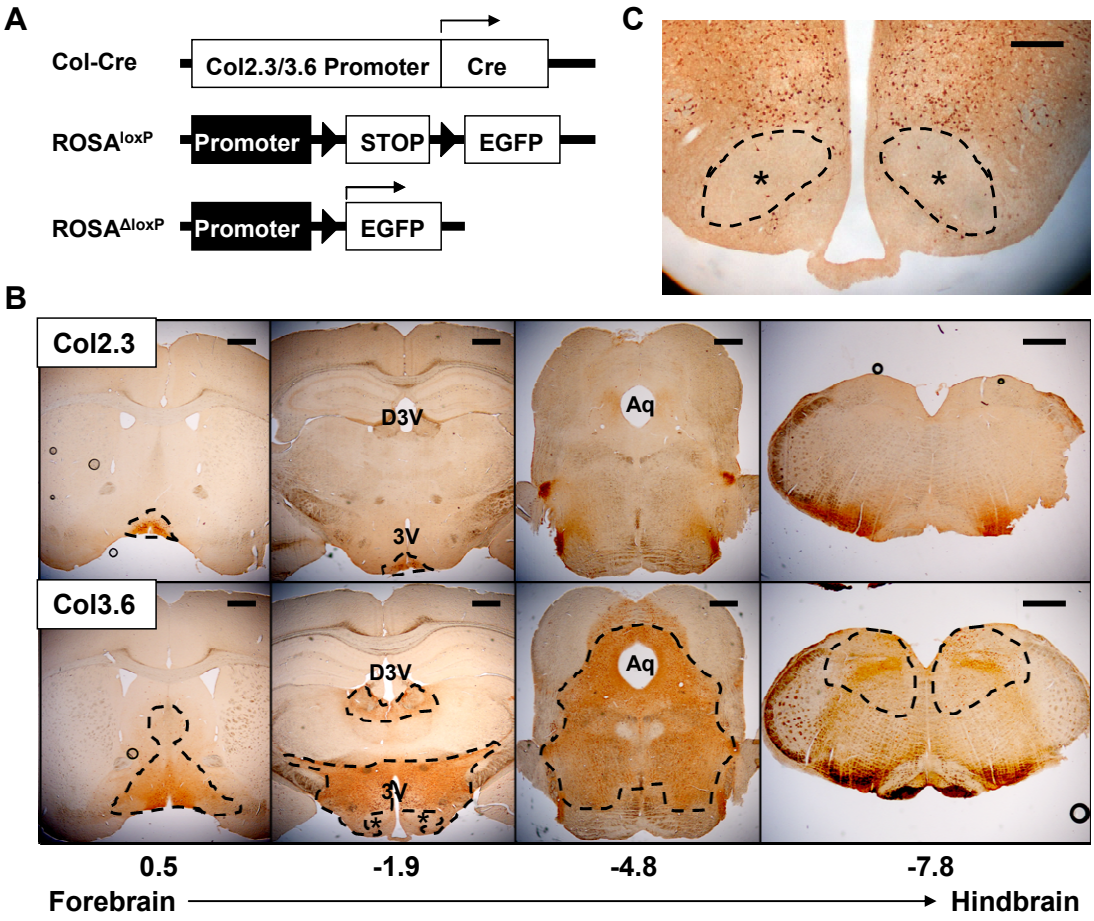


**Figure 26.** Ectopic expression of Col2.3 and Col3.6 promoters in the brain. **(A)** Col2.3-Cre and Col3.6-Cre were bred with GFP ROSA reporter mice. Cre driven recombination of loxP sites (triangles) facilitated expression of EGFP. **(B)** Resulting expression of EGFP in the brain was analyzed. **(C)** Col3.6-Cre driven neural deletion was nearly absent in the ventral medial hypothalamus. D3V: dorsal third ventricle, 3V: thrid ventricle, Aq: aqueduct, *Ventral Medial Hypothalamus. Credit: (Scheller, Leinninger et al. 2011)

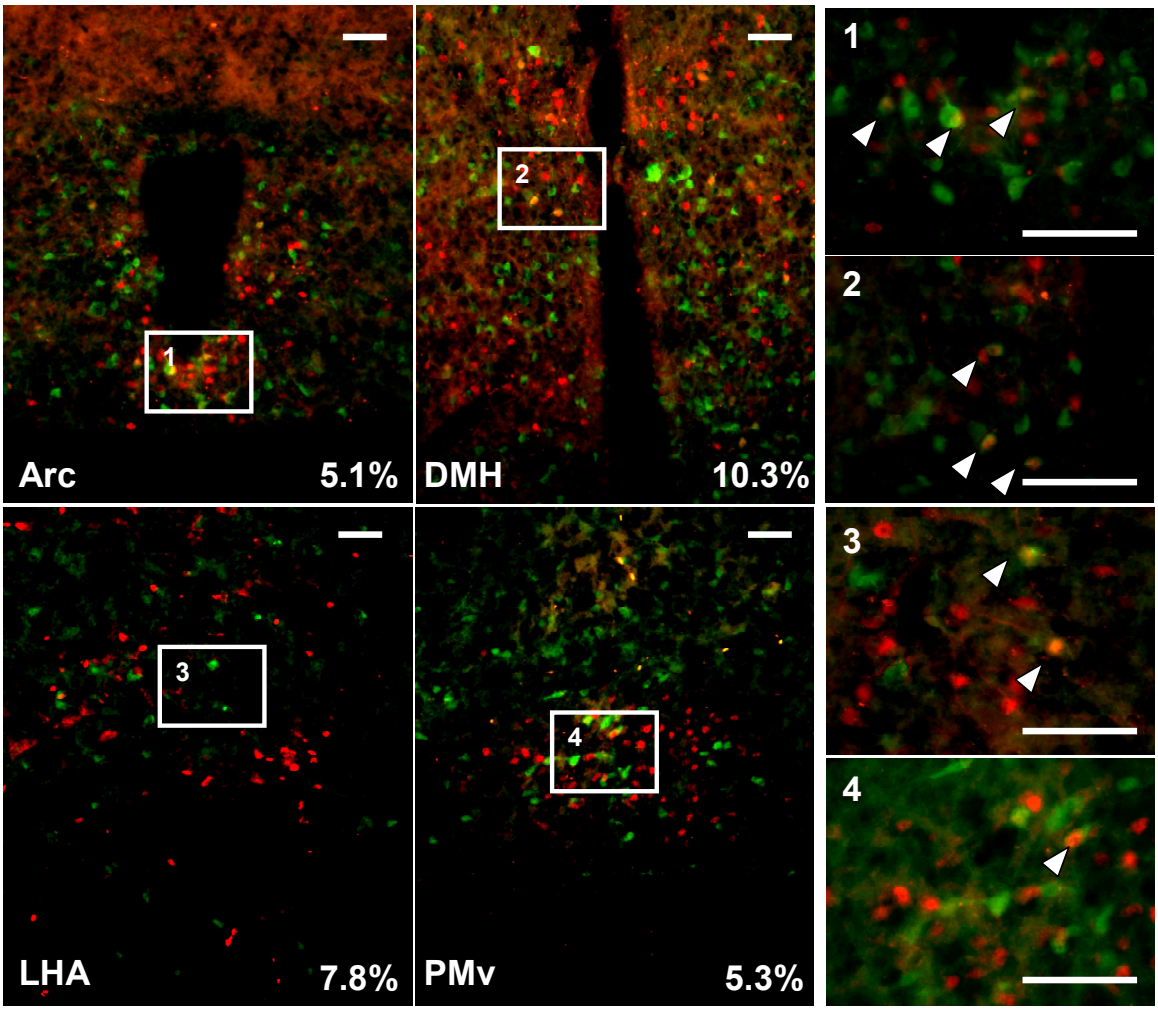


**Figure 27.** Co-localization of Col3.6 driven loxP recombination and leptin induced P-Stat3 in the hypothalamus. $3.6^{ROSA\text{-}GFP}$ mice were treated with leptin directly into the lateral ventricle of the brain. Leptin-responsive P-Stat3 neurons are pictured in red and EGFP positive neurons in green. Approximately 5-10% co-localization of P-Stat3 neurons with EGFP was noted in the arcuate nucleus (Arc), dorsal medial hypothalamus (DMH), lateral hypothalamic area (LHA), and ventral premammillary nucleus (PMv). Credit: (Scheller, Leinninger et al. 2011)

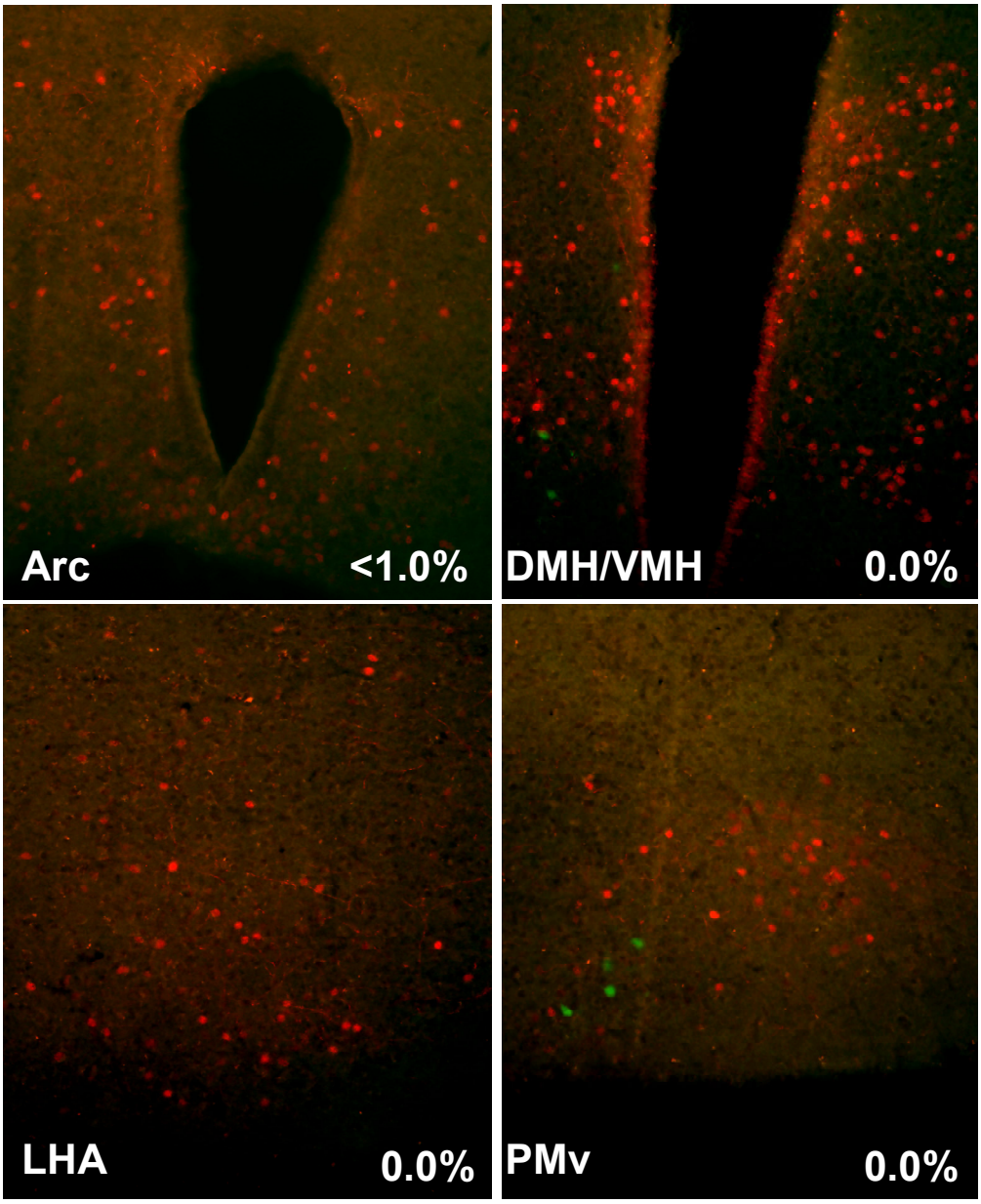


**Figure 28.** Co-localization of Col2.3 driven loxP recombination and leptin induced P-Stat3 in the hypothalamus. $2.3^{ROSA\text{-}GFP}$ mice were treated with leptin directly into the lateral ventricle of the brain. Leptin-responsive P-Stat3 neurons are pictured in red and EGFP positive neurons in green. Approximately 0-1% co-localization of P-Stat3 neurons with EGFP was noted in the arcuate nucleus (Arc), dorsal medial hypothalamus (DMH), lateral hypothalamic area (LHA), and ventral premammillary nucleus (PMv). Credit: (Scheller, Leinninger et al. 2011)

### *Aged 3.6$^{Cre+F/F}$ mice have intact, but decreased central leptin response*

The presence of co-localization of P-Stat3 and EGFP$^{+}$ neurons implies that leptin signaling may be decreased in the 3.6$^{Cre+F/F}$ mice. In addition, it has been previously reported that obesity enhances leptin resistance (Faouzi, Leshan et al. 2007). Therefore, we examined the combination of ObRb deletion and leptin resistance on the P-Stat3 response in 42 week old male 3.6$^{Cre+F/F}$ mice. We found that 3.6$^{Cre+F/F}$ mice had increased baseline P-Stat3 staining in regions such as the PMV (Figure 29). The 3.6$^{Cre+F/F}$ mice also had decreased P-Stat3 response to IP-delivered leptin in the LHA, Arc and DMH/VMH when compared to controls (Figure 29). Due to high background P-Stat3 staining in the arcuate nucleus a significant increase in staining could not be detected after leptin addition in either group (Figure 29). However, there was a significant reduction of P-Stat3 positive neurons in the Arc of leptin-treated 3.6$^{Cre+F/F}$ mice when compared to controls (Figure 29). Longitudinal food intake analysis of 24 to 28 week old female mice revealed that after 14 days significant differences in chow consumption were noted (Figure 29a). These changes continued to be significant after 28 days, though no change in average body mass was noted in the 3.6$^{Cre-}$ or 3.6$^{Cre+F/F}$ animals during that time (Figure 29a).

## 4.5 Discussion

The first goal of this study was to examine expression of the Col3.6 and Col2.3 promoters in the brain to determine the potential role for non-specific central ObRb deletion in the bone phenotype of the 3.6$^{Cre+F/F}$ mice (Table 6). We found significant cre-induced loxP recombination with both promoters, though Col3.6-Cre induced much more

widespread deletion that centered on the 3V, D3V, and Aq. Unanticipated neural expression is not unique to these promoters and has also been found with the previously-assumed adipose-specific Fabp4-Cre, Jackson Labs stock no:005069 (Heffner and Sharma 2010). These unexpected findings highlight the need to perform full body

**A**

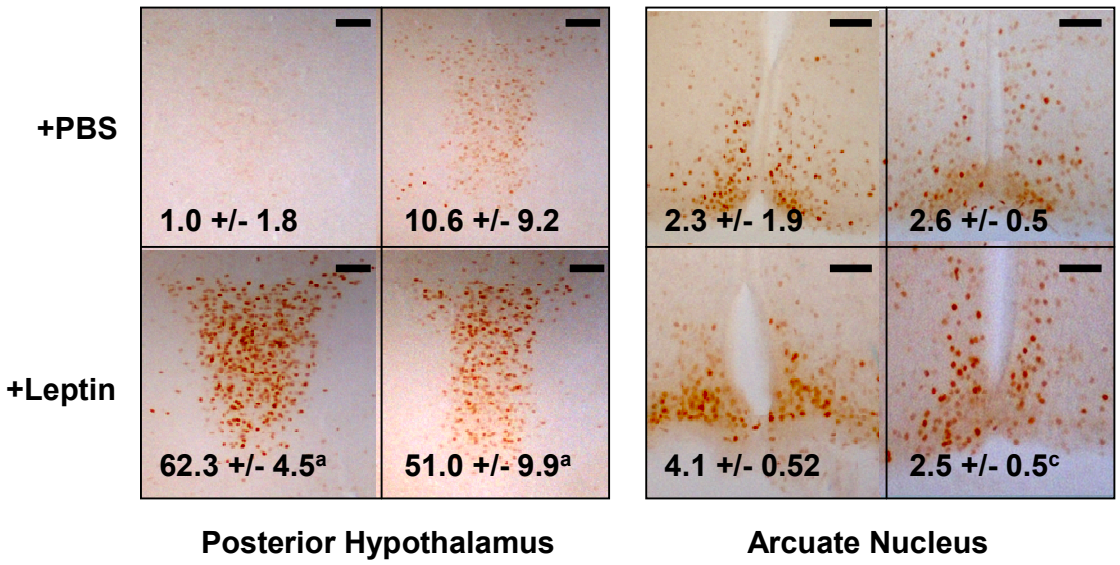


**B**

| | DMH/VMH | LHA | PMV |
|---|---|---|---|
| **Cre- PBS** | 0.04+/-0.07 | 0.40+/-0.44 | 0.21+/-0.04 |
| **Cre- Lep** | 17.0+/-12.2[d] | 7.17+/-3.32[a] | 7.18+/-2.1[a] |
| **Cre+ PBS** | 0.89+/-1.49 | 0.16+/-0.21 | 1.58+/-0.30[b] |
| **Cre+ Lep** | 4.36+/-2.02[d] | 2.70+/-1.7[a,c] | 10.8+/-4.6[a] |

**Figure 29.** Leptin induces a P-Stat3 response in both control and $3.6^{Cre+F/F}$ mice. Fourty-two week old mice received intraperitoneal injection of 5mg/kg leptin two hours before perfusion and analysis. **(A)** Representative images from the posterior hypothalamus and arcuate nucleus. **(B)** Additional quantified data from hypothalamic brain regions. N=3. a: significant over matched PBS; b: significant over control PBS; c: significant over control leptin; d: non-significant trend over matched control $p<0.100$. Credit: (Scheller, Leinninger et al. 2011)

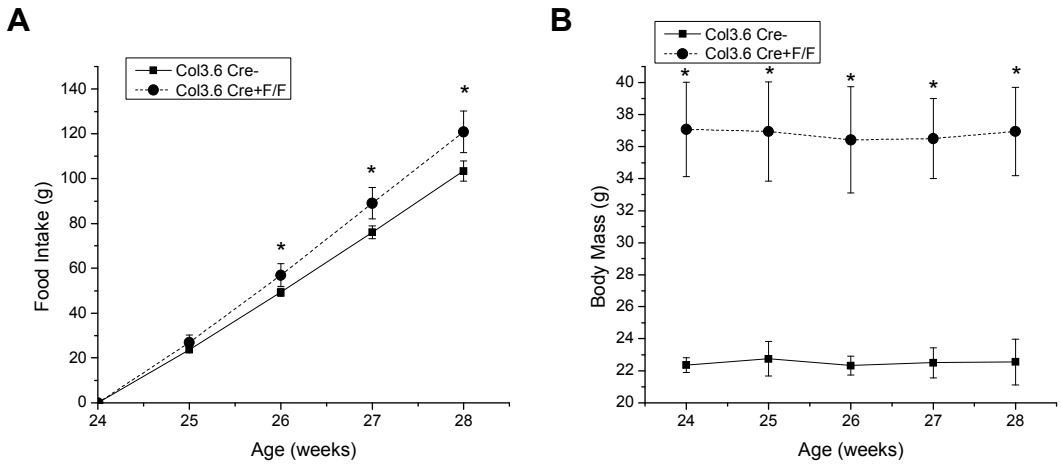


**Figure 29a.** Longitudinal food intake analysis of $3.6^{Cre-}$ and $3.6^{Cre+F/F}$ mice. Female mice from 24 to 28 weeks were single housed and provided 90-100g of food per week. Chow consumption and body mass was quantified every seven days. Bedding was checked for dropped food particles. **(A)** Total chow consumption. **(B)** Average body mass. N=4. *: significant over matched control. Credit: E.L. Scheller, unpublished data.

analysis when characterizing tissue-specific transgenic animals. The further address the aim of this study we examined co-localization of neurons lacking ObRb with leptin-induced P-Stat3 signaling. Co-localization studies revealed that while Col3.6 was expressed widely in the brain, the neurons that were affected only overlapped with leptin-responsive P-Stat3 neurons in 5-10% of cases. In the case of Col2.3, co-localization was nearly absent. As previously discussed, complete ObRb KO mice have decreased femur length. It is thus unlikely that removal of 5-10% of central leptin signaling would result in the opposite phenotype of increased femur length through a mechanism that involves direct sympathetic regulation of osteoblasts or osteoclasts (Ducy, Amling et al. 2000).

The second goal of this study was to determine the potential contribution of central leptin signaling to the increased accumulation of peripheral fat observed in our $3.6^{Cre+F/F}$ mice (Figure 18). Though we believe that the observed 5-10% co-localization is unlikely to

drive the observed bone phenotype, it is highly possible that neural modulation of food intake is dose dependently related to the number of active leptin receptors in the hypothalamus. Thus, decreasing the ability of leptin to signal through P-Stat3, even by only 5-10%, may result in a slight change in food intake and adipose accumulation. Development of slight central leptin resistance with age as we also observed may further compound this hyperphagia. However, it should be noted that both $3.6^{Cre-}$ and $3.6^{Cre+F/F}$ animals had similarly high levels of background P-Stat3 in the arcuate nucleus making any effect of leptin impossible to determine. The arcuate nucleus is thought to be the main center controlling leptin regulation of food intake (Satoh, Ogawa et al. 1997). This, combined with the modest 5-10% co-localization, may explain why food intake changes were only observed longitudinally and not significant enough to be detected upon acute analysis.

### 4.6 Acknowledgments

Supported by R01-DE13835 (PHK), F30-DE019577 (ELS) and NIH DK57768 (MGM)

# CHAPTER 5

# ZOLEDRONIC ACID INHIBITS MACROPHAGE SOCS3 EXPRESSION AND ENHANCES CYTOKINE PRODUCTION

## 5.1 Summary

Suppressor of cytokine signaling-3 (SOCS3) has multiple functions including inhibition of Janus kinase activity, regulation of protein degradation, and suppression of cytokine signaling. SOCS3 modulates macrophage response to cytokines such as IL-6 and leptin that are systemically induced in obesity. Obesity is a suspected risk factor for SOCS3-related pathology such as rheumatoid arthritis and Crohn's disease as well as zoledronic acid (ZA)-induced osteonecrosis of the jaw (ONJ). Thus, understanding the ability of bisphosphonates to modulate SOCS3 is necessary to qualify their contribution to these disorders. ONJ occurs in up to 10% of patients using intravenous bisphosphonates and has an unknown pathogenesis that may be linked to decreased bone turnover, altered vascularity, bacterial invasion, and compromised wound healing. Given the increased risk of ONJ with obesity and importance of macrophages in wound healing, we hypothesized that amino-bisphosphonates could contribute to the pathogenesis of ONJ by regulating macrophage responses to cytokines such as leptin and IL-6. We report that zoledronic acid is a novel inhibitor of SOCS3 in primary macrophages and human ONJ biopsy specimens. Inhibition of SOCS3 by ZA resulted in significant increases in IL-6 production. SOCS3 transcription is regulated by nuclear accumulation of phosphorylated-Stat3 (P-Stat3). We found that ZA decreased phosphorylation of Stat3 in

a mevalonate-pathway dependent manner. However, restoration of P-Stat3 was not sufficient to correct SOCS3 inhibition. We propose that disruption of macrophage SOCS3 expression by amino-bisphosphonates such as ZA may be a novel contributor to inflammatory phenotypes in obesity and the pathogenesis of ONJ.

## 5.2 Introduction

Suppressor of Cytokine Signaling-3 (SOCS3), a member of the SOCS family of proteins, has multiple domain-specific functions that include inhibition of Janus kinase (Jak) activity, competition with signal transducer and activator of transcription (Stat) proteins, regulation of protein degradation, and suppression of cytokine signaling (Piessevaux, Lavens et al. 2008). Expression of SOCS3 is induced by extracellular binding proteins such as interleukin 6 (IL-6), IL-10, interferon gamma (IFN-y), bacterial lipopolysaccharide (LPS), and leptin. Complete deficiency of SOCS3 in mice is lethal due to placental defects (Yasukawa, Ohishi et al. 2003), however, conditional deletion has revealed a wide role for SOCS3 in cells and tissues including macrophages (Ohishi, Matsumura et al. 2005), the central nervous system (Mori, Hanada et al. 2004), T cells (Kinjyo, Inoue et al. 2006), the pancreas (Mori, Shichita et al. 2007), and the liver (Ogata, Chinen et al. 2006). Alterations in SOCS3 protein levels may play a significant role in the pathogenesis of inflammatory diseases including rheumatoid arthritis (Isomaki, Alanara et al. 2007), inflammatory bowel disease (Suzuki, Hanada et al. 2001), and Crohn's disease (Lovato, Brender et al. 2003).

Zoledronic acid (ZA) is a commonly used amino-bisphosphonate medication that is approved in the United States for treatment of Paget's disease, postmenopausal osteoporosis, multiple myeloma, and bone metastases from solid tumors (Ibrahim, Scher et al. 2003). Additional off-label uses such as treatment of osteoarthritis and rheumatoid arthritis are growing increasingly popular (Jarrett, Conaghan et al. 2006; Zoler 2010). ZA is highly potent with a half-life potentially exceeding 10 years and becomes incorporated in the bone after initial administration (Khan, Kanis et al. 1997). The compound is then gradually released during bone remodeling. This generates potential for long-term systemic effects and has been linked to complications such as osteonecrosis of the jaw (ONJ). ONJ is diagnosed when a patient with a history of bisphosphonate use and without previous radiation treatment presents with exposed bone in the oral cavity that fails to heal after eight weeks (Novince, Ward et al. 2009). A survey of over 700,000 medical claims revealed that those taking IV bisphosphonates were at a four to six-fold increased risk of requiring jaw surgery due to inflammatory changes (Cartsos, Zhu et al. 2008) and a survey of cancer patients specifically taking ZA found a 30-fold increase in risk of ONJ (Wessel, Dodson et al. 2008).

In patients taking ZA, obesity is also a risk factor for development of ONJ (Wessel, Dodson et al. 2008). Obesity has been linked to significant increases in systemic markers of inflammation such as c-reactive protein and circulating inflammatory cytokines such as leptin, IL-6, and TNF-α (Considine, Sinha et al. 1996; Das 2001; Fontana, Eagon et al. 2007). Obesity is also a suspected risk factor for SOCS3-related inflammatory disorders such as rheumatoid arthritis and Crohn's disease (Voigt, Koepsell et al. 1994; Mendall,

Gunasekera et al. 2011). Given the increasing prevalence of amino-bisphosphonate use, understanding the ability of these compounds to modulate inflammation and macrophage cytokine production is necessary to qualify their contribution to these disorders.

The main function of amino-bisphosphonates such as ZA is to reduce osteoclast activity both by induction of osteoclast apoptosis (Sudhoff, Jung et al. 2003) and inhibition of osteoclast maturation through blockage of protein prenylation and geranyl-geranylation in myeloid precursor cells (Coxon, Helfrich et al. 2000; Russell, Watts et al. 2008). Although the macrophage and the osteoclast originate from a common precursor, much less is known about the effects of bisphosphonates on macrophage gene expression. Macrophages play an important role in the early phase of wound healing. In addition to the phagocytosis of debris and bacteria, macrophages release cytokines that promote proliferation of fibroblasts and endothelial cells. Some studies have suggested that reduced macrophage infiltration may, in part, be responsible for the increased rate of healing in oral mucosa compared to dermal sites (Szpaderska, Zuckerman et al. 2003). We previously demonstrated that macrophages are present in human ONJ biopsy specimens with a trend toward increased macrophage numbers in patients with IV bisphosphonate-induced ONJ (Scheller, Baldwin et al. 2011). Thus, understanding the mechanisms by which bisphosphonates regulate macrophage functions, such as cytokine secretion, may provide insight into the pathogenesis of ONJ and lead to discovery of new therapeutic targets. Given the increased risk of ONJ with obesity and the importance of macrophages in wound healing, we hypothesized that amino-bisphosphonates could

contribute to the progression of ONJ and other inflammatory disorders by regulating macrophage responses to systemic cytokines such as leptin and IL-6.

## 5.3 Materials and Methods

### *Transgenic Mice*

All procedures were approved by the University Committee on the Use and Care of Animals. Mice with the coding sequence for exon17 of the long-form leptin receptor (ObRb) flanked by loxP were obtained from Dr. Martin Myers (University of Michigan) with permission of Dr. Streamson Chua (Columbia University) (McMinn, Liu et al. 2004). Mice with germline transmission of the recombined floxed region and inactivation of leptin receptor signaling were used in our study and are referred to as knockout (KO) mice. ObRb transgenic s/s (point mutation at tyrosine 1138) and l/l (point mutation at tyrosine 985) mice were the generous gift of Dr. Peter Mancuso (University of Michigan) and are also available from Jackson Labs (Stock No. 008518 and 008385). Genotyping of s/s, l/l, and ObRb KO mice was performed from tail biopsy as described previously (Bates, Stearns et al. 2003; McMinn, Liu et al. 2004; Bjornholm, Munzberg et al. 2007). Recombination and deletion of the loxP flanked allele was determined using a three-primer system designed by McMinn et al (McMinn, Liu et al. 2004).

### *Cell Culture*

#### Human

Primary human bone marrow macrophages (hBMMs) were differentiated from primary marrow of iliac crest specimens (60 year old male) obtained with University of Michigan

Institutional Review Board (IRB) approval. Fragments were washed extensively with PBS and marrow suspension processed with Lympholyte® Mammal gradient cell separation media (Cedarlane® Laboratories, Cat:CL5110) to remove dead cells and erythrocytes. Briefly, 4mL cell suspension was layered on 3mL Lympholyte® and centrifuged at 800g for 20 minutes at room temperature. The lymphocyte layer was harvested with a Pasteur pipet and washed three times in media. Cells were plated in macrophage growth medium (α-Modified Eagle's Medium (α-MEM; Invitrogen/Gibco), 10% FBS (Gibco, Lot no.451459), 100U/ml penicillin, 100mg/ml streptomycin sulfate (Gibco Cat:15140)) at a density of 700,000 cells/$cm^2$ in 100ng/mL recombinant human macrophage colony stimulating factor (M-CSF) (Peprotech, Cat:300-25). Media was replenished after two days. At day four serum free media ± ZA was added overnight before stimulation with 50ng/mL IL-6 (Peprotech, Cat:200-06) for five hours.

**Mouse**

Bone marrow macrophages (BMMs) were generated by plating the total marrow from two mice (femora, tibiae, and humeri) to 36-wells of two 24-well plates for ELISA or five 60mm dishes for Western blot analysis. Cells were derived in macrophage growth medium plus 70ng/mL M-CSF (Peprotech, Cat:315-02)) for 2-3 days. Primary BMMs were serum starved in the presence of ZA ((Novartis, Zometa®) overnight (16-18 hours) before treatment with 100nM recombinant mouse leptin (R&D Systems, Cat:398-LP-01M), 20% fetal bovine serum, or 25ng/mL IL-6 (PeproTech, Cat:216-16) for 1 hour for qPCR, 3 hours for Western blot analysis, or 24 hours for ELISA. Cells were treated with

5-10μM *trans,trans*-Farnesol (FOH) (Sigma:277541) or geranylgeraniol (GGOH) (Sigma:G3278) where indicated.

***ELISA***

BMMs were plated in 24-well plates, six wells per data point per experiment. All experiments were repeated at least twice. After three days of BMM differentiation, cells were serum starved in the presence of $10^{-7}$ to $10^{-5}$M ZA overnight. Subsequently, 250uL of α-MEM + 0.5% BSA (Sigma, Cat:A8806) containing fresh ZA and 100nM Leptin as added as indicated. Supernatant was harvested after 24 hours and stored at -80$^{o}$C until analyzed. Post-supernatant removal, genomic DNA was harvested using the QIAGEN DNeasy kit (Cat:69506) by adding PBS, proteases, and buffer directly to each well followed by incubation of the whole plate at 55$^{o}$C. Harvested DNA was quantified using a UV spectrophotometer at 260nm. Ratio of 260nm to 280nm absorbance was greater than 1.4 for sample acceptance. Ten to twenty-five microliters of supernatant was analyzed with an IL-6 ELISA kit (R&D Systems, Cat:M6000B). Results from each well were normalized to total genomic DNA.

***Western Blot Analysis***

Protein was harvested using NP-40 lysis buffer (10% glycerol, 1% NP-40, 50mM Tris pH 7.4, 200mM NaCl, 2mM $MgCl_2$, 1mM PMSF, 1xProtease Inhibitor Cocktail (Sigma Cat:P8340)). Cells were collected and pelleted in 1mL ice cold PBS at 4$^{o}$C. Cell pellets were resuspended in 25-50μL of lysis buffer, incubated for 30min on ice, centrifuged at 13,000rpm for 10 minutes, and supernatant harvested. Protein concentration was

measured at 595nm with Bio-Rad protein assay dye concentrate (Cat:500-0006). Protein extracts (30-80µg) were boiled in 2x SDS sample buffer 5min and separated on a 12% Tris-HCl polyacrylamide gel (Bio-Rad). Protein was transferred to PVDF membranes using a wet transfer system (Bio-Rad Cat:170-3930). Membranes were blocked in 5% milk (Stat3, P-Stat3, GAPDH; Bio-Rad, Cat:170-6404) or 5% BSA (SOCS3, Sigma, Cat:A7906) one hour and probed overnight with 1:1000 P-Stat3 (Cell Signaling:9131) or 1:1000 SOCS3 (Cell Signaling:2923) and stripped and re-probed the next day with 1:1000 Stat3 (Cell Signaling:9132) and/or 1:1000 GAPDH (Chemicon® International:MAB374). Signals were amplified with 1:3000 HRP-conjugated secondary antibody (Santa Cruz Biotechnology) and SuperSignal® West Pico Chemiluminescent Substrate (Thermo Scientific, Pierce Product) and developed using film exposure.

***Human Tissue Collection***

Biopsies were accessioned with University of Michigan IRB approval. Biopsies were identified as described previously (Scheller, Baldwin et al. 2011) and assigned to one of two groups, no BP history (control) or ONJ. H&E stained slides of all cases were examined to ensure that each specimen contained epithelium and connective tissue. Histological identification of non-vital bone with associated bacterial colonies, consistent with osteonecrosis, was also required.

***Immunofluorescence***

Cells were fixed for 5 minutes in methanol at -20$^{o}$C before PBS wash and permeabilization with 1% Triton-X-100 in PBS. Cells were blocked in PBS+2.5% goat

serum+2.5% donkey serum+0.1% Triton-X-100 for 30 minutes. CD68 primary antibody (1:500, AbCam:ab955) was added in 1:10 diluted block for one hour and after washing signal was amplified with secondary antibody (1:500 Donkey anti-mouse Cy$^{TM}$3, Jackson ImmunoResearch) for 45 minutes. Nucleic acids were visualized with DAPI.

***Immunohistochemistry***

Immunohistochemistry was performed as described previously (Scheller, Baldwin et al. 2011). Formalin-fixed sections were deparaffinized in xylene and rehydrated. Antigen retrieval was performed in pH 6.0 citrate buffer. Endogenous peroxidase was quenched in 3% hydrogen peroxide for 30 minutes followed by permeabilization in 0.1% Triton-X-100 in PBS. Slides were blocked with 2.5% normal horse serum. Primary antibodies were added overnight at 4$^{o}$C: CD68 (1:500, Abcam:ab955) and SOCS3 (1:500, Abcam:ab16030). Signal was amplified with ImmPRESS reagent (VectorLabs:MP-7500) and imaged with ImmPACT DAB substrate (VectorLabs:SK-4105). Slides were counterstained with hematoxylin. Serial sections were stained for CD68 and SOCS3. Comparison was performed by generating a representative image composite of all CD68 or SOCS3 stained sections to ensure identical analysis of all images (40x magnification), images were then processed with Adobe Photoshop CS3 by using select→color range→reds to remove background blue hematoxylin staining. The resulting composite was thresholded with ImageJ (Scion Corp., Frederick, MD, USA) and total pixel density of stain per total field size of each specimen recorded. Results are expressed as the ratio of SOCS3 stain density to CD68 stain density in percent.

***PCR***

Total RNA was extracted from primary BMMs using TRIzol reagent (Invitrogen). Total RNA (0.6μg) was converted to cDNA using the SuperScript® III First-Strand Synthesis SuperMix Kit (Invitrogen:11752). Resulting cDNA was diluted 1:20 and used for 20μL reactions in SYBR® Green PCR master mix (Applied Biosystems). PCR and determination of the computed threshold was performed on an iCycler (Bio-Rad). SOCS3 primers based on sequence NM_007707 are as follows: Right_AACTTGCTGTGGGTGACCAT, Left_ AAGGCCGGAGATTTCGCT.

***Statistical Analysis***

A two-tailed, homoscedastic t test was used to calculate statistical differences between control and experimental groups. Values are reported as the mean ± the standard deviation. $P<0.050$ was considered statistically significant. For western blot, band density was measured with UVP® VisionWorksLS$^{TM}$ image acquisition and analysis software. For Figure 2 and 3, SOCS3 band density was normalized to GAPDH band density. For Figure 3, P-Stat3 band density was normalized to Stat3 band density. The resulting value was then normalized to GAPDH. To evaluate significance, the control ratio of [(P-Stat3/Stat3)/GAPDH] for each time point was set to 1.0. The value from the corresponding ZA treated time point was then assigned a proportional fraction of 1.0. This fraction was then compared between multiple independent blots, three to five blots per time point, and statistics calculated as above.

## 5.4 Results

### *Zoledronic Acid enhances leptin-induced IL-6 production in an ObRb Tyr985-dependent manner*

Primary bone marrow macrophages (BMMs) from control and complete long-form leptin receptor (ObRb) knockout (KO) mice were stimulated with 100nM leptin and $10^{-7}$ to $10^{-5}$M zoledronic acid (ZA) (Figure 30). The conditioned medium was subsequently analyzed for IL-6 and normalized to total genomic DNA per well. ZA alone induced a 1.68 fold ($p=0.006$) increase of IL-6 in control cells and a 2.44 fold ($p<0.001$) increase in KO cells (Figure 30). Administration of 100nM leptin induced a leptin-specific 2.01 fold ($p<0.001$) increase of IL-6 in control cells with no change in ObRb KO cells confirming the ability of leptin to induce IL-6 through ObRb (Figure 30). Combination treatment with $10^{-5}$M ZA and 100nM leptin produced a synergistic 5.78 fold ($p<0.001$) increase in IL-6 above that induced by ZA or leptin alone (Figure 30). This synergy was not observed in the KO cells (Figure 30).

To determine which signaling pathway was responsible for the increased cytokine production with combined leptin and ZA treatment, we utilized two mouse models with gene targeted deletions in the signaling components of the leptin receptor, ObRb. ObRb has two signaling phosphotyrosines, Tyr1138 and Tyr985, on the cytoplasmic domain of the receptor. Point mutation of Tyr1138, which was generated in s/s gene targeted mice, blocks leptin signaling through P-Stat3 and SOCS3. In contrast, mutation of Tyr985 of the leptin receptor in l/l mice blocks 70-100% of downstream Erk signaling (Myers 2004). The signaling deficits of s/s and l/l mice have been previously verified in the

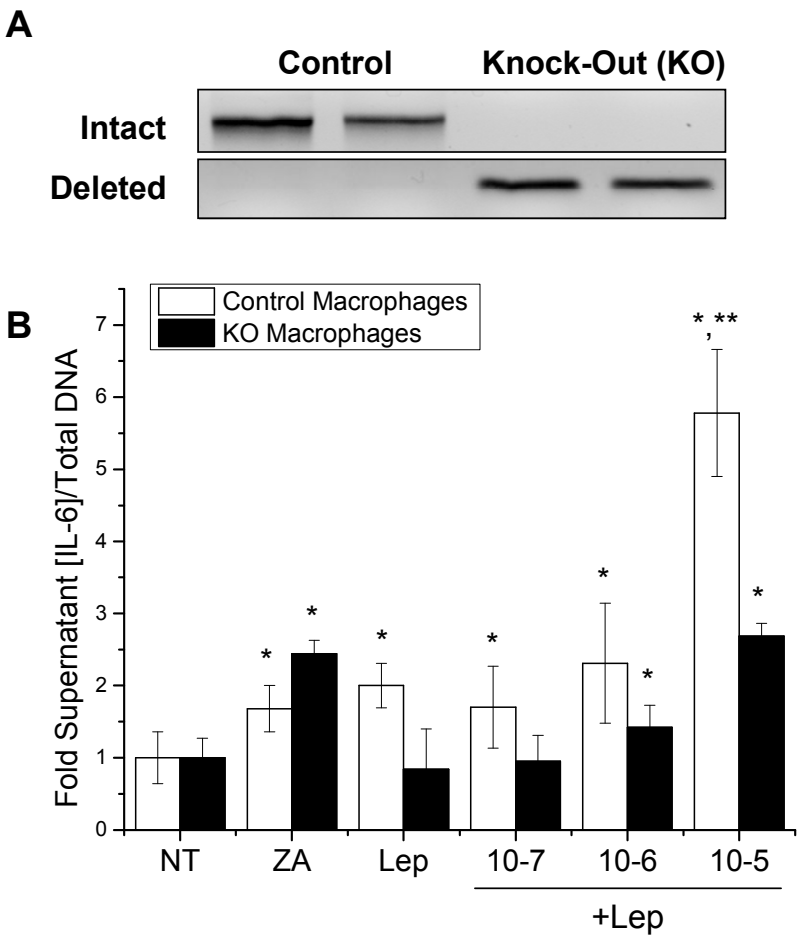


**Figure 30.** Zoledronic acid and leptin induce synergistic IL-6 production. **(A)** Genomic DNA PCR confirming complete cre-lox recombination of the bone marrow macrophages from the long-form leptin-receptor (ObRb) knockout (KO) animals and intact ObRb in the controls. **(B)** IL-6 ELISA of control and KO BMMs after 16-18 hour pretreatment with ZA followed by induction with 100nM leptin for 24 hours. N=6. *: significant over NT control, **: significant over ZA only control. Credit: (Scheller, Hankenson et al. 2011)

central nervous system (Bates, Stearns et al. 2003; Bjornholm, Munzberg et al. 2007) and in peripheral macrophages (Mancuso, Peters-Golden et al. 2011). BMMs harvested from s/s and l/l mice were genotyped (Figure 31) and treated as described above. Repetition of the ELISA experiment revealed a 16.87 fold ($p=0.001$) synergistic increase in IL-6 after combined leptin and $10^{-5}$M ZA treatment in the s/s BMMs but not in the l/l BMMs (Figure 31). This implies that synergistic induction of IL-6 production by Leptin and ZA requires Tyr985-directed Erk signaling.

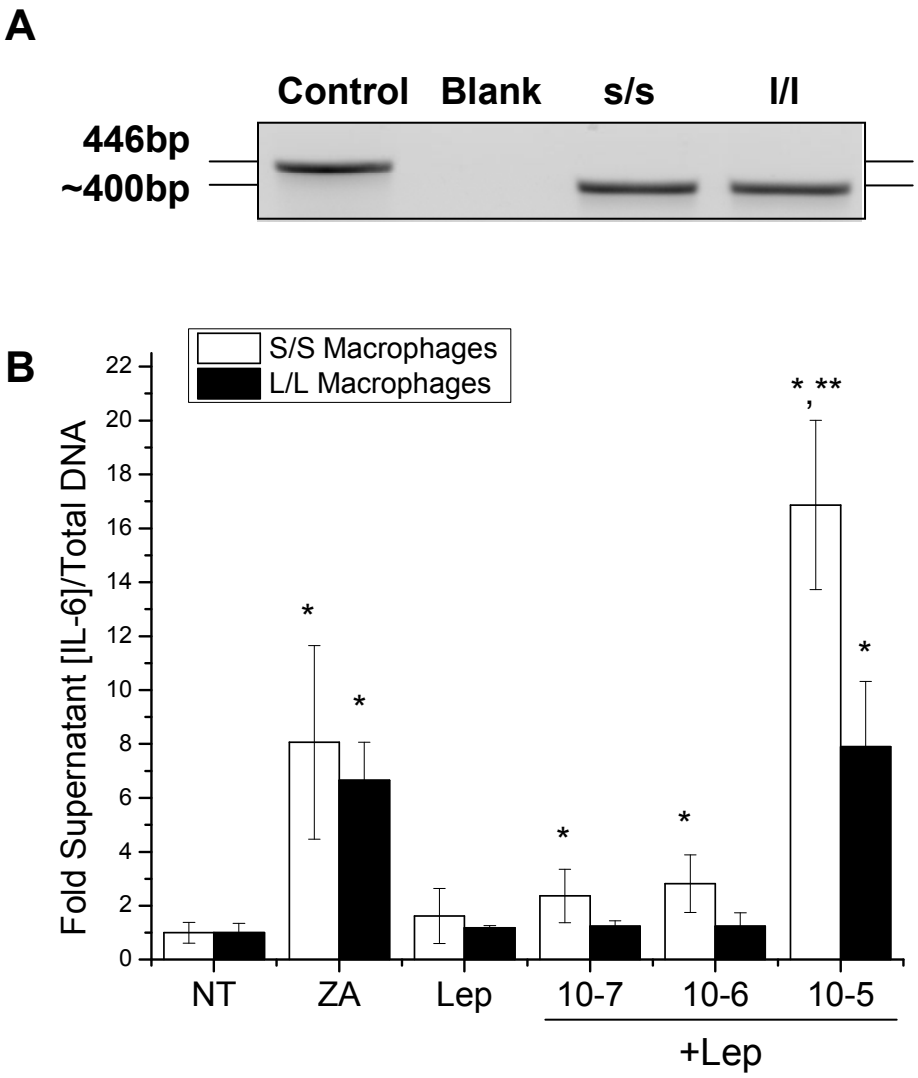


**Figure 31.** Leptin-induced IL-6 production is mediated by ObRb tyrosine 985. **(A)** Confirmatory genotyping of s/s (point mutation ObRb Tyr1138) and l/l (point mutation ObRb Tyr985) mice. **(B)** IL-6 ELISA of s/s and l/l bone marrow macrophages after 16-18 hour pretreatment with zoledronic acid (ZA) followed by induction with 100nM leptin for 24 hours. N=6. *: significant over NT control, **: significant over ZA only control. Credit: (Scheller, Hankenson et al. 2011)

### *ZA blocks SOCS3 protein accumulation by BMMs*

The s/s transgenic mice that lack the ability to signal through P-Stat3 and SOCS3 demonstrated a robust synergistic increase in macrophage IL-6 output. A similar increase was observed after treatment of control macrophages with leptin and $10^{-5}$M ZA. Since SOCS3 is a known inhibitor of leptin signaling, we hypothesized that ZA may be

regulating cellular SOCS3 accumulation. SOCS3 is a negative-feedback regulator of signaling molecules such as leptin and IL-6, and induction of SOCS3 expression can decrease macrophage cytokine production (Yoshimura, Naka et al. 2007). We found that stimulation of BMMs with 20% FBS for three hours increased SOCS3 protein 1.8-fold (Figure 32). Treatment with $10^{-6}$M or $10^{-5}$M ZA inhibited this increase in a dose dependent manner. Leptin induction of SOCS3 protein levels by 2.4-fold at three hours was also inhibited dose dependently by $10^{-6}$ or $10^{-5}$M ZA (Figure 32). Similarly, SOCS3 inhibition after stimulation with 25ng/mL IL-6 by ZA was noted (Figure 32).

***ZA reduces phosphorylation of Stat3 in a mevalonate-pathway dependent manner***

Since SOCS3 RNA is induced by nuclear accumulation of P-Stat3 and previous reports have suggested that ZA can modulate P-Stat3 levels in clonal macrophages (Reuben, Dinh et al. 2011), we investigated the ability of ZA to regulate P-Stat3 in primary BMMs. Addition of 25ng/mL IL-6 for 0 to 180 minutes increased phosphorylation of Stat3 from 5-30 minutes and again from 120-180 minutes (Figure 33). Pre-treatment with $10^{-5}$M ZA for 16-18 hours resulted in both an increase in total Stat3 at all time points and a reduction in Stat3 phosphorylation (Figure 33). This approximately 50% reduction in the ratio of P-Stat3 to Stat3, normalized to GAPDH, was statistically significant from 5 to 15 minutes (Figure 33). Many of the functions of amino-bisphosphonates are mediated by their ability to inhibit the mevalonate pathway. Therefore, mevalonate pathway intermediates GGOH and FOH were added to determine the extent to which specific intermediates may rescue the bisphosphonate-induced P-Stat3 defect. Addition of 10μM

GGOH did not alter phosphorylation of Stat3. In contrast, the addition of 10μM FOH fully restored levels of P-Stat3 in the presence of $10^{-5}$M ZA (Figure 34).

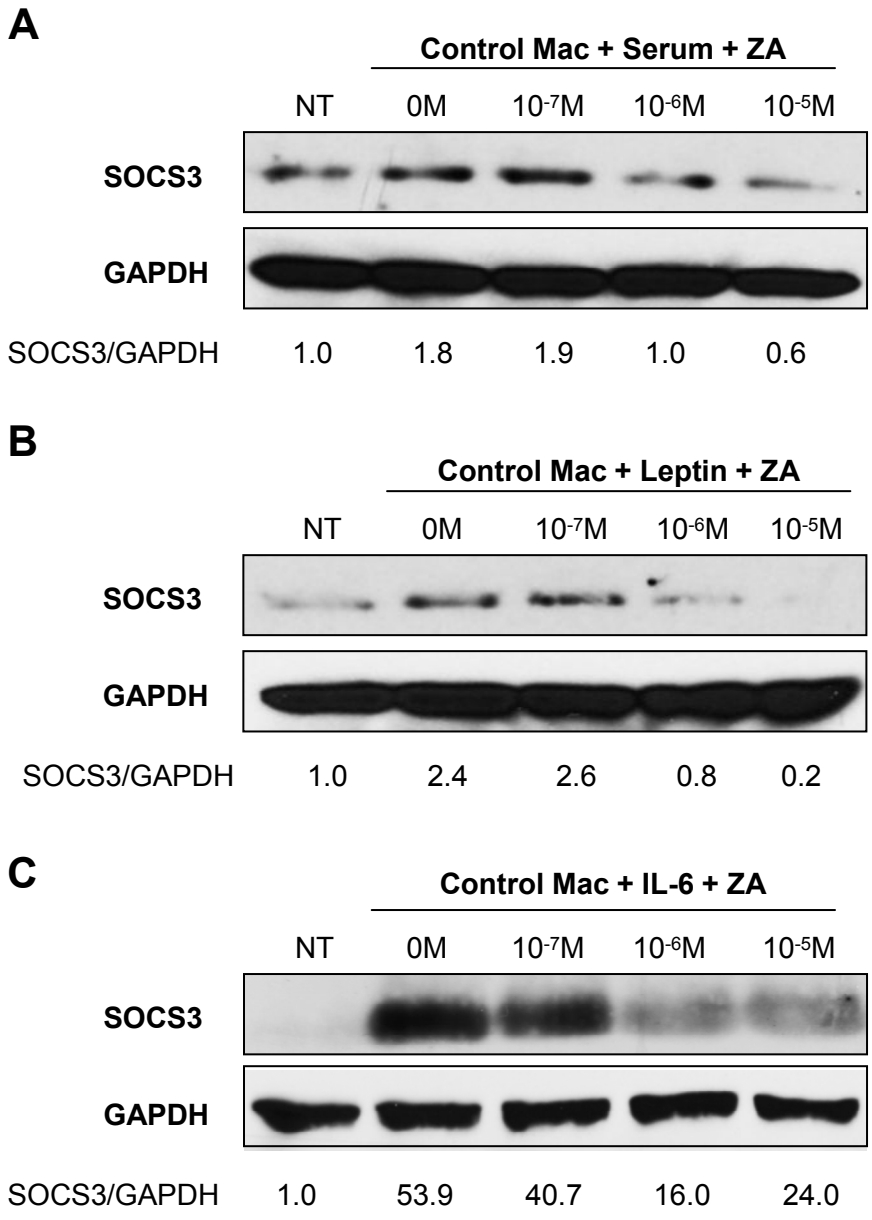


**Figure 32.** Zoledronic acid (ZA) inhibits SOCS3 protein accumulation in primary bone marrow macrophages. Western blot densitometry data was normalized to GAPDH control. **(A,B,C)** ZA pretreatment for 16-18 hours from $10^{-7}$ to $10^{-5}$M dose-dependently inhibited induction of SOCS3 in BMMs by 20% serum, 100nM leptin, or 25ng/mL IL-6 respectively after three hours. Representative blots shown, all experiments repeated at least twice. Credit: (Scheller, Hankenson et al. 2011)

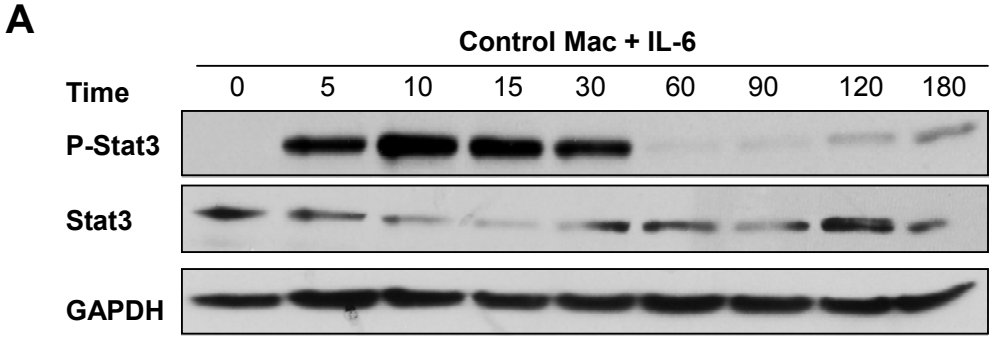


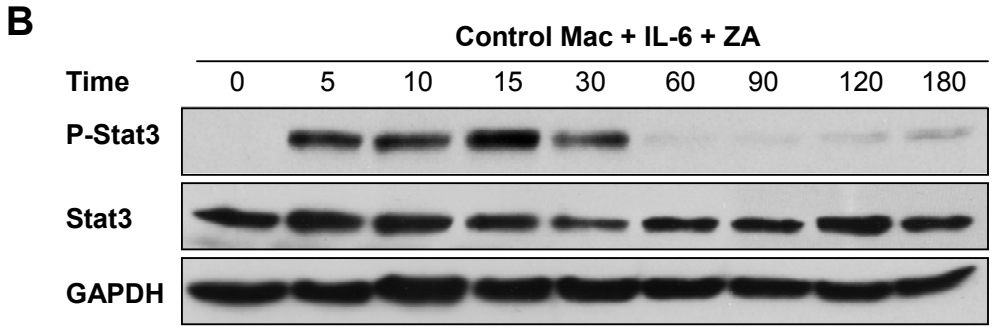


C

| | (P-Stat3/Stat3)/GAPDH | | | | | | | |
|---|---|---|---|---|---|---|---|---|
| **Time (min)** | **5** | **10** | **15** | **30** | **60** | **90** | **120** | **180** |
| **Control** | 1.0 | 1.0 | 1.0 | 1.0 | 1.0 | 1.0 | 1.0 | 1.0 |
| **ZA** | 0.38* | 0.41* | 0.47* | 1.12 | 0.93 | 1.11 | 1.42 | 0.52 |

**Figure 33.** Zoledronic acid (ZA) inhibits Stat3 phosphorylation. **(A)** Control western blot of P-Stat3, Stat3, and GAPDH after bone marrow macrophage stimulation with 25ng/mL IL-6 for 0 to 180 minutes. **(B)** Paired western blot after treatment with $10^{-5}$M ZA. **(C)** Statistical analysis of the ratio of phosphorylation of Stat3 after ZA treatment to control at each time point. Control densitometry ratio [(P-Stat3/Stat3)/GAPDH] was set to 1.0 and corresponding ZA treated ratio given a proportional value before statistical comparison of independent blots. N=3. Credit: (Scheller, Hankenson et al. 2011)

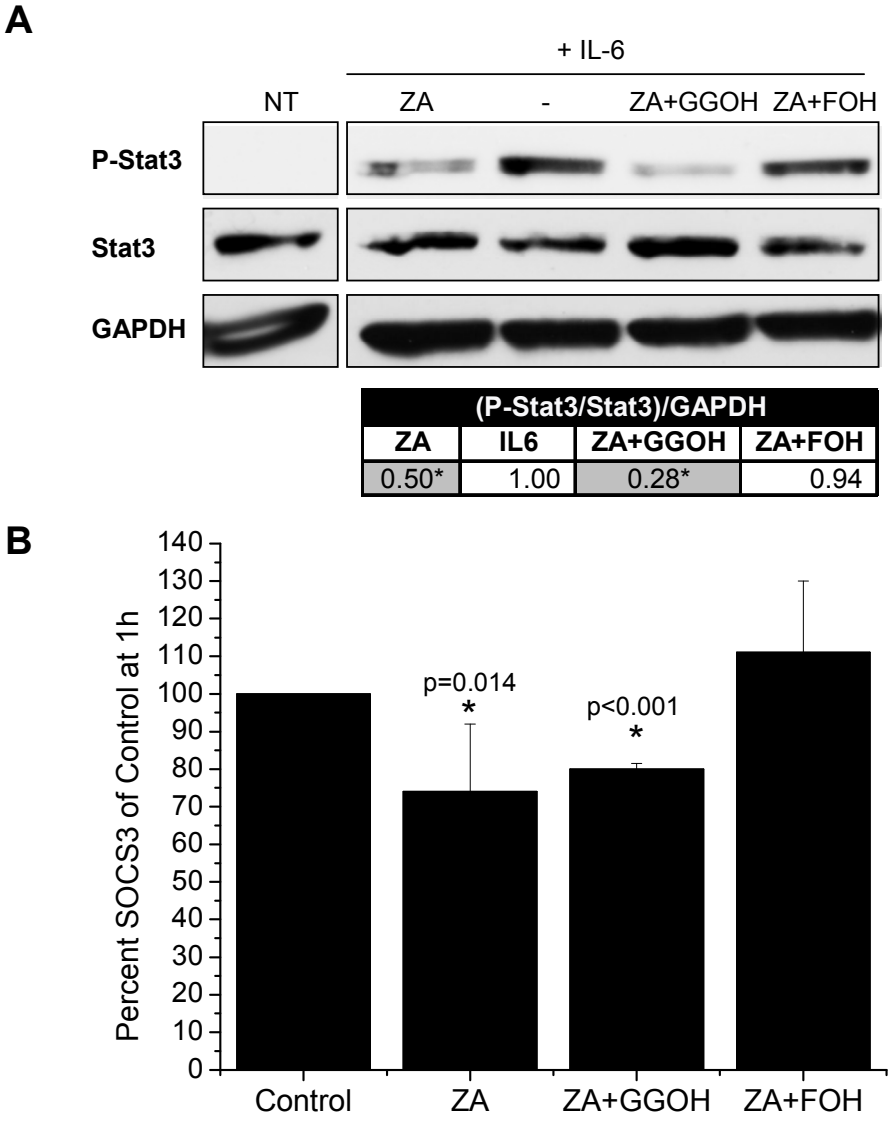


| (P-Stat3/Stat3)/GAPDH | | | |
|---|---|---|---|
| ZA | IL6 | ZA+GGOH | ZA+FOH |
| 0.50* | 1.00 | 0.28* | 0.94 |

**Figure 34.** Farnesyl intermediates rescue zoledronic acid (ZA) mediated inhibition of P-Stat3 and SOCS3 mRNA. **(A)** Western blot of bone marrow macrophages pre-treated with $10^{-5}$M ZA and 10μM GGOH or FOH overnight, '-' indicates lack of ZA treatment. Pre-treated cells were stimulated with 25ng/mL IL-6 for 10-15 minutes. Tabulated results report the ratio of phosphorylation of Stat3 after ZA treatment to control at each time point as in figure 33. N=3. **(B)** Quantitative PCR analysis of SOCS3 mRNA after one hour, treatments as above. Results are reported as percent of control SOCS3 mRNA. N=3-5. *: significantly less than control. Credit: (Scheller, Hankenson et al. 2011)

***Correction of P-Stat3 signaling is not sufficient to rescue SOCS3 protein inhibition***

P-Stat3 nuclear accumulation induces SOCS3 mRNA transcription (Banks, Davis et al. 2000). Therefore, we sought to determine if cytokine treatment had a similar effect in our system. Addition of 25ng/mL IL-6 significantly induced SOCS3 mRNA accumulation after one hour. This increase was significantly blunted by treatment with $10^{-5}$M ZA and rescued by concomitant treatment with 10μM FOH, but not 10μM GGOH (Figure 34). Despite the complete rescue of P-Stat3 protein and SOCS3 mRNA levels, FOH at 5μM or 10μM was not sufficient to rescue SOCS3 protein production (Figure 35).

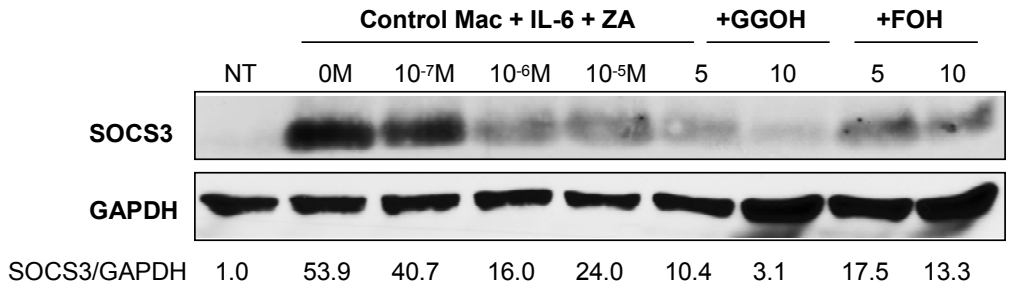


**Figure 35.** Rescue of P-Stat3 and SOCS3 mRNA with FOH does not correct SOCS3 protein inhibition. Representative western blot of SOCS3 after ZA/GGOH/FOH overnight pre-treatment where indicated and three hour 25ng/mL IL-6 stimulation of bone marrow macrophages. GGOH and FOH concentrations are reported as μM and combined with $10^{-5}$M zoledronic acid. Experiment was repeated three times with similar results. Credit: (Scheller, Hankenson et al. 2011)

***Macrophage-associated SOCS3 levels are decreased in human specimens***

To determine if alterations in SOCS3 were present in human cells and tissue, we analyzed both primary human macrophages and ONJ biopsy specimens (Scheller, Hankenson et al. 2011). Human bone marrow macrophages (hBMMs) were harvested from iliac crest bone marrow of a 60 year old male donor. Harvested cells were strongly positive for CD68, a macrophage marker, when analyzed with immunofluorescence (Figure 36). SOCS3 protein accumulation induced after five hours of 50ng/mL IL-6

treatment was inhibited by pre-incubation of the cells with $10^{-5}$M ZA (Figure 36) similar to studies with mouse BMMs (Figure 32). Immunohistochemistry for SOCS3 and CD68 was performed on serial sections of biopsies derived from control human oral ulcerations or ulcerations associated with ONJ (Table 8). Comparison of SOCS3 staining density in the areas of macrophage infiltration revealed a significant decrease in SOCS3 in the ONJ specimens (16.8±16.2%, p=001) when compared to controls (70.5±27.1%) (Figure 36).

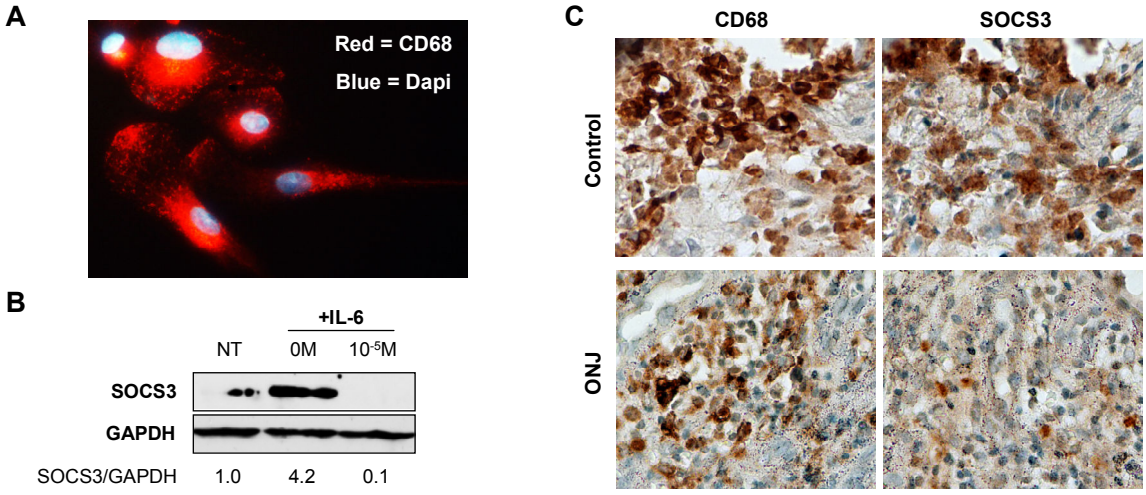


**Figure 36.** Bisphosphonates decrease SOCS3 in human CD68+ macrophages and human ONJ biopsies. **(A)** Cellular immunofluorescence of primary human macrophages. Red = CD68, Blue = Dapi. 40x magnification. **(B)** Representative western blot of primary macrophage SOCS3 after treatment with 50ng/mL IL-6 alone or IL-6 + $10^{-5}$M zoledronic acid. Experiment was performed in duplicate with similar results. **(C)** Representative serially stained sections of control ulcerated tissue and an ONJ lesion. 40x magnification. Credit: (Scheller, Hankenson et al. 2011)

| Patient | Group | Age | Gender | Specimen Diagnosis | Bisphosphonate | SOCS3 (%) | Avg+/-SD (%) | P Value |
|---|---|---|---|---|---|---|---|---|
| 1 | Control | 57 | M | Nonspecific Ulcer | | 100.0 | 70.5+/-27.1 | 0.001 |
| 2 | Control | 65 | M | Traumatic Ulcer | | 60.2 | | |
| 3 | Control | 78 | M | Traumatic Ulcer | | 41.4 | | |
| 4 | Control | 81 | M | Bony Sequestrum | | 100.0 | | |
| 5 | Control | 54 | F | Granulomatous Reaction | | 40.8 | | |
| 6 | Control | 65 | M | Bony Sequestrum | | 80.5 | | |
| 1 | IV BP | 65 | M | ONJ | Zometa® | 14.4 | 16.8+/-16.2 | |
| 2 | IV BP | 67 | F | ONJ | Zometa® | 17.2 | | |
| 3 | IV BP | 55 | F | ONJ | Zometa® | 5.0 | | |
| 4 | IV BP | 82 | M | ONJ | Zometa® | 45.0 | | |
| 5 | BP NOS | 81 | F | ONJ | Unknown | 3.6 | | |
| 6 | Oral BP | 88 | F | ONJ | Fosamax® | 31.4 | | |
| 7 | Oral BP | 67 | F | ONJ | Fosamax® | 1.1 | | |

**Table 8.** Patient information, condition, treatment, and SOCS3 percent staining density of human specimens. Credit: (Scheller, Hankenson et al. 2011)

## 5.5 Discussion

SOCS3 is an essential regulator of diverse cellular functions including cytokine production and has been implicated in the pathogenesis of inflammatory pathology such as Crohn's disease and rheumatoid arthritis. We found that the amino-bisphosphonate zoledronic acid has the potential to enhance macrophage cytokine secretion by inhibiting SOCS3 protein accumulation. Due to the extended half-life of bisphosphonates and their ability to incorporate into the bone matrix (Kozloff, Volakis et al. 2010), it is possible that long-term systemic persistence of these drugs may contribute to inflammatory pathologic processes through the inhibition of SOCS3.

Indeed, ONJ, an increasingly recognized complication of amino-bisphosphonate treatment, may be linked to altered macrophage SOCS3 activity, as preliminary evidence suggests that SOCS3 protein levels are decreased in ONJ biopsy specimens when compared to controls. However, it is important to recognize a limitation of this study. Except for specimen number five that contained a granulomatous reaction, both the controls and the ONJ biopsy specimens represented clinical ulcerations of similar appearance. In all specimens one would expect to see an inflammatory reaction including induction of SOCS3. However, the duration of the ulcers is unknown and their status as acute vs chronic inflammatory lesions may also influence SOCS3 protein levels. Despite this level of information, the approximately four-fold decrease in SOCS3 protein levels in the ONJ specimens suggests that further investigation in this area may provide additional insights on the mechanisms responsible for ONJ.

The pathogenesis of ONJ is currently unknown but may be linked to decreased bone turnover, altered vascularity, bacterial invasion, and compromised wound healing (Novince, Ward et al. 2009). Osteoimmunology is an emerging field of research that views regulation of bone metabolism within the context of immune function (Lorenzo, Horowitz et al. 2008). While the macrophage has long been appreciated as a key component of the immune system, an essential role for macrophages in bone homeostasis was only recently confirmed when induced depletion of macrophages in a mouse model ablated mature osteoblast bone-forming surface (Chang, Raggatt et al. 2008). In addition to regulation of osteogenesis, macrophage-released cytokines are regulators of fibroblast and endothelial cell proliferation and studies have speculated that reduced macrophage infiltration may, in part, be responsible for increased rates of healing of oral mucosa compared to keratinized dermal sites (Szpaderska, Zuckerman et al. 2003). Thus, dysregulation of critical macrophage functions such as cytokine production may contribute to altered bone remodeling and decreased healing potential observed at sites of ONJ.

We found that zoledronic acid at concentrations of $10^{-6}$ to $10^{-5}$M is a novel inhibitor of serum and cytokine-induced SOCS3 in macrophages *in vitro*. Inhibition of SOCS3 was also observed in human ONJ biopsy specimens *in vivo*. SOCS3 is a potent regulator of macrophage responses to systemic cytokines such as IL-6 and leptin that are upregulated in states of obesity. Analysis of alendronate release kinetics in rat bone have demonstrated local bisphosphonate concentrations of $10^{-3}$ to $10^{-4}$M at sites of active resorption after 0.4mg/kg treatment (Sato, Grasser et al. 1991). In addition, secreted

concentrations of $10^{-5}$M ZA are readily achieved with ZA-loaded bone cement that has been proposed for local treatment of giant cell tumor and multiple myeloma (Zwolak, Manivel et al. 2010). This study reveals that the future use of such devices must consider complications due to inhibition of SOCS3 and enhancement of a destructive inflammatory response. Though our study has focused on SOCS3 inhibition in the context of ONJ, this may also play important roles in other inflammatory conditions such as rheumatoid arthritis (Isomaki, Alanara et al. 2007), inflammatory bowel disease (Suzuki, Hanada et al. 2001), and Crohn's disease (Lovato, Brender et al. 2003).

In summary, we conclude that ZA is a novel inhibitor of SOCS3 protein accumulation in macrophages, essentially 'inhibiting the inhibitor' of signaling by molecules such as leptin and IL-6 (Figure 37). Functionally, administration of ZA with leptin promoted a synergistic induction of downstream IL-6 production by primary BMMs that was not present in BMMs lacking the long-form leptin receptor (ObRb). This effect was dependent on ObRb tyrosine 985, likely mediated by the downstream Erk pathway (Figure 37). Though ZA was found to decrease both phosphorylation of Stat3 and initial induction of SOCS3 mRNA in a mevalonate-pathway dependent manner, rescue of these defects with FOH was not sufficient to restore SOCS3 protein levels. Thus, the specific mechanism of SOCS3 inhibition is unclear at this point but may involve a post-transcriptional process. Though this study focused on SOCS3 induction by obesity-related cytokines leptin and IL-6, our results suggest wider implications for regulation of additional SOCS3 dependent signaling molecules such as IL-10, LPS and IFN-γ. In conclusion, we propose that inhibition of SOCS3 and dysregulation of macrophage

cytokine output may contribute to obesity-associated inflammatory disorders and potentially the pathogenesis of ZA-induced ONJ.

## 5.6 Acknowledgments

Supported by R01 DE13835 (PHK/KDH), F30 DE019577 (ELS) and the Baylor Oral Health Foundation (JSR). Special thanks to Paul Edwards and Sean Edwards for their help with the human biopsies and primary marrow samples respectively.

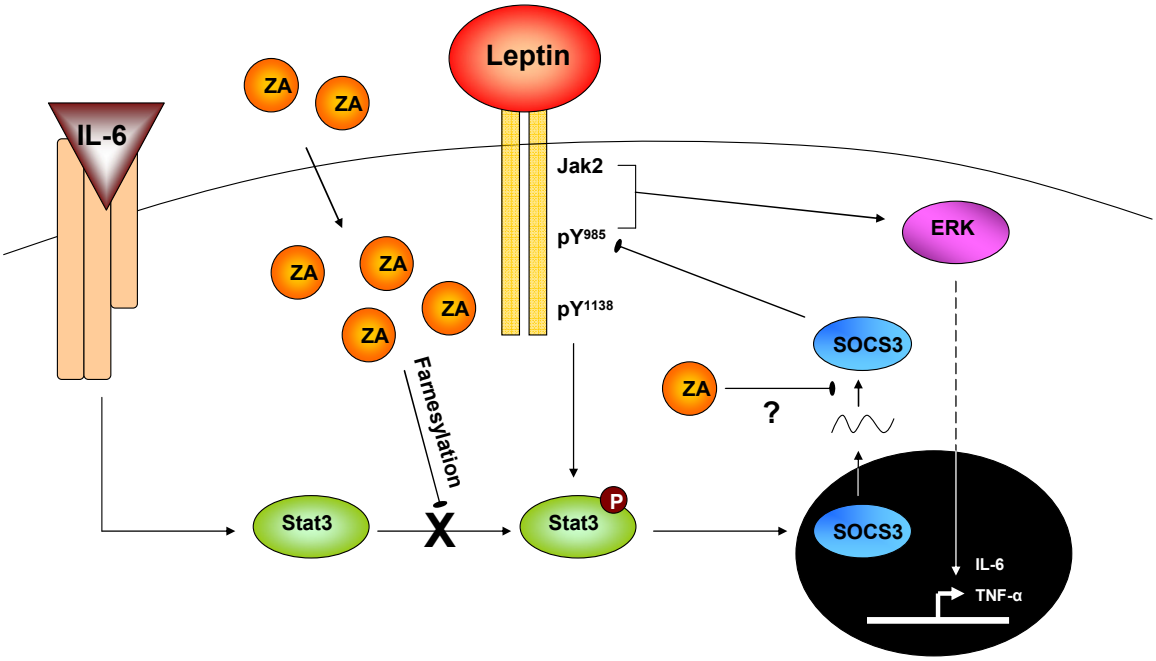


**Figure 37.** Theoretical model of zoledronic acid (ZA) regulation of SOCS3. ZA taken up by the cell blocks phosphorylation of Stat3 in a farnesylation-dependent manner. ZA, via a secondary mechanism that may involve inhibition of protein translation, blocks protein accumulation of SOCS3. Functionally, this results in increased cytokine output of leptin-induced IL-6 in an ObRb Tyr985, Erk signaling dependent manner. Credit: (Scheller, Hankenson et al. 2011)

# CHAPTER 6

# PROSPECTUS AND CONCLUSIONS

## 6.1 Further consideration of the $3.6^{Cre+F/F}$ phenotype

### *Investigation of peripheral obesity*

The $3.6^{Cre+F/F}$ mice presented with an unexpected increase in body mass that was primarily attributed to the higher fat content of the transgenic mice (Figure 19). This could be explained by alterations in adipose progenitor cell differentiation, central changes in food intake, and/or altered regulation of adipocyte hypertrophy. We found that the Col3.6 promoter was capable of driving loxP recombination in peripheral adipose depots, likely due to recombination in an adipocyte precursor cell such as the MPC or adipose stem cell (ASC) (Figure 23). The realization that adipose tissue is a rich source of precursor cells has progressed since the late 19th century and in recent years has consisted of a switch in nomenclature from "adipocyte precursor" to "adipose stem cell" when it was realized that cells within the stromal vascular fraction (SVF) of adipose tissue could differentiate into cells other than adipocytes.

Fractionation of adipose tissue as performed in our study consists of collagenase digestion and centrifugation to separate floating, lipid-laden adipocytes from a pellet referred to as the SVF (Rodbell 1964). In 1973 growth of fibroblast-like cells from the SVF was reported *in vitro* (Poznanski, Waheed et al. 1973) followed by confirmatory

reports of their ability to serve as an adipocyte precursor (Van, Bayliss et al. 1976). Despite recognition of this adipocyte precursor in 1976 and appearance of the stem cell concept as early as 1909 (Maximow 2009), these two findings were not merged until 2001 in the first report of a unique, multipotent adipose stem cell (Zuk, Zhu et al. 2001).

At first inspection it appears that ASCs are a subset of the larger class of so-called mesenchymal stem cells and share many similarites with MSCs of other tissues. *In vitro* clonal expansion of single cell preparations of tissues such as bone marrow, synovium, adipose, or dental pulp reveals stromovascular progenitor cells (SVCs) capable of multilineage *in vitro* differentiation toward adipocytes, osteoblasts, and chondroblasts (Friedenstein, Chailakhjan et al. 1970; Poznanski, Waheed et al. 1973; Gronthos, Mankani et al. 2000; De Bari, Dell'Accio et al. 2001). The ability to form these tissues *in vivo* varies. Origin of adipose lineages is thought to occur from both the mesoderm and the neural crest during development (Billon, Iannarelli et al. 2007). This dual origin is similar to that of bone which derives from neuroectoderm (craniofacial skeleton) and axial and lateral specifications of mesoderm (Olsen, Reginato et al. 2000). However, despite definition of an early, transient MSC-like population of neuroectoderm (Takashima, Era et al. 2007), adult progenitors appear to have a unique origin that is not yet defined. The subtle differences between SVC populations may represent a similar cell of origin that was epigenetically programmed once within its tissue of residence (Boquest, Noer et al. 2006). This epigenetic silencing of certain promoters may explain the enhanced ability of the adipose SVC to differentiate toward fat (Boquest, Noer et al. 2006), *in vivo* dentin formation by dental pulp SVCs (Shi and Gronthos 2003), enhanced

chondrogensis of synovial SVCs (De Bari, Dell'Accio et al. 2001), or the greater hematopoetic supportive capacity of the bone marrow SVC (Casteilla, Planat-Benard et al. 2011). If the Col3.6 promoter is able to drive recombination in precursor cells from diverse tissues including bone and adipose, this may point to a common origin of these cells and provide significant developmental insight.

In support of the contribution of adipocyte hyperplasia to the obesity of Col3.6$^{Cre+F/F}$ mice, we demonstrated that SVC lacking ObRb isolated from both the bone marrow and peripheral adipose tissue could differentiate more robustly to adipocytes *in vitro* (Figure 14, Figure 23). This finding has never been replicated *in vivo*, and thus the contribution of this mechanism to peripheral fat pad size remains unknown. In addition to increases in food intake driving obesity, specific knock-down of ObRb using siRNA in the white adipose tissue of mice also results in increased body mass suggesting that leptin regulation of fat depot size is regulated peripherally as well as centrally (Huan, Li et al. 2003). To further evaluate differentiation *in vivo*, it would be interesting to cross an ObRb null adipose SVC from our 3.6$^{Cre+F/F}$ animals with a PPARγ linked LacZ reporter cell (Tang, Zeve et al. 2008). These cells could then be implanted into adipose depots *in vivo* in wild type mice fed a high fat diet as described previously (Rodeheffer, Birsoy et al. 2008) and the contribution of implanted cells compared to ObRb-replete LacZ-expressing controls. We would hypothesize that the SVCs lacking ObRb could generate increased numbers of adipocytes *in vivo* in the presence of excess food intake due to the lack of leptin differentiation inhibition.

In addition to effects on precursor cell differentiation, understanding the accumulation of fat in $3.6^{Cre+F/F}$ mice requires analysis of central regulation of food intake. We explored the metabolic phenotype of the animals using CLAMS. We also measured the ability of leptin to signal centrally through the hypothalamus. CLAMS metabolic analysis failed to reveal any change in spontaneous activity or acute food intake that could explain the peripheral obesity (Figure 20). However, during central analysis, we found that the Col3.6 promoter drove non-specific loxP recombination in 5-10% of hypothalamic leptin-responsive neurons (Figure 27). Though it is unlikely that this is directly responsible for the observed bone phenotype, it is highly possible that elimination of a small proportion of leptin-responsive neurons could result in a proportional increase in food intake. Acute analysis of food intake failed to reveal any differences (Figure 20), however, a longitudinal study of mice from 24 to 28 weeks of age revealed an approximately 16% increase in chow consumption (Figure 29a). It is unknown if this increase is sufficient to cause and/or maintain the average 63% increase in body mass of these same animals. Paired food provision during development may lead to a resolution of this question.

In addition to evidence for adipocyte hyperplasia, the contribution of adipocyte hypertrophy to the obesity of the $3.6^{Cre+F/F}$ mice could be determined. In complete leptin deficient ob/ob mice the rate of lipogenesis in liver and adipose tissue is twice that of controls and an increase in adipocyte size is observed at two weeks of age (Coleman 1978). As previously mentioned, specific knock-down of ObRb in the white adipose of mice *in vivo* results in increased body mass in the absence of central alteration (Huan, Li

et al. 2003). This may represent changes in both differentiation of adipose precursors or modulation of properties of mature adipocytes. Glucose and insulin have been shown to stimulate leptin production by mature adipocytes *in vitro*, while inhibitors of glycolysis induce dose dependent inhibition of secretion (Mueller, Gregoire et al. 1998). However, even at high concentrations (200-2000ng/mL), leptin is not able to modulate basal or insulin-stimulated glucose metabolism of either freshly isolated or cultured adipocytes (Mick, Vanderbloomer et al. 1998). Thus, leptin modulation of adipocyte hypertrophy may occur through central mechanisms. Quantification of adipocyte size as well as the central and peripheral contribution of leptin to lipogenesis may further explain the obesity of $3.6^{Cre+F/F}$ mice.

***Contribution of obesity to the bone phenotype***

It has been established in mice that increases in body mass increase femoral cortical bone parameters independent of leptin signaling (Iwaniec, Dube et al. 2009). This increase in cortical bone parameters was accompanied by an increase in femur length (Iwaniec, Dube et al. 2009). Conversely, caloric restriction in mice decreases femoral cortical bone mineral content and thickness without changes in femur length (Hamrick, Ding et al. 2008). In both instances, either males fed a high fat diet from 16-24 weeks or subject to calorie restriction from 14-24 weeks, femoral trabecular bone volume fraction remained unchanged (Hamrick, Ding et al. 2008; Iwaniec, Dube et al. 2009). The mass increase of our $3.6^{Cre+F/F}$ animals is comparable to that observed in animals fed a high fat diet. Thus, it is likely that our observed changes in femoral length and increases in cortical parameters at 12 weeks and 42 weeks are related to this change. However, the observed

40-70% increases in trabecular bone volume and bone mineral content can not be explained by changes in body weight and are thus assumed to be linked directly to alterations in leptin signaling.

### *Leptin and Chondrogenesis*

Though it appears that increases in body mass of the $3.6^{Cre+F/F}$ animals may be responsible for the increased femur length, the appearance of a bone length phenotype warrants discussion of the ability of leptin to regulate chondrogenesis. In ob/ob mice the cartilaginous growth plates have disturbed columnar structure, decreased type X collagen expression, increased apoptosis, and premature mineralization (Kishida, Hirao et al. 2005). In addition, *in vitro* matrix mineralization of ob/ob chondrocytes is higher than that of wild-type mice (Kishida, Hirao et al. 2005). These observations are similar to our findings with primary ob/ob and db/db BMSCs (Scheller, Song et al. 2010). Thus, it appears that leptin may regulate terminal differentiation of chondrocytes and play a role in endochondral ossification at the growth plate. Since the chondrocyte, osteoblast, and adipocyte are derived from a common mesenchymal progenitor it is possible that ObRb is not present on chondrocytes in the $3.6^{Cre+F/F}$ mice. If true, precise determination of the cause of the bone length increase would require independent evaluation of the contribution of body mass and leptin-related alterations in endochondral ossification.

## 6.2 Potential use of recombinant leptin to treat human disease

Exploring the diverse roles of adipose and leptin signaling in the marrow could provide clues to understanding bone metabolism and obesity linked inflammatory disorders such

as rheumatoid arthritis, Crohn's disease, and osteonecrosis of the jaw. Further application of this knowledge to the regeneration of the marrow-supporting osseous and cartilaginous structures is a primary goal of the field of bone tissue engineering. In addition to previously published central mechanisms (Ducy, Amling et al. 2000), we have explored the ability of leptin to modulate bone formation through peripheral cells such as the macrophage, the osteoblast, and the mesenchymal precursor cell. Our studies have reaffirmed the complexity of the relationship between leptin and bone and provided insight on its potential use as a therapeutic agent for bone tissue engineering. It is now apparent that leptin modulation of bone formation is dependent on multiple factors such as gender, age, inflammatory state, and presence of central leptin resistance. This results in diverse correlations between leptin and bone mineral density that range from a negative correlation prominent in males (Table 1) to a positive correlation often observed in post-menopausal females (Table 2). Our studies revealed that this gender discordance may be related to leptin regulation of the myeloid lineage as our $LysM^{Cre+F/F}$ transgenic mouse was the first to demonstrate a gender-specific leptin-related bone phenotype (Table 3). We also determined that leptin regulation of osteoblast function is minimal at physiologic equilibrium, though positive effects are possible *in vitro*. In addition, based on our studies with the $3.6^{Cre+F/F}$ animals we hypothesize that leptin may negatively regulate the differentiation of mesenchymal precursor cells. Thus, in the context of leptin regulation of bone formation one is left with three negative modulators (brain, MPCs, and myeloid lineage) and two potentially positive modulators (osteoblast and myeloid lineage) (Figure 38).

The myeloid lineage is listed in both groups due to the divergent, gender-specific bone phenotype observed in the 42 week old LysM$^{Cre+F/F}$ mice (Table 3). The LysM promoter is known to drive deletion on myeloid lineage cells such as monocytes, macrophages, granulocytes and osteoclasts. Thus, at this time, it is not possible for us to definitively determine the individual contribution of these cell types. In addition, it is possible that the observed cortical changes in the 52 week old LysM$^{Cre+F/F}$ males occurred due to their average 11% body mass increase (36g vs 39.6g, $p=0.009$, $N=6$). However, this mass differential is far less than the 23% increase observed in the 42 week old 3.6$^{Cre+F/F}$ males (37.2g vs 45.8g, $p<0.001$, $N=6$), yet the increases in cortical parameters are similar or more prominent in the aged LysM$^{Cre+F/F}$ animals (Table 3, Table 6). This lack of proportional increase of body mass and cortical values implies that impaired leptin signaling may be driving the changes in bone metabolism directly through the myeloid lineage of the LysM$^{Cre+F/F}$ animals. In summary, the diversity of our findings implies that leptin is not a likely candidate for direct bone tissue engineering. However, the effects on the bone are minimal enough to consider its use for treatment of other disorders.

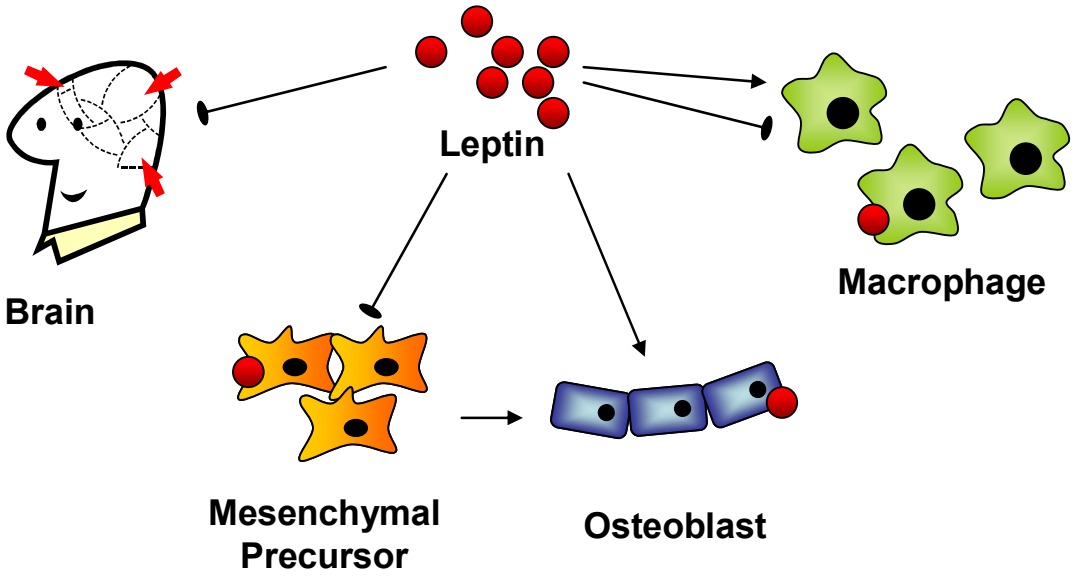


**Figure 38.** Summary of leptin modulation of bone formation. Circulating leptin has the ability to modulate bone formation both by acting centrally through the hypothalamus and by acting peripherally on individual cells. Negative mediators of skeletal bone mass include the sympathetic nervous system, the mesenchymal precursor, and the myeloid lineage in males. Positive modulators include the osteoblast and the myeloid lineage in females.

## REFERENCES


Abramoff, M. D., P. J. Magelhaes, et al. (2004). "Image Processing with ImageJ." Biophotonics International **11**(7): 36-42.

Aust, L., B. Devlin, et al. (2004). "Yield of human adipose-derived adult stem cells from liposuction aspirates." Cytotherapy **6**(1): 7-14.

Banks, A. S., S. M. Davis, et al. (2000). "Activation of downstream signals by the long form of the leptin receptor." J Biol Chem **275**(19): 14563-72.

Bates, S. H., W. H. Stearns, et al. (2003). "STAT3 signalling is required for leptin regulation of energy balance but not reproduction." Nature **421**(6925): 856-9.

Benayahu, D., D. Zipori, et al. (1993). "Marrow adipocytes regulate growth and differentiation of osteoblasts." Biochem Biophys Res Commun **197**(3): 1245-52.

Bianco, P., M. Riminucci, et al. (2001). "Bone marrow stromal stem cells: nature, biology, and potential applications." Stem Cells **19**(3): 180-92.

Billon, N., P. Iannarelli, et al. (2007). "The generation of adipocytes by the neural crest." Development **134**(12): 2283-92.

Bjorbaek, C., J. K. Elmquist, et al. (1998). "Identification of SOCS-3 as a potential mediator of central leptin resistance." Mol Cell **1**(4): 619-25.

Bjornholm, M., H. Munzberg, et al. (2007). "Mice lacking inhibitory leptin receptor signals are lean with normal endocrine function." J Clin Invest.

Bjornholm, M., H. Munzberg, et al. (2007). "Mice lacking inhibitory leptin receptor signals are lean with normal endocrine function." J Clin Invest **117**(5): 1354-60.

Boquest, A. C., A. Noer, et al. (2006). "Epigenetic programming of mesenchymal stem cells from human adipose tissue." Stem Cell Rev **2**(4): 319-29.

Breslow, M. J., K. Min-Lee, et al. (1999). "Effect of leptin deficiency on metabolic rate in ob/ob mice." Am J Physiol **276**(3 Pt 1): E443-9.

Burkhardt, R., G. Kettner, et al. (1987). "Changes in trabecular bone, hematopoiesis and bone marrow vessels in aplastic anemia, primary osteoporosis, and old age: a comparative histomorphometric study." Bone **8**(3): 157-64.

Burks, D. J., J. Font de Mora, et al. (2000). "IRS-2 pathways integrate female reproduction and energy homeostasis." Nature **407**(6802): 377-82.

Cao, J. J., B. R. Gregoire, et al. (2009). "High-fat diet decreases cancellous bone mass but has no effect on cortical bone mass in the tibia in mice." Bone **44**(6): 1097-104.

Cartsos, V. M., S. Zhu, et al. (2008). "Bisphosphonate use and the risk of adverse jaw outcomes: a medical claims study of 714,217 people." J Am Dent Assoc **139**(1): 23-30.

Casteilla, L., V. Planat-Benard, et al. (2011). "Adipose-derived stromal cells: Their identity and uses in clinical trials, an update." World J Stem Cells **3**(4): 25-33.

CDC (1998). NIH, NHLBI Obesity Education Initiative. Clinical Guidelines on the Identification, Evaluation, and Treatment of Overweight and Obesity in Adults. CDC.

Chang, M. K., L. J. Raggatt, et al. (2008). "Osteal tissue macrophages are intercalated throughout human and mouse bone lining tissues and regulate osteoblast function in vitro and in vivo." J Immunol **181**(2): 1232-44.
Chang, Y. J., D. T. Shih, et al. (2006). "Disparate mesenchyme-lineage tendencies in mesenchymal stem cells from human bone marrow and umbilical cord blood." Stem Cells **24**(3): 679-85.
Chanprasertyothin, S., N. Piaseu, et al. (2005). "Association of circulating leptin with bone mineral density in males and females." J Med Assoc Thai **88**(5): 655-9.
Charlton, H. M. (1984). "Mouse mutants as models in endocrine research." Q J Exp Physiol **69**(4): 655-76.
Clausen, B. E., C. Burkhardt, et al. (1999). "Conditional gene targeting in macrophages and granulocytes using LysMcre mice." Transgenic Res **8**(4): 265-77.
Cochrane, R. L., S. H. Clark, et al. (2007). "Rearrangement of a conditional allele regardless of inheritance of a Cre recombinase transgene." Genesis **45**(1): 17-20.
Cohen, P., C. Zhao, et al. (2001). "Selective deletion of leptin receptor in neurons leads to obesity." J Clin Invest **108**(8): 1113-21.
Coleman, D. L. (1978). "Obese and diabetes: two mutant genes causing diabetes-obesity syndromes in mice." Diabetologia **14**(3): 141-8.
Considine, R. V., M. K. Sinha, et al. (1996). "Serum immunoreactive-leptin concentrations in normal-weight and obese humans." N Engl J Med **334**(5): 292-5.
Cornish, J., K. E. Callon, et al. (2002). "Leptin directly regulates bone cell function in vitro and reduces bone fragility in vivo." J Endocrinol **175**(2): 405-15.
Coxon, F. P., M. H. Helfrich, et al. (2000). "Protein geranylgeranylation is required for osteoclast formation, function, and survival: inhibition by bisphosphonates and GGTI-298." J Bone Miner Res **15**(8): 1467-76.
Cusin, I., F. Rohner-Jeanrenaud, et al. (1996). "The weight-reducing effect of an intracerebroventricular bolus injection of leptin in genetically obese fa/fa rats. Reduced sensitivity compared with lean animals." Diabetes **45**(10): 1446-50.
Das, U. N. (2001). "Is obesity an inflammatory condition?" Nutrition **17**(11-12): 953-66.
De Bari, C., F. Dell'Accio, et al. (2001). "Multipotent mesenchymal stem cells from adult human synovial membrane." Arthritis Rheum **44**(8): 1928-42.
Dennison, E. M., H. E. Syddall, et al. (2004). "Plasma leptin concentration and change in bone density among elderly men and women: the Hertfordshire Cohort Study." Calcif Tissue Int **74**(5): 401-6.
Ducy, P., M. Amling, et al. (2000). "Leptin inhibits bone formation through a hypothalamic relay: a central control of bone mass." Cell **100**(2): 197-207.
Dunbar, J. C., Y. Hu, et al. (1997). "Intracerebroventricular leptin increases lumbar and renal sympathetic nerve activity and blood pressure in normal rats." Diabetes **46**(12): 2040-3.
Ealey, K. N., D. Fonseca, et al. (2006). "Bone abnormalities in adolescent leptin-deficient mice." Regul Pept **136**(1-3): 9-13.
Elefteriou, F., J. D. Ahn, et al. (2005). "Leptin regulation of bone resorption by the sympathetic nervous system and CART." Nature **434**(7032): 514-20.

Emilsson, V., Y. L. Liu, et al. (1997). "Expression of the functional leptin receptor mRNA in pancreatic islets and direct inhibitory action of leptin on insulin secretion." Diabetes **46**(2): 313-6.
Faouzi, M., R. Leshan, et al. (2007). "Differential accessibility of circulating leptin to individual hypothalamic sites." Endocrinology **148**(11): 5414-23.
Fontana, L., J. C. Eagon, et al. (2007). "Visceral fat adipokine secretion is associated with systemic inflammation in obese humans." Diabetes **56**(4): 1010-3.
Foulk, D. A. and R. M. Szabo (1995). "Diaphyseal humerus fractures: natural history and occurrence of nonunion." Orthopedics **18**(4): 333-5.
Franklin, K. B. J. and G. Paxinos (1997). The Mouse Brain in Stereotaxic Coordinates. San Diego, CA.
Friedenstein, A. J., R. K. Chailakhjan, et al. (1970). "The development of fibroblast colonies in monolayer cultures of guinea-pig bone marrow and spleen cells." Cell Tissue Kinet **3**(4): 393-403.
Friedenstein, A. J., U. F. Deriglasova, et al. (1974). "Precursors for fibroblasts in different populations of hematopoietic cells as detected by the in vitro colony assay method." Exp Hematol **2**(2): 83-92.
Friedenstein, A. J., J. F. Gorskaja, et al. (1976). "Fibroblast precursors in normal and irradiated mouse hematopoietic organs." Exp Hematol **4**(5): 267-74.
Friedman, J. M. and J. L. Halaas (1998). "Leptin and the regulation of body weight in mammals." Nature **395**(6704): 763-70.
Gainsford, T., T. A. Willson, et al. (1996). "Leptin can induce proliferation, differentiation, and functional activation of hemopoietic cells." Proc Natl Acad Sci U S A **93**(25): 14564-8.
Gilbert, L., X. He, et al. (2000). "Inhibition of osteoblast differentiation by tumor necrosis factor-alpha." Endocrinology **141**(11): 3956-64.
Gordeladze, J. O., C. A. Drevon, et al. (2002). "Leptin stimulates human osteoblastic cell proliferation, de novo collagen synthesis, and mineralization: Impact on differentiation markers, apoptosis, and osteoclastic signaling." J Cell Biochem **85**(4): 825-36.
Gronthos, S., D. M. Franklin, et al. (2001). "Surface protein characterization of human adipose tissue-derived stromal cells." J Cell Physiol **189**(1): 54-63.
Gronthos, S., M. Mankani, et al. (2000). "Postnatal human dental pulp stem cells (DPSCs) in vitro and in vivo." Proc Natl Acad Sci U S A **97**(25): 13625-30.
Gruen, M. L., M. Hao, et al. (2007). "Leptin requires canonical migratory signaling pathways for induction of monocyte and macrophage chemotaxis." Am J Physiol Cell Physiol.
Gura, T. (1999). "Leptin not impressive in clinical trial." Science **286**(5441): 881-882.
Gutierrez, G. M., E. Kong, et al. (2008). "Impaired bone development and increased mesenchymal progenitor cells in calvaria of RB1-/- mice." Proc Natl Acad Sci U S A **105**(47): 18402-7.
Halaas, J. L., K. S. Gajiwala, et al. (1995). "Weight-reducing effects of the plasma protein encoded by the obese gene." Science **269**(5223): 543-6.
Hamrick, M. W., M. A. Della-Fera, et al. (2005). "Leptin treatment induces loss of bone marrow adipocytes and increases bone formation in leptin-deficient ob/ob mice." J Bone Miner Res **20**(6): 994-1001.

Hamrick, M. W., K. H. Ding, et al. (2008). "Caloric restriction decreases cortical bone mass but spares trabecular bone in the mouse skeleton: implications for the regulation of bone mass by body weight." J Bone Miner Res **23**(6): 870-8.
Hamrick, M. W., C. Pennington, et al. (2004). "Leptin deficiency produces contrasting phenotypes in bones of the limb and spine." Bone **34**(3): 376-83.
Hardie, D. G. and D. Carling (1997). "The AMP-activated protein kinase--fuel gauge of the mammalian cell?" Eur J Biochem **246**(2): 259-73.
Heffner, C. and Y. Sharma. (2010). "B6.Cg-Tg(Fabp4-cre)1Rev/J (Stock No:005069)." from http://cre.jax.org/Fabp4/Fabp4-cre_.html.
Hess, R., A. M. Pino, et al. (2005). "High affinity leptin receptors are present in human mesenchymal stem cells (MSCs) derived from control and osteoporotic donors." J Cell Biochem **94**(1): 50-7.
Heymsfield, S. B., A. S. Greenberg, et al. (1999). "Recombinant leptin for weight loss in obese and lean adults: a randomized, controlled, dose-escalation trial." Jama **282**(16): 1568-75.
Hoggard, N., J. G. Mercer, et al. (1997). "Localization of leptin receptor mRNA splice variants in murine peripheral tissues by RT-PCR and in situ hybridization." Biochem Biophys Res Commun **232**(2): 383-7.
Howard, J. K., B. J. Cave, et al. (2004). "Enhanced leptin sensitivity and attenuation of diet-induced obesity in mice with haploinsufficiency of Socs3." Nat Med **10**(7): 734-8.
Huan, J. N., J. Li, et al. (2003). "Adipocyte-selective reduction of the leptin receptors induced by antisense RNA leads to increased adiposity, dyslipidemia, and insulin resistance." J Biol Chem **278**(46): 45638-50.
Huang, K. C., W. C. Cheng, et al. (2004). "Lack of independent relationship between plasma adiponectin, leptin levels and bone density in nondiabetic female adolescents." Clin Endocrinol (Oxf) **61**(2): 204-8.
Huggins, C. and B. H. Blocksom Jr (1936). "Changes in Outlying Bone Marrow Accompanying a Local Increase of Temperature Within Physiological Limits." J Exp Med **64**: 253-274.
Hummel, K. P., M. M. Dickie, et al. (1966). "Diabetes, a new mutation in the mouse." Science **153**(740): 1127-8.
Ibanez, L., N. Potau, et al. (2000). "Increased bone mineral density and serum leptin in non-obese girls with precocious pubarche: relation to low birthweight and hyperinsulinism." Horm Res **54**(4): 192-7.
Ibrahim, A., N. Scher, et al. (2003). "Approval summary for zoledronic acid for treatment of multiple myeloma and cancer bone metastases." Clin Cancer Res **9**(7): 2394-9.
Ingalls, A. M., M. M. Dickie, et al. (1950). "Obese, a new mutation in the house mouse." J Hered **41**(12): 317-8.
Isomaki, P., T. Alanara, et al. (2007). "The expression of SOCS is altered in rheumatoid arthritis." Rheumatology (Oxford) **46**(10): 1538-46.
Iwaniec, U. T., S. Boghossian, et al. (2007). "Central leptin gene therapy corrects skeletal abnormalities in leptin-deficient ob/ob mice." Peptides **28**(5): 1012-9.
Iwaniec, U. T., M. G. Dube, et al. (2009). "Body mass influences cortical bone mass independent of leptin signaling." Bone **44**(3): 404-12.

Jarrett, S. J., P. G. Conaghan, et al. (2006). "Preliminary evidence for a structural benefit of the new bisphosphonate zoledronic acid in early rheumatoid arthritis." Arthritis Rheum **54**(5): 1410-4.
Kalajzic, Z., P. Liu, et al. (2002). "Directing the expression of a green fluorescent protein transgene in differentiated osteoblasts: comparison between rat type I collagen and rat osteocalcin promoters." Bone **31**(6): 654-60.
Khan, S. A., J. A. Kanis, et al. (1997). "Elimination and biochemical responses to intravenous alendronate in postmenopausal osteoporosis." J Bone Miner Res **12**(10): 1700-7.
Kielar, D., J. S. Clark, et al. (1998). "Leptin receptor isoforms expressed in human adipose tissue." Metabolism **47**(7): 844-7.
Kinjyo, I., H. Inoue, et al. (2006). "Loss of SOCS3 in T helper cells resulted in reduced immune responses and hyperproduction of interleukin 10 and transforming growth factor-beta 1." J Exp Med **203**(4): 1021-31.
Kishida, Y., M. Hirao, et al. (2005). "Leptin regulates chondrocyte differentiation and matrix maturation during endochondral ossification." Bone **37**(5): 607-21.
Kozloff, K. M., L. I. Volakis, et al. (2010). "Near-infrared fluorescent probe traces bisphosphonate delivery and retention in vivo." J Bone Miner Res **25**(8): 1748-58.
Krebsbach, P. H., J. R. Harrison, et al. (1993). "Transgenic expression of COL1A1-chloramphenicol acetyltransferase fusion genes in bone: differential utilization of promoter elements in vivo and in cultured cells." Mol Cell Biol **13**(9): 5168-74.
Krebsbach, P. H., S. A. Kuznetsov, et al. (1997). "Bone formation in vivo: comparison of osteogenesis by transplanted mouse and human marrow stromal fibroblasts." Transplantation **63**(8): 1059-69.
Krech, S., J. R. McNeill, et al. (2004). Encyclopedia of world environmental history, Volume 3. Routledge.
La Cava, A. and G. Matarese (2004). "The weight of leptin in immunity." Nat Rev Immunol **4**(5): 371-9.
Laharrague, P., D. Larrouy, et al. (1998). "High expression of leptin by human bone marrow adipocytes in primary culture." Faseb J **12**(9): 747-52.
Lamghari, M., L. Tavares, et al. (2006). "Leptin effect on RANKL and OPG expression in MC3T3-E1 osteoblasts." J Cell Biochem **98**(5): 1123-9.
Lee, G. H., R. Proenca, et al. (1996). "Abnormal splicing of the leptin receptor in diabetic mice." Nature **379**(6566): 632-5.
Leinninger, G. M., Y. H. Jo, et al. (2009). "Leptin acts via leptin receptor-expressing lateral hypothalamic neurons to modulate the mesolimbic dopamine system and suppress feeding." Cell Metab **10**(2): 89-98.
Lengner, C. J., H. A. Steinman, et al. (2006). "Osteoblast differentiation and skeletal development are regulated by Mdm2-p53 signaling." J Cell Biol **172**(6): 909-21.
Lewis, D. B., H. D. Liggitt, et al. (1993). "Osteoporosis induced in mice by overproduction of interleukin 4." Proc Natl Acad Sci U S A **90**(24): 11618-22.
Li, M., Y. Shen, et al. (1996). "Comparative study of skeletal response to estrogen depletion at red and yellow marrow sites in rats." Anat Rec **245**(3): 472-80.
Lin, S., T. C. Thomas, et al. (2000). "Development of high fat diet-induced obesity and leptin resistance in C57Bl/6J mice." Int J Obes Relat Metab Disord **24**(5): 639-46.

Liu, F., H. W. Woitge, et al. (2004). "Expression and activity of osteoblast-targeted Cre recombinase transgenes in murine skeletal tissues." Int J Dev Biol **48**(7): 645-53.
Loffreda, S., S. Q. Yang, et al. (1998). "Leptin regulates proinflammatory immune responses." Faseb J **12**(1): 57-65.
Lollmann, B., S. Gruninger, et al. (1997). "Detection and quantification of the leptin receptor splice variants Ob-Ra, b, and, e in different mouse tissues." Biochem Biophys Res Commun **238**(2): 648-52.
Lord, G. M., G. Matarese, et al. (1998). "Leptin modulates the T-cell immune response and reverses starvation-induced immunosuppression." Nature **394**(6696): 897-901.
Lorentzon, M., K. Landin, et al. (2006). "Leptin is a negative independent predictor of areal BMD and cortical bone size in young adult Swedish men." J Bone Miner Res **21**(12): 1871-8.
Lorenzo, J., M. Horowitz, et al. (2008). "Osteoimmunology: interactions of the bone and immune system." Endocr Rev **29**(4): 403-40.
Lovato, P., C. Brender, et al. (2003). "Constitutive STAT3 activation in intestinal T cells from patients with Crohn's disease." J Biol Chem **278**(19): 16777-81.
Maingrette, F. and G. Renier (2003). "Leptin increases lipoprotein lipase secretion by macrophages: involvement of oxidative stress and protein kinase C." Diabetes **52**(8): 2121-8.
Mancuso, P., M. Peters-Golden, et al. (2011). "Disruption of leptin receptor-STAT3 signaling enhances leukotriene production and pulmonary host defense against pneumococcal pneumonia." J Immunol **186**(2): 1081-90.
Mao, X., Y. Fujiwara, et al. (2001). "Activation of EGFP expression by Cre-mediated excision in a new ROSA26 reporter mouse strain." Blood **97**(1): 324-6.
Martini, G., R. Valenti, et al. (2001). "Influence of insulin-like growth factor-1 and leptin on bone mass in healthy postmenopausal women." Bone **28**(1): 113-7.
Maurin, A. C., P. M. Chavassieux, et al. (2000). "Influence of mature adipocytes on osteoblast proliferation in human primary cocultures." Bone **26**(5): 485-9.
Maximow, A. (2009). "The Lymphocyte as a stem cell common to different blood elements in embryonic development and during post-fetal life of mammals (1909). Originally in German: Folia Haematologica 8.1909, 125-134." Cell Ther Transplant **1**(3).
McMinn, J. E., S. M. Liu, et al. (2004). "An allelic series for the leptin receptor gene generated by CRE and FLP recombinase." Mamm Genome **15**(9): 677-85.
Menahan, L. A. (1983). "Age-related changes in lipid and carbohydrate metabolism of the genetically obese mouse." Metabolism **32**(2): 172-8.
Mendall, M. A., A. V. Gunasekera, et al. (2011). "Is obesity a risk factor for Crohn's disease?" Dig Dis Sci **56**(3): 837-44.
Metcalf, D. (2007). "Concise review: hematopoietic stem cells and tissue stem cells: current concepts and unanswered questions." Stem Cells **25**(10): 2390-5.
Mick, G., T. Vanderbloomer, et al. (1998). "Leptin does not affect adipocyte glucose metabolism: studies in fresh and cultured adipocytes." Metabolism **47**(11): 1360-5.
Minokoshi, Y., Y. B. Kim, et al. (2002). "Leptin stimulates fatty-acid oxidation by activating AMP-activated protein kinase." Nature **415**(6869): 339-43.

Morberg, C. M., I. Tetens, et al. (2003). "Leptin and bone mineral density: a cross-sectional study in obese and nonobese men." J Clin Endocrinol Metab **88**(12): 5795-800.
Mori, H., R. Hanada, et al. (2004). "Socs3 deficiency in the brain elevates leptin sensitivity and confers resistance to diet-induced obesity." Nat Med **10**(7): 739-43.
Mori, H., T. Shichita, et al. (2007). "Suppression of SOCS3 expression in the pancreatic beta-cell leads to resistance to type 1 diabetes." Biochem Biophys Res Commun **359**(4): 952-8.
Morikawa, Y., E. Ueyama, et al. (2004). "Fasting-induced activation of mitogen-activated protein kinases (ERK/p38) in the mouse hypothalamus." J Neuroendocrinol **16**(2): 105-12.
Motyl, K. J. and L. R. McCabe (2009). "Leptin treatment prevents type I diabetic marrow adiposity but not bone loss in mice." J Cell Physiol **218**(2): 376-84.
Mueller, W. M., F. M. Gregoire, et al. (1998). "Evidence that glucose metabolism regulates leptin secretion from cultured rat adipocytes." Endocrinology **139**(2): 551-8.
Myers, M. G. (2004). "Leptin Receptor Signaling and the Regulation of Mammalian Physiology." Recent Prog Horm Res **59**: 287-304.
Naveiras, O., V. Nardi, et al. (2009). "Bone-marrow adipocytes as negative regulators of the haematopoietic microenvironment." Nature **460**(7252): 259-63.
Niswender, K. D., G. J. Morton, et al. (2001). "Intracellular signalling. Key enzyme in leptin-induced anorexia." Nature **413**(6858): 794-5.
Novince, C. M., B. B. Ward, et al. (2009). "Osteonecrosis of the jaw: an update and review of recommendations." Cells Tissues Organs **189**(1-4): 275-83.
Ogata, H., T. Chinen, et al. (2006). "Loss of SOCS3 in the liver promotes fibrosis by enhancing STAT3-mediated TGF-beta1 production." Oncogene **25**(17): 2520-30.
Oguz, S., O. L. Tapisiz, et al. (2009). "Is leptin a significant predictor of bone mineral density in postmenopausal Turkish women?" Rheumatol Int **29**(4): 393-6.
Ohishi, M., Y. Matsumura, et al. (2005). "Suppressors of cytokine signaling-1 and -3 regulate osteoclastogenesis in the presence of inflammatory cytokines." J Immunol **174**(5): 3024-31.
Olsen, B. R., A. M. Reginato, et al. (2000). "Bone development." Annu Rev Cell Dev Biol **16**: 191-220.
Ozata, M., I. C. Ozdemir, et al. (1999). "Human leptin deficiency caused by a missense mutation: multiple endocrine defects, decreased sympathetic tone, and immune system dysfunction indicate new targets for leptin action, greater central than peripheral resistance to the effects of leptin, and spontaneous correction of leptin-mediated defects." J Clin Endocrinol Metab **84**(10): 3686-95.
Pasco, J. A., M. J. Henry, et al. (2001). "Serum leptin levels are associated with bone mass in nonobese women." J Clin Endocrinol Metab **86**(5): 1884-7.
Pelleymounter, M. A., M. J. Cullen, et al. (1995). "Effects of the obese gene product on body weight regulation in ob/ob mice." Science **269**(5223): 540-3.
Phinney, D. G. and D. J. Prockop (2007). "Concise review: mesenchymal stem/multipotent stromal cells: the state of transdifferentiation and modes of tissue repair--current views." Stem Cells **25**(11): 2896-902.

Piessevaux, J., D. Lavens, et al. (2008). "The many faces of the SOCS box." Cytokine Growth Factor Rev **19**(5-6): 371-81.
Poznanski, W. J., I. Waheed, et al. (1973). "Human fat cell precursors. Morphologic and metabolic differentiation in culture." Lab Invest **29**(5): 570-6.
Ranvier, L. A. (1889). "Traite technique d'histologie." Paris, F. Savy **264**.
Reseland, J. E., U. Syversen, et al. (2001). "Leptin is expressed in and secreted from primary cultures of human osteoblasts and promotes bone mineralization." J Bone Miner Res **16**(8): 1426-33.
Reuben, J. S., L. Dinh, et al. (2011). "Bisophosphonates inhibit phosphorylation of signal transducer and activator of transcription 3 and expression of suppressor of cytokine signaling 3: implications for their effects on innate immune function and osteoclastogenesis." Oral Surg Oral Med Oral Pathol Oral Radiol Endod **111**(2): 196-204.
Rhee, S. D., Y. Y. Sung, et al. (2008). "Leptin inhibits rosiglitazone-induced adipogenesis in murine primary adipocytes." Mol Cell Endocrinol **294**(1-2): 61-9.
Rifas, L., S. Arackal, et al. (2003). "Inflammatory T cells rapidly induce differentiation of human bone marrow stromal cells into mature osteoblasts." J Cell Biochem **88**(4): 650-9.
Rodbell, M. (1964). "Metabolism of Isolated Fat Cells. I. Effects of Hormones on Glucose Metabolism and Lipolysis." J Biol Chem **239**: 375-80.
Rodeheffer, M. S., K. Birsoy, et al. (2008). "Identification of white adipocyte progenitor cells in vivo." Cell **135**(2): 240-9.
Roemmich, J. N., P. A. Clark, et al. (2003). "Relationship of leptin to bone mineralization in children and adolescents." J Clin Endocrinol Metab **88**(2): 599-604.
Roux, C., A. Arabi, et al. (2003). "Serum leptin as a determinant of bone resorption in healthy postmenopausal women." Bone **33**(5): 847-52.
Ruhl, C. E. and J. E. Everhart (2002). "Relationship of serum leptin concentration with bone mineral density in the United States population." J Bone Miner Res **17**(10): 1896-903.
Russell, R. G., N. B. Watts, et al. (2008). "Mechanisms of action of bisphosphonates: similarities and differences and their potential influence on clinical efficacy." Osteoporos Int **19**(6): 733-59.
Sahin, G., G. Polat, et al. (2003). "Body composition, bone mineral density, and circulating leptin levels in postmenopausal Turkish women." Rheumatol Int **23**(2): 87-91.
Santos-Alvarez, J., R. Goberna, et al. (1999). "Human leptin stimulates proliferation and activation of human circulating monocytes." Cell Immunol **194**(1): 6-11.
Sato, M., W. Grasser, et al. (1991). "Bisphosphonate action. Alendronate localization in rat bone and effects on osteoclast ultrastructure." J Clin Invest **88**(6): 2095-105.
Sato, M., N. Takeda, et al. (2001). "Association between serum leptin concentrations and bone mineral density, and biochemical markers of bone turnover in adult men." J Clin Endocrinol Metab **86**(11): 5273-6.
Satoh, N., Y. Ogawa, et al. (1997). "The arcuate nucleus as a primary site of satiety effect of leptin in rats." Neurosci Lett **224**(3): 149-52.

Sauer, B. and N. Henderson (1988). "Site-specific DNA recombination in mammalian cells by the Cre recombinase of bacteriophage P1." Proc Natl Acad Sci U S A **85**(14): 5166-70.
Scheller, E. L., C. M. Baldwin, et al. (2011). "Bisphosphonates Inhibit Expression of p63 by Oral Keratinocytes." J Dent Res.
Scheller, E. L., K. D. Hankenson, et al. (2011). "Zoledronic acid inhibits macrophage SOCS3 expression and enhances cytokine production." J Cell Biochem **Epub ahead of print**.
Scheller, E. L., G. M. Leinninger, et al. (2011). "Ectopic expression of col2.3 and col3.6 promoters in the brain and association with leptin signaling." Cells Tissues Organs **194**(2-4): 268-73.
Scheller, E. L., J. Song, et al. (2010). "Leptin functions peripherally to regulate differentiation of mesenchymal progenitor cells." Stem Cells **28**(6): 1071-80.
Shi, S. and S. Gronthos (2003). "Perivascular niche of postnatal mesenchymal stem cells in human bone marrow and dental pulp." J Bone Miner Res **18**(4): 696-704.
Shi, Y., V. K. Yadav, et al. (2008). "Dissociation of the neuronal regulation of bone mass and energy metabolism by leptin in vivo." Proc Natl Acad Sci U S A **105**(51): 20529-33.
Steppan, C. M., D. T. Crawford, et al. (2000). "Leptin is a potent stimulator of bone growth in ob/ob mice." Regul Pept **92**(1-3): 73-8.
Sudhoff, H., J. Y. Jung, et al. (2003). "Zoledronic acid inhibits osteoclastogenesis in vitro and in a mouse model of inflammatory osteolysis." Ann Otol Rhinol Laryngol **112**(9 Pt 1): 780-6.
Sun, A. J., T. Jing, et al. (2003). "Relationship of leptin and sex hormones to bone mineral density in men." Acta Diabetol **40 Suppl 1**: S101-5.
Suzuki, A., T. Hanada, et al. (2001). "CIS3/SOCS3/SSI3 plays a negative regulatory role in STAT3 activation and intestinal inflammation." J Exp Med **193**(4): 471-81.
Szpaderska, A. M., J. D. Zuckerman, et al. (2003). "Differential injury responses in oral mucosal and cutaneous wounds." J Dent Res **82**(8): 621-6.
Takashima, Y., T. Era, et al. (2007). "Neuroepithelial cells supply an initial transient wave of MSC differentiation." Cell **129**(7): 1377-88.
Takeda, S., F. Elefteriou, et al. (2002). "Leptin regulates bone formation via the sympathetic nervous system." Cell **111**(3): 305-17.
Tamasi, J. A., B. J. Arey, et al. (2003). "Characterization of bone structure in leptin receptor-deficient Zucker (fa/fa) rats." J Bone Miner Res **18**(9): 1605-11.
Tang, W., D. Zeve, et al. (2008). "White fat progenitor cells reside in the adipose vasculature." Science **322**(5901): 583-6.
Tartaglia, L. A., M. Dembski, et al. (1995). "Identification and expression cloning of a leptin receptor, OB-R." Cell **83**(7): 1263-71.
Thomas, T., B. Burguera, et al. (2001). "Role of serum leptin, insulin, and estrogen levels as potential mediators of the relationship between fat mass and bone mineral density in men versus women." Bone **29**(2): 114-20.
Thomas, T., F. Gori, et al. (1999). "Leptin acts on human marrow stromal cells to enhance differentiation to osteoblasts and to inhibit differentiation to adipocytes." Endocrinology **140**(4): 1630-8.

Ura, K., I. Morimoto, et al. (2000). "Interleukin (IL)-4 and IL-13 inhibit the differentiation of murine osteoblastic MC3T3-E1 cells." Endocr J **47**(3): 293-302.
Ushiroyama, T., A. Ikeda, et al. (2003). "Inverse correlation between serum leptin concentration and vertebral bone density in postmenopausal women." Gynecol Endocrinol **17**(1): 31-6.
Van, R. L., C. E. Bayliss, et al. (1976). "Cytological and enzymological characterization of adult human adipocyte precursors in culture." J Clin Invest **58**(3): 699-704.
Voigt, L. F., T. D. Koepsell, et al. (1994). "Smoking, obesity, alcohol consumption, and the risk of rheumatoid arthritis." Epidemiology **5**(5): 525-32.
Weiss, L. A., E. Barrett-Connor, et al. (2006). "Leptin predicts BMD and bone resorption in older women but not older men: the Rancho Bernardo study." J Bone Miner Res **21**(5): 758-64.
Wessel, J. H., T. B. Dodson, et al. (2008). "Zoledronate, smoking, and obesity are strong risk factors for osteonecrosis of the jaw: a case-control study." J Oral Maxillofac Surg **66**(4): 625-31.
Wronski, T. J., J. M. Smith, et al. (1981). "Variations in mineral apposition rate of trabecular bone within the beagle skeleton." Calcif Tissue Int **33**(6): 583-6.
Yamauchi, M., T. Sugimoto, et al. (2001). "Plasma leptin concentrations are associated with bone mineral density and the presence of vertebral fractures in postmenopausal women." Clin Endocrinol (Oxf) **55**(3): 341-7.
Yang, D. C., H. J. Tsay, et al. (2008). "cAMP/PKA Regulates Osteogenesis, Adipogenesis and Ratio of RANKL/OPG mRNA Expression in Mesenchymal Stem Cells by Suppressing Leptin." PLoS ONE **3**(2): e1540.
Yasukawa, H., M. Ohishi, et al. (2003). "IL-6 induces an anti-inflammatory response in the absence of SOCS3 in macrophages." Nat Immunol **4**(6): 551-6.
Yilmazi, M., I. Keles, et al. (2005). "Plasma leptin concentrations in postmenopausal women with osteoporosis." Endocr Res **31**(2): 133-8.
Yoneda, T., Y. Maruyama, et al. (2001). "A possible role for leptin in normo- or hypoparathyroid uremic bone in postmenopausal dialysis women." J Bone Miner Metab **19**(2): 119-24.
Yoshimura, A., T. Naka, et al. (2007). "SOCS proteins, cytokine signalling and immune regulation." Nat Rev Immunol **7**(6): 454-65.
Zastrow, O., B. Seidel, et al. (2003). "The soluble leptin receptor is crucial for leptin action: evidence from clinical and experimental data." Int J Obes Relat Metab Disord **27**(12): 1472-8.
Zhang, F., Y. Chen, et al. (2005). "Leptin: structure, function and biology." Vitam Horm **71**: 345-72.
Zhang, Y., R. Proenca, et al. (1994). "Positional cloning of the mouse obese gene and its human homologue." Nature **372**(6505): 425-32.
Zhao, T., M. Hou, et al. (2005). "Globular adiponectin decreases leptin-induced tumor necrosis factor-alpha expression by murine macrophages: involvement of cAMP-PKA and MAPK pathways." Cell Immunol **238**(1): 19-30.
Zhong, N., X. P. Wu, et al. (2005). "Relationship of serum leptin with age, body weight, body mass index, and bone mineral density in healthy mainland Chinese women." Clin Chim Acta **351**(1-2): 161-8.

Zoico, E., M. Zamboni, et al. (2003). "Relationship between leptin levels and bone mineral density in the elderly." Clin Endocrinol (Oxf) **59**(1): 97-103.
Zoler, M. L. (2010). Zoledronic acid relieves knee OA pain and shrinks bone marrow lesions. Elsevier Global Medical News, International Medical News Group.
Zuk, P. A., M. Zhu, et al. (2001). "Multilineage cells from human adipose tissue: implications for cell-based therapies." Tissue Eng **7**(2): 211-28.
Zwolak, P., J. C. Manivel, et al. (2010). "Cytotoxic effect of zoledronic acid-loaded bone cement on giant cell tumor, multiple myeloma, and renal cell carcinoma cell lines." J Bone Joint Surg Am **92**(1): 162-8.